389
3-24-83
(1) I-8446 Dr. 1270

SANDIA REPORT SAND79-2291 • TTC-308 • Unlimited Release • UC-71
Printed February 1983

SAND--79-2291

DE83 008976

A Study and Full-Scale Test of a High-Velocity Grade-Crossing Simulated Accident of a Locomotive and a Nuclear-Spent-Fuel Shipping Cask

Michael Huerta, H. Richard Yoshimura

Prepared by
Sandia National Laboratories
Albuquerque, New Mexico 87185 and Livermore, California 94550
for the United States Department of Energy
under Contract DE-AC04-76DP00789

DISTRIBUTION OF THIS DOCUMENT IS UNLIMITED

SF 2900-Q(6-82)

MASTER

DISCLAIMER

This report was prepared as an account of work sponsored by an agency of the United States Government. Neither the United States Government nor any agency Thereof, nor any of their employees, makes any warranty, express or implied, or assumes any legal liability or responsibility for the accuracy, completeness, or usefulness of any information, apparatus, product, or process disclosed, or represents that its use would not infringe privately owned rights. Reference herein to any specific commercial product, process, or service by trade name, trademark, manufacturer, or otherwise does not necessarily constitute or imply its endorsement, recommendation, or favoring by the United States Government or any agency thereof. The views and opinions of authors expressed herein do not necessarily state or reflect those of the United States Government or any agency thereof.

DISCLAIMER

Portions of this document may be illegible in electronic image products. Images are produced from the best available original document.

Issued by Sandia National Laboratories, operated for the United States Department of Energy by Sandia Corporation.
NOTICE: This report was prepared as an account of work sponsored by an agency of the United States Government. Neither the United States Government nor any agency thereof, nor any of their employees, nor any of their contractors, subcontractors, or their employees, makes any warranty, express or implied, or assumes any legal liability or responsibility for the accuracy, completeness, or usefulness of any information, apparatus, product, or process disclosed, or represents that its use would not infringe privately owned rights. Reference herein to any specific commercial product, process, or service by trade name, trademark, manufacturer, or otherwise, does not necessarily constitute or imply its endorsement, recommendation, or favoring by the United States Government, any agency thereof or any of their contractors or subcontractors. The views and opinions expressed herein do not necessarily state or reflect those of the United States Government, any agency thereof or any of their contractors or subcontractors.

Printed in the United States of America
Available from
National Technical Information Service
U.S. Department of Commerce
5285 Port Royal Road
Springfield, VA 22161

NTIS price codes
Printed copy: A04
Microfiche copy: A01

SAND79-2291
TTC-308
Unlimited Release
Printed February 1983

Distribution
Category UC-71

A Study and Full-Scale Test of a High-Velocity Grade-Crossing Simulated Accident of a Locomotive and a Nuclear-Spent-Fuel Shipping Cask

NOTICE
PORTIONS OF THIS REPORT ARE ILLEGIBLE.
It has been reproduced from the best available copy to permit the broadest possible availability.

Michael Huerta
Southwest Engineering Associates
El Paso, Texas

H. Richard Yoshimura
Transportation Systems Development and Testing Division 9783

Transportation Technology Center
Sandia National Laboratories
Albuquerque, NM 87185

DISCLAIMER

This report was prepared as an account of work sponsored by an agency of the United States Government. Neither the United States Government nor any agency thereof, nor any of their employees, makes any warranty, express or implied, or assumes any legal liability or responsibility for the accuracy, completeness, or usefulness of any information, apparatus, product, or process disclosed, or represents that its use would not infringe privately owned rights. Reference herein to any specific commercial product, process, or service by trade name, trademark, manufacturer, or otherwise does not necessarily constitute or imply its endorsement, recommendation, or favoring by the United States Government or any agency thereof. The views and opinions of authors expressed herein do not necessarily state or reflect those of the United States Government or any agency thereof.

Abstract

This report describes structural analyses of a high-speed impact between a locomotive and a tractor-trailer system carrying a nuclear-spent-fuel shipping cask. The analyses included both mathematical and physical scale-modeling of the system. The report then describes the full-scale test conducted as part of the program. The system response is described in detail, and a comparison is made between the analyses and the actual hardware response as observed in the full-scale test.

DISTRIBUTION OF THIS DOCUMENT IS UNLIMITED

Acknowledgments

Many Sandia personnel contributed to this work. D. C. Bickel and R. L. Lucas of the Track and Cables Division headed the design of the propulsion system and the conduct of the full-scale test. D. R. Stenberg of Missouri Research Labs (MRL), assisted in designing the scale models, preparing hardware for the test, and taking measurements after the test. M. E. Barnett and W. V. Hereford of the Telemetry Development Division were responsible for the instrumentation and telemetered data acquisition. T. A. Leighley of the Photometrics and Optical Development Division provided high-speed film coverage. John E. CdeBaca of the Test Data Analysis Division was responsible for digitizing and reducing the film data. A. W. Dennis of the Applied Mechanics Division assisted in designing the models and provided some significant pretest analyses. The authors thank the individuals mentioned above and others who have assisted them in this work and in preparing this document.

Contents

Figures

Figures (cont)

A Study and Full-Scale Test of a High-Velocity Grade-Crossing Simulated Accident of a Locomotive and a Nuclear-Spent-Fuel Shipping Cask

Introduction

This report presents the analysis and results of a full-scale grade-crossing simulated accident involving a locomotive and a nuclear-spent-fuel shipping cask, the fourth in a series of transportation tests conducted by Sandia National Laboratories. Reference 1 describes the rationale and purposes of the tests. The first two tests provided information on the response of a tractor-trailer system impacting a rigid barrier at two different velocities.[2] The third test involved a railcar and cask system impacting a rigid barrier at high velocity.[3] In this, the final test to be reported, a tractor-trailer system was placed across a simulated grade crossing and impacted by a rocket propelled locomotive traveling at 130 km/h (81 mph). The system was carefully monitored with instrumentation and many high-speed cameras.

As with the previous transportation-system tests, mathematical and scale modeling studies were made before the full-scale test. These studies predicted the response of the system, and the full-scale test served as a confirmatory test. The present report describes the analyses (mathematical and scale modeling) and the full-scale grade-crossing test. Results of the analyses are compared with the actual response of the full-scale system.

Accident Scenario and Hardware

The scenario chosen for this particular test was to impact a tractor-trailer system stalled at a grade crossing by a locomotive traveling at 129 km/h (80 mph). The cask was centered over and perpendicular to the tracks and mounted on the same shipping trailer that was used during its time in service. Figure 1 is a schematic of the test configuration. The road grade of the crossing was constructed to be 5% on each side to represent a standard design.

Available hardware included a locomotive weighing 109 metric tons (240,000 lb), a shipping cask weighing 25.45 metric tons (56,000 lb) and a three-axle trailer weighing 5.9 metric tons (13,000 lb). Also available was a used gasoline tractor to be attached to the trailer.

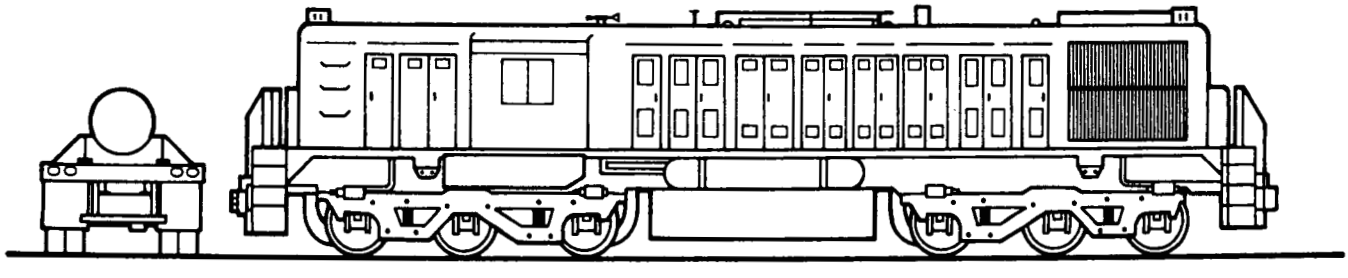

Figure 1. Schematic of Test Configuration

Figure 2 illustrates the cask's construction. The design utilized lead shielding and 304 stainless-steel materials. The outer shell was 2.54 cm (1 in.) thick; the inside shell was 1.9 cm (0.75 in.) thick. A 21.3-cm (8.37-in.) layer of lead shielding was used between the shells; the head and bottom had a slightly thinner layer. The head was held in place with eight 2.54-cm (1-in.) bolts. The cask was tied down to the trailer structure with heavy steel bands and four 3.2-cm (1.25-in.) bolts at each connection.

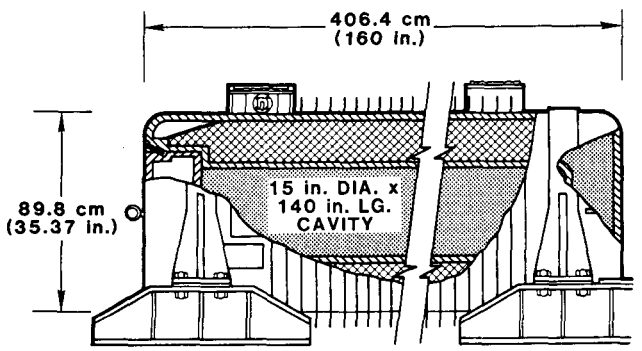

Figure 2. Schematic of the Shipping Cask

The locomotive for the test was a used military-surplus unit. Its structural construction features are briefly described as pertinent to the analysis. The available unit followed typical locomotive construction in that the main structural members consisted of two massive I-beams running the full length of the vehicle. On the test unit the I-beams were 50 cm (20 in.) tall with flanges 1.9 cm (0.75 in.) thick and 30.5 cm (12 in.) wide. The web portion of the beam was 1.27 cm (0.5 in.) thick. The ends of the I-beams were covered with 1.9 cm (0.75 in.) thick steel plate to form a bumper system above the couplers on both ends of the vehicle. Near the ends of the vehicle, the I-beam structure was reinforced with a cross I-beam placed 99 cm (39 in.) behind the end plate. The top of the I-beam was covered with a 0.5 cm (0.2 in.)-steel decking. The lower I-beam flanges were also heavily reinforced with steel plate on the bottom. These features will become more apparent when the scale model is described. Photographs of the system and additional information are included in the section describing the full-scale test.

The impact relationship between the locomotive and the cask (see Figure 1) was such that the top of the locomotive frame was 20.3 cm (8 in.) below the centerline of the cask. With this configuration, the coupler clears the bottom of the trailer frame. The geometric relationship just described occurs when the hardware, as manufactured, is used with a 5% grade in the crossing. This geometric relationship was used in the analyses as well as in the full-scale test.

Mathematical Analysis

Introduction

Analyzing a locomotive impacting a shipping cask is a very complicated, even intractable problem to handle mathematically. Some simplifying assumptions have to be made. The approach that one has to take is to simplify the problem down to its most basic structures using sound engineering judgments. In this case it is reasonable to assume that for the impact situation the important structures are the locomotive underframe and the cask. The mass of the locomotive is also important in that the locomotive momentum provides the driving force.

A grade-crossing accident with the same velocity and cask but using a heavier 186-metric-ton locomotive has previously been analyzed by Dennis.[4] He used a combination of lumped-parameter and static finite-element modeling. His results indicated that an impact between a locomotive and a cask placed on its normal shipping trailer would not breach the cask, on the basis that the calculated cask deformations were small. Dennis also concluded that the trailer structure was insignificant in the impact except that it supported the cask at a given elevation. He calculated that the trailer structure would be crushed and forced under the cask with negligible cask motion. He also calculated that the tie downs would be broken and that the locomotive underframe would impact the cask 0.034 s after it contacted the side of the trailer.

The work of Dennis is used as a basis for a finite-element analysis where only the mass of the locomotive, the locomotive underframe, and the mass of the cask are considered; the trailer structure is ignored. The relatively soft locomotive superstructure and cask appurtenances are neglected.

In the past, finite-element solutions for end-impact calculations have proven feasible and have provided reasonable results.[2] An end-on impact is two-dimensional (2D) in that the cask structure can be modeled as an axisymmetric body. The problem of analyzing a shipping cask impacted by a locomotive underframe, on the other hand, is a much more complex three-dimensional (3D) problem. At the time of the test, a 3D large-deformation, finite-element solution was impractical in terms of computer time and possibly man-hours required to set it up. C. M. Stone[5]

attempted a 3D solution where he assumed the underframe was an infinitely rigid structure and gave the cask an initial velocity into it. He used the computer program WULFF[6] and a CDC 6600 machine. The computer run times were excessive, on the order of 15 h of computation time for <1 ms of real time. The rigid-frame assumption turned out to be impractical and the problem could not be run to completion. Plots of the deformed mesh for early times in the impact, however, did appear approximately correct in shape.

Because of these difficulties, we resorted to a 2D calculation to obtain an approximate solution. With a 2D calculation, simplifying assumptions can be made and some parametric studies run to obtain a feeling for the solution sensitivity to the various assumptions. In this way it is possible to obtain a reasonable approximation to the structural response of the system.

A 2D finite-element solution made with the HONDO[7] computer code was used in the present study to predict the cask response. HONDO is a large displacement dynamic finite-element program which uses a finite difference technique to solve the equations of motion in time steps. An analysis of this type was done by Dennis[8] before we ran the full-scale test. In that work Dennis concluded that the under frame would buckle before the cask was seriously deformed, but because of mathematical instabilities occurring at large element deformations, the analysis could not be carried out very far. Since then, the HONDO code has been modified to include a 4-point Gauss integration technique as an option. This modification adds more stability to the finite element calculations, and large-deformation solutions can be carried out further. The problem has been independently redone using the HONDO code. This section describes the finite element modeling that was done for this independent formulation.

For a better understanding of the assumptions, we will review the construction of the front part of the underframe in more detail. As discussed previously, the underframe consists of two large I-beams covered with a 1.9-cm (0.75-in.)-steel plate on the front end. The I-beams also have stiffening plates under the bottom flange. These features can readily be seen in Figure 3, a schematic of the underframe front-end view. The width of the underframe measured from the outside edges of the I-beam flanges is 188 cm (74-in.). The area under the I-beams, called the coupler housing, is not significant to the problem except that in this analysis it is used as vertical support for the upper portion of the underframe. In the actual locomotive, the top of the I-beams is covered with steel plating 0.5 cm (0.187 in.) thick and skip welded to the structure. The underframe, with a width of 188 cm (74 in.), impacts only the central portion of the cask, which has an overall length of 406 cm (160 in.).

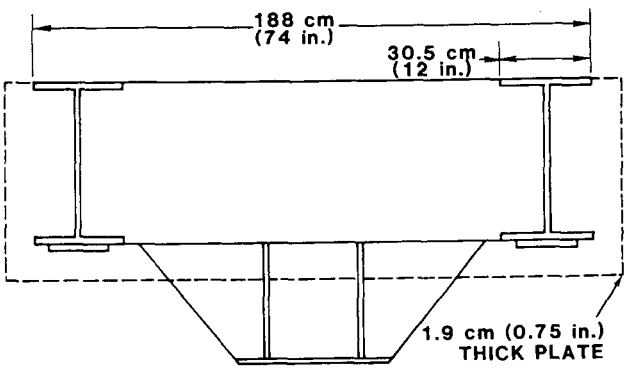

Figure 3. Schematic of the Locomotive Underframe

The first step in the analysis was to determine whether the cask could be bowed by the impact; that is, whether the cask would tend to wrap itself around the underframe. By using simple hand calculations based on the estimated yield strength of the underframe, we determined that the underframe could not deliver enough force to bend the cask body. This meant that damage to the cask would be limited to where contact occurs between cask and underframe. A HONDO finite-element model was then constructed to estimate the deformation response of the cask.

Figure 4 schematically illustrates the 2D plane strain model constructed to analyze this problem. (Appendix A is a detailed description of the model). Because the model is 2D, the I-beam flanges are assumed solid through the width of the locomotive frame as indicated in this figure, resulting in some conservatism. The model was constructed on the basis of the width of the underframe; therefore, to give the cask the proper inertia, the lead material was made artificially heavy. The calculated lead density to achieve this was 2.88 x 104 kg/m^3 (1.04 lb/in.^{3}). The total weight of the locomotive was taken as 113.6 metric tons (250,000 lb). Because the plane strain calculation is done on the basis of a unit thickness, the density used for the locomotive mass was based on the width of the under frame and the area allotted to the locomotive mass in the model (Figure 4). The material density calculated for the locomotive mass was 1.245 $\times$ 105 kg/m^3 (4.5 lb/in.^{3}). A very high stiffness was also assigned to this material. The I-beam web material properties were calculated by determining that frontal area of the webs represented 1.35% of the area. Based on this, the yield strength of the material was set at 0.0135 times the yield strength of the mild steel. The modulus for the web area was calculated by using this same ratio. This material was

also given a very low Poisson's ratio to simulate a buckling or crushing behavior, which would be the failure mode for a relatively thin web. The rationale for spreading the web loading across the entire width of the underframe was that the 1.9 cm (0.75 in.)-thick plate at the front would serve as a load spreader.

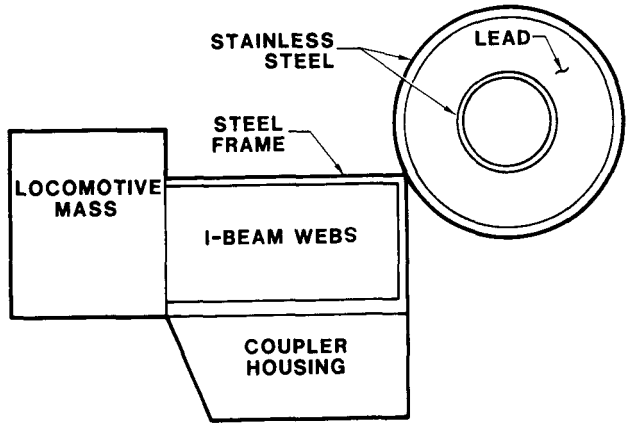

Figure 4. Geometry of the Finite-Element Model

Figure 5 illustrates the finite-element mesh for the model generated with the program QMESH.[9] The locomotive portion was given an initial velocity of 129 km/h (80 mph) in the direction of the stationary cask. The underframe was supported in the vertical direction as shown in Figure 5. This is conservative, because the underframe will deflect downward less than is possible in the real structure. This boundary condition was imposed because the bending stiffness of the underframe could not be modeled very accurately, and a choice was therefore made to use this conservative assumption. The area representing the coupler housing was given the same material properties as the I-beam web material.

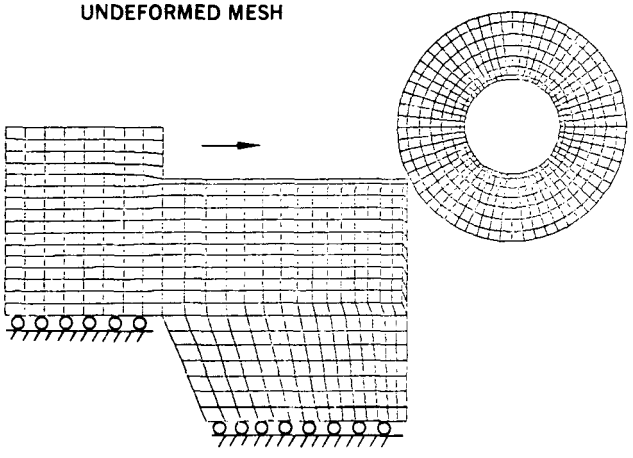

Figure 5. The Finite-Element Mesh

Cask cooling fins are very significant in terms of energy absorption and cask deformation. This is especially true of this design because the fins were designed quite large and closely spaced. On this cask, the fins were 7.30 cm (2.875 in.) deep, 0.71 cm (0.28 in.) thick, and along the impact portion of the cask they were placed at 3.8 cm (1.5 in) centers. Adding (smearing) the fin area to the shell thickness resulted in an addition of 1.63 cm (0.644 in) to the 2.54 cm (1 in.)-thick basic shell. In the finite-element model, the shell thickness was assumed to be 3.81 cm (1.5 in.). Thus the fin material was smeared to the basic shell, with some reduction in thickness for an added conservatism. This assumption is conservative not only because the area has been reduced, but also because the effective bending stiffness (directly proportional to the moment of inertia) of the entire shell section is greatly reduced by assuming that the fin area is smeared onto the basic shell.

Results

The results are discussed in terms of the deformations calculated for the cask under the assumptions previously described.

Figure 6 illustrates the results from the HONDO calculations for a 129 km/h (80 mph) impact. This figure indicates separate times in the same finite-element solution measured from the time of contact. As illustrated here, at 153 ms, the calculations indicated that the cask had significantly crushed the corner of the underframe, while sustaining only a relatively mild deformation (there is a slight ovaling of the inner cavity). Proceeding with the calculations to 300 ms produced the results shown at the bottom of the figure. Here the cask has almost separated from the underframe and has sustained its maximum deformations. These results indicated that the inner cross sectional area was reduced by 5%.

To test the solution sensitivity to the web stiffness, the stiffness was doubled in a later run. This change made only a very minor difference in cask deformation.

Discussion

The finite-element analysis indicated that in the worst case the cask would sustain a deformation that reduces the inner cross-sectional area of the cask by 5% in the area of impact. If the underframe impacts only about half the cask length, and if the cross-sectional area is reduced by about 5% in this area, in the worst case the interior volume of the cask might be reduced by about 2-1/2%. Because water-filled casks are normally shipped with a void volume of about

10%, this amount of deformation should not cause over-pressurization possibly leading to cask failure. Failure by other mechanisms also appears very unlikely.

The analysis presented above is very conservative for the following reasons. In reality, the front end of the underframe deflects downward when the cask impact occurs (the impact is off-center). This downward deflection of the underframe results in a less damaging condition to the cask. Also, the assumption that the I-beam flanges are solid through the underframe thickness gives the frame much added stiffness. Further, the assumption that the fin area is smeared on the outer shell makes the shell more susceptible to bending or denting. The analytical analysis presented above is then considered to be quite conservative. However, even with these conservatisms, the analysis indicates that the cask will not be breached by the impact.

Scale Model Test

Introduction

As in the studies of References 2 and 3, scale models were designed and tested before conducting the full-scale test. A discussion of modeling theory is included in Reference 2. Only a very brief discussion of physical scale modeling and a description of the models and test results are presented here. The models discussed in this section were designed by A. W. Dennis, H. R. Yoshimura, and D. R. Stenberg. They included a model cask, trailer, tiedowns, and locomotive. Construction details for these are included in Appendix B.

The philosophy adopted in the design of the models was to construct what is usually termed an "adequate model." This means that the model is simplified compared to the prototype; only the structural features pertinent to the problem are included in detail. For this study, the front end of the locomotive underframe as well as the shipping cask were modeled in considerable detail. Other parts of the structure were modeled with less detail; for example, only a rough approximation of the trailer structure with ballast on the end to simulate the mass of the tractor was used for the tractor-trailer model. These simplifications were based on engineering judgments and the earlier work of Dennis,[4] which indicated that the pertinent parameters were the stiffness of the locomotive underframe, the mass of the locomotive and the construction details of the cask. The models were constructed to one-eighth scale and were designed to run on a sled track.

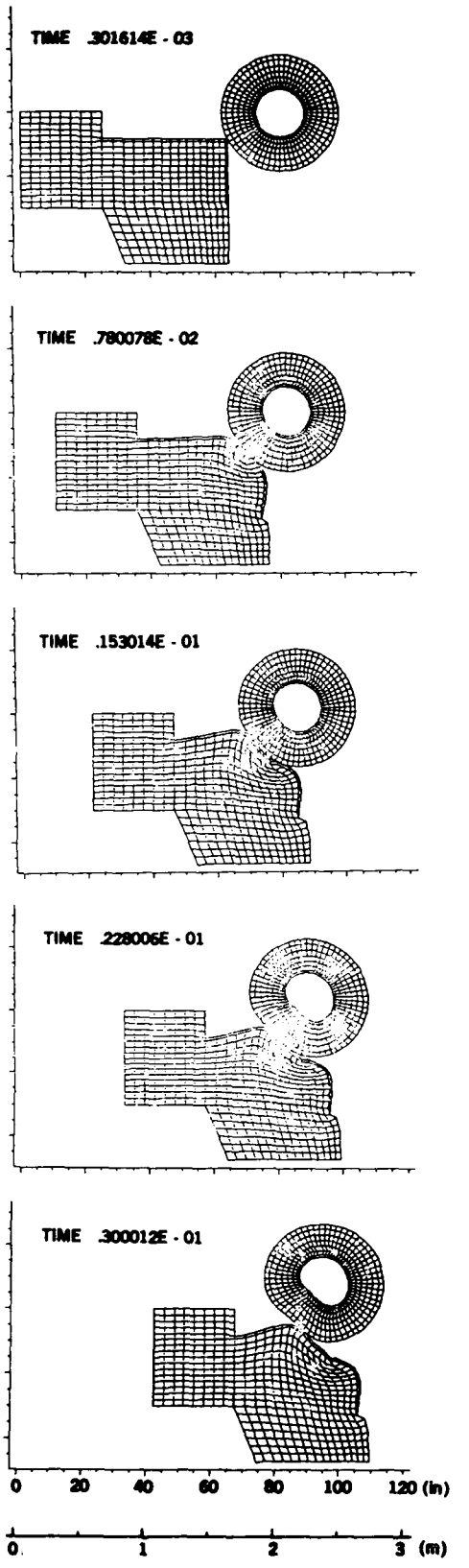

Figure 6. Deformed Finite-Element Mesh for Different Times in the Impact

Figure 7 is a photograph of the cask model. Much detail was included in this model to obtain as accurate a response as possible. The model included detailed inner and outer stainless-steel shells, the external fins, and the head and bolting system. Lead was cast into the annular region between the shells as well as into the hollow volume in the head. The model weighed 50 kg (110 lb); it was attached to the model trailer with a scaled tie down system.

The locomotive model shown in Figures 8 and 9 was designed with a detailed front-end structure, where the impact would occur. The rest of the model was simplified with the total mass adjusted by means of steel plate ballast to scale correctly. The superstructure included a sheet-metal cover and simplified models of the alternator and engine as illustrated in Figure 8, which also shows the rail shoes that allowed the model to run on the track. Figure 10 illustrates the features of the front part of the underframe with the cab removed. The axial and cross I-beams were hand-constructed to very accurately model the full-scale units. The front plate that covers the ends of the axial I-beams was also very carefully modeled.

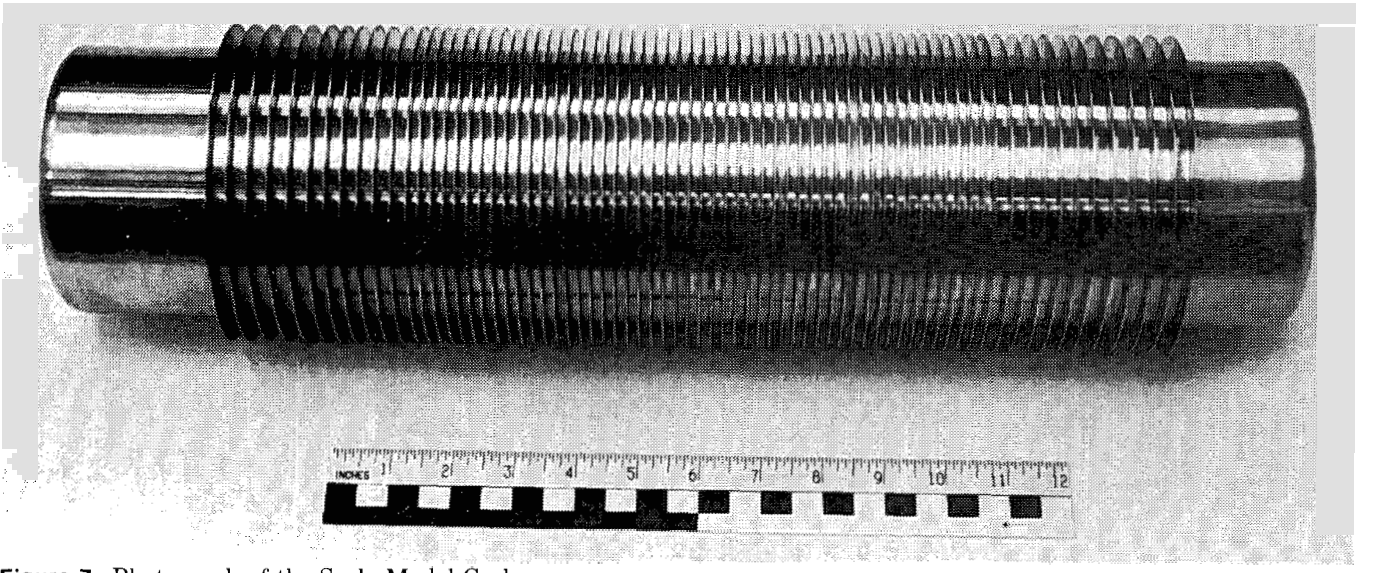

Figure 7. Photograph of the Scale-Model Cask

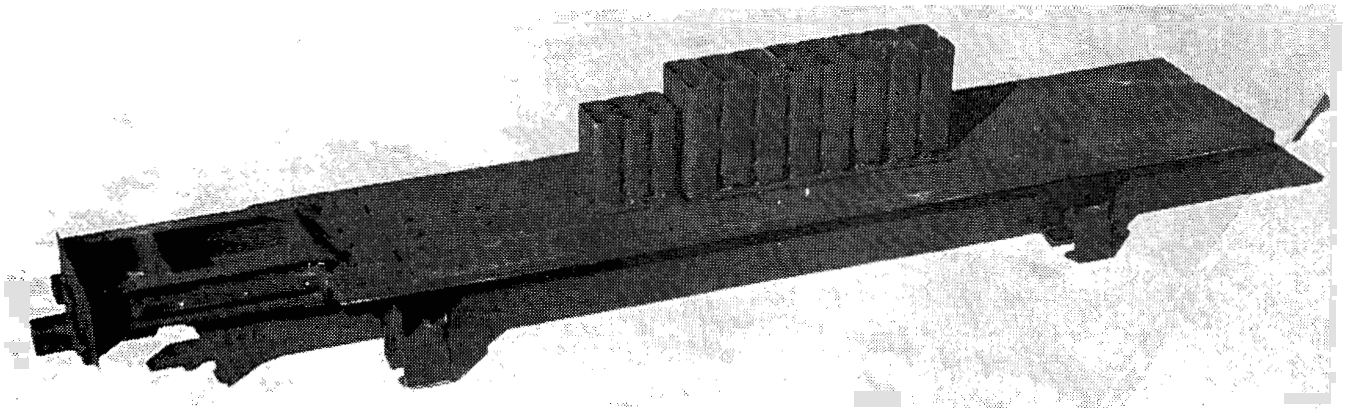

Figure 8. Photograph of the Scale-Model Locomotive With the Sheet-Metal Cover Removed

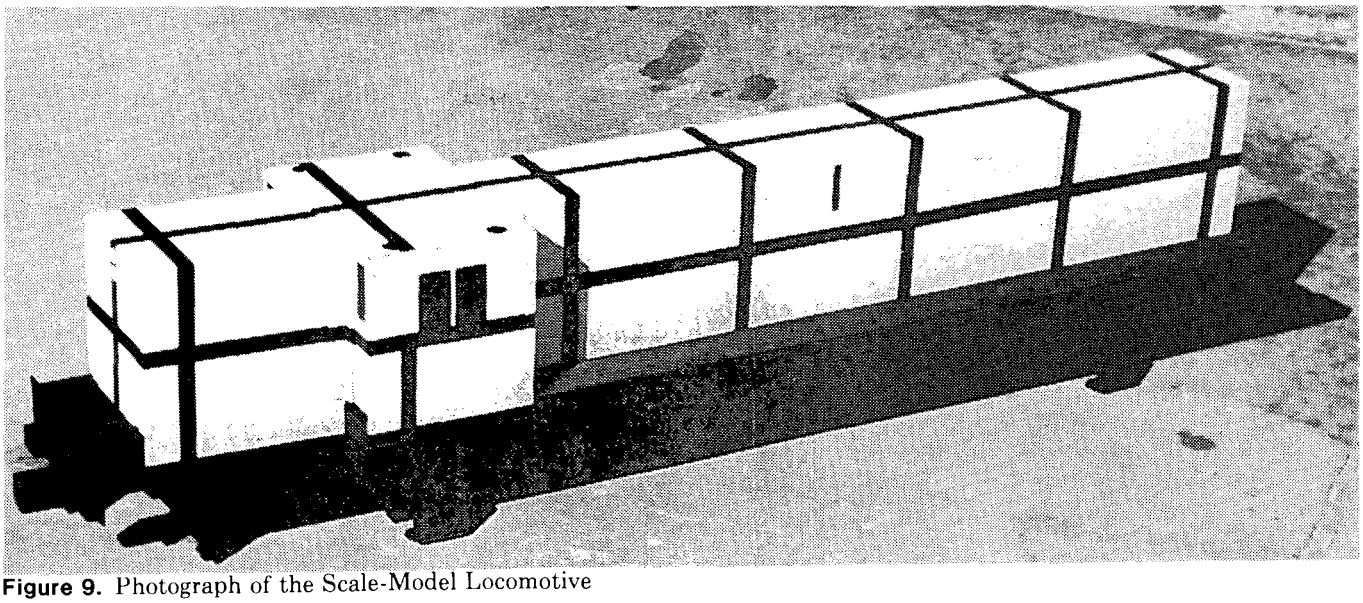

Figure 9. Photograph of the Scale-Model Locomotive

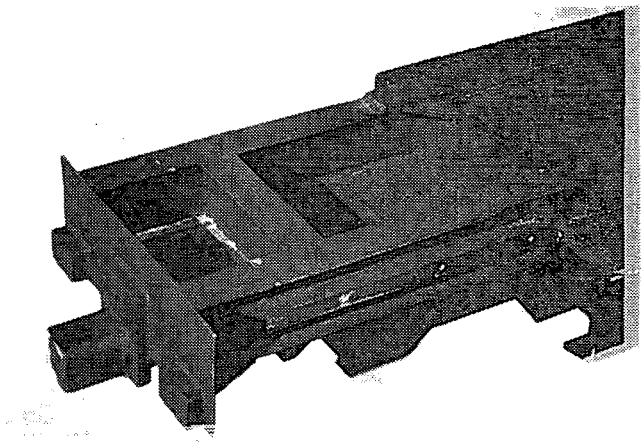

Figure 10. Closeup Photograph of the Model Locomotive Underframe

Figure 11 shows the models at the sled track and the elevation relationship between the cask and the locomotive underframe. Here the top of the locomotive underframe is 2.54 cm (1 in.) below the center line of the cask. This correctly modeled the full-scale test where it had been determined that the corresponding dimension would be 20.3 cm (8 in.). Using this geometric relationship, we accelerated the model locomotive up to speed by means of a small rocket motor and allowed it to coast into the cask at an impact of 130 km/h (80 mph).

Scale-Model Test Results

The scale-model test was successful achieving an impact velocity of 126 km/h (78 mph). (Film test data are included in Appendix C). The system response was about as expected; the model trailer was quickly crushed and pushed under the cask without appreciable cask motion. The locomotive underframe then impacted the cask, causing the underframe I-beams to buckle.

The underframe gave local deformations to the cooling fins and the outer shell of the cask. The underframe impact also caused the cask to rotate and then roll up into the sheet-metal superstructure of the locomotive crushing it back about 30.5 cm (12 in.). Figure 12 illustrates the locomotive underframe and superstructure after impact. The rounded deformation left by the cask in the superstructure is clearly seen. Note that the cask cleanly stripped the superstructure from the frame. The rounded superstructure indentation also indicates that the cask did not elevate very much as it rolled over the underframe. The top 2.54 cm (1 in.) of the front bumper plate was bent back through an angle of about 50° from vertical (Figure 12).

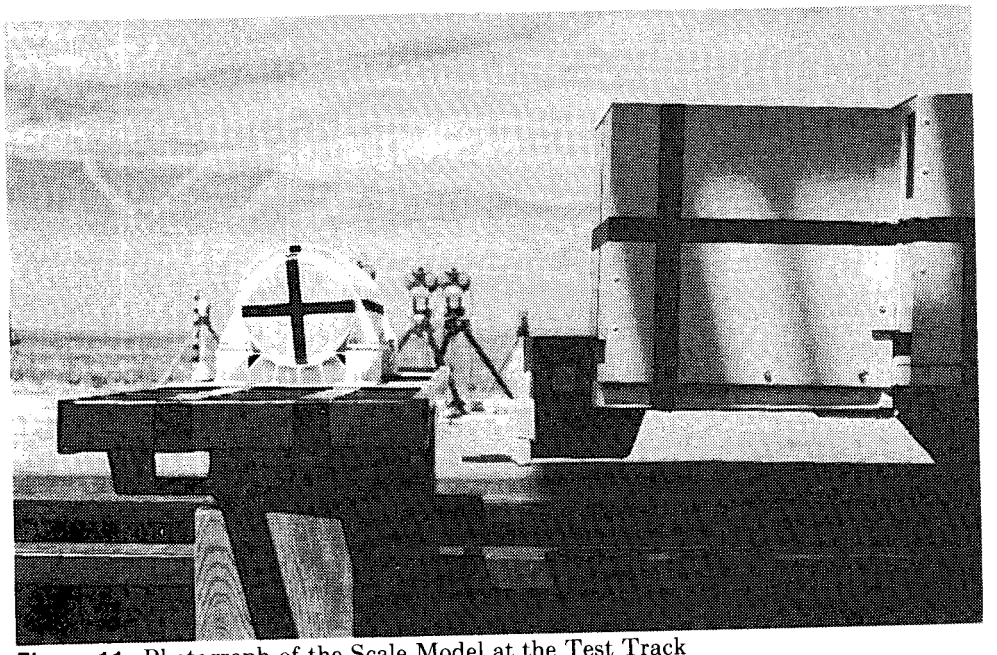

Figure 11. Photograph of the Scale Model at the Test Track

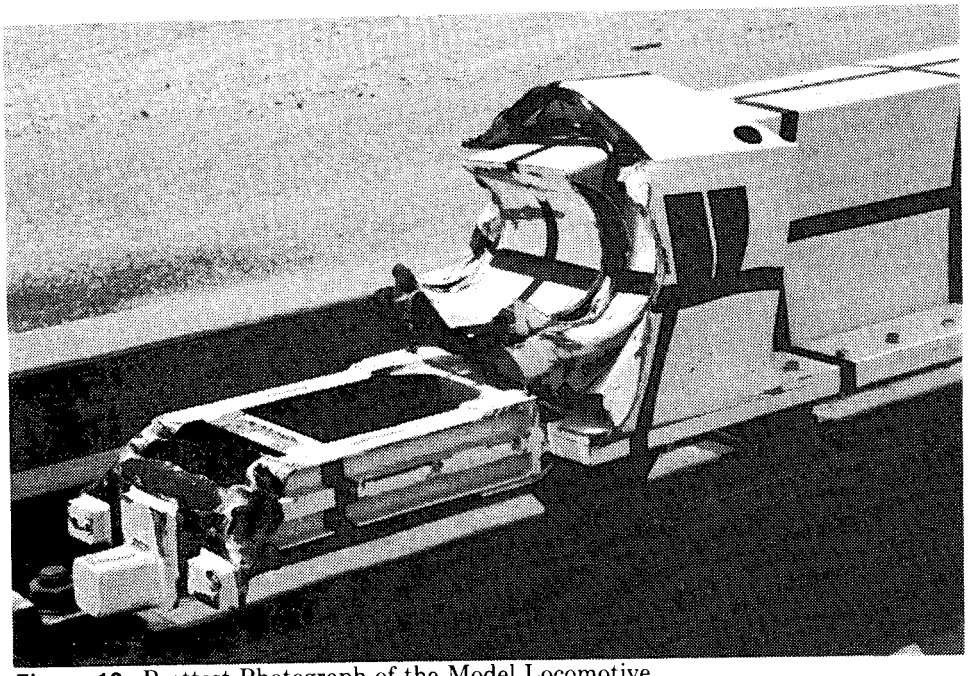

Figure 12. Posttest Photograph of the Model Locomotive

Figure 13 shows the cask after impact. The local indentations and crushed fins coincided with the underframe axial members. Measurements on the cask indicated that the indentations to the outer shell averaged between left and right were 0.254 cm (0.1 in.) at their deepest point. The left indentation was about 10% deeper. Measurements made of the inside diameter of the cask indicated that it was not distorted at any point. The cask head remained firmly in place. Figures C-1 through C-5 of Appendix C illustrate data obtained from the high-speed films. Included are the velocity-time curve for the locomotive, displacement-time and velocity-time curves for the cask, and a plot of the cask rotation about its own axis (as viewed from one end) vs time.

Discussion

The data indicate that the locomotive slows down considerably during impact and that a maximum horizontal velocity of about 97 km/h (60 mph) is imparted to the cask. The data also indicate that the vertical displacement and vertical velocity imparted to the cask were quite small. Thus, the plot for the total cask velocity as a function of time is almost identical to the plot of the horizontal cask velocity vs time. The scale-model data predicted that the cask will obtain its maximum horizontal velocity in about 0.055 s, which corresponds to 0.44 s for the prototype, since events occur faster in the model by the scale factor. At this time (0.055 s) the cask's horizontal displacement was about 1 m (39.4 in.).

The plot of cask rotation vs time (Figure C-5) indicates that the off-center blow caused the cask to spin at a high rate. The value of angular velocity corresponds to the slope of the curve in Figure C-5. The cask spin reached its maximum value of about 1300 rpm at about 0.006 s.

In summary, the scale-model test indicated that an impact of 130 km/h (80 mph) between a moving locomotive and a stalled shipping system results in some localized external deformation to the shipping cask but does not impair its containment ability. The test indicated that the interior cavity of the cask would not be distorted. It also indicated that extensive damage would occur to the locomotive and that the impact would buckle the locomotive underframe creating a ramp that would allow the cask to move up into the superstructure.

Full-Scale Test

The full-scale test was run at a Sandia National Laboratories' track facility in Albuquerque, NM. The test scenario described previously was successfully accomplished. Six large rocket motors accelerated the locomotive to speed impacting it into the tractor-trailer system at 130 km/h (81 mph). This section describes the hardware and instrumentation that were used, and the response of the system.

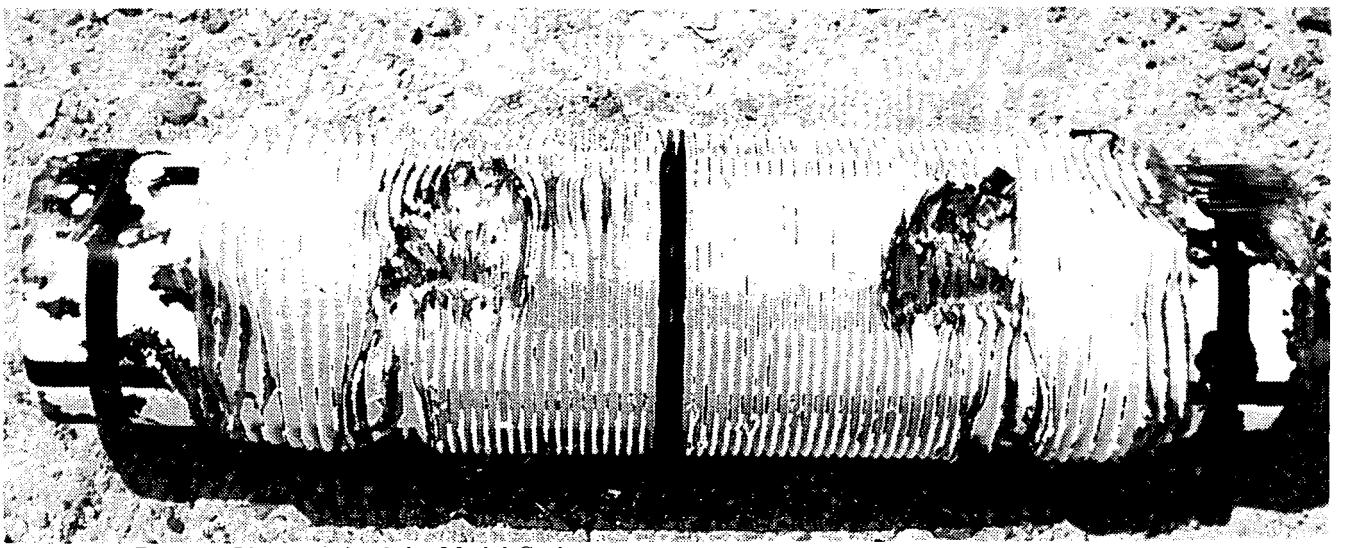

Figure 13. Posttest Photograph of the Model Cask

Test Hardware and Instrumentation

Figure 14 shows the cask and tractor-trailer system in the test orientation at the track facility, with the cask centered directly over and perpendicular to the tracks. Its elevation was determined by the standard trailer height and the 5% grade on both sides of the track. The box adjacent to the cask head housed the telemetry package used for data transmission. The trailer and tiedowns were those that were used while the system was in service. The trailer was attached to a gasoline tractor obtained for use on this test.

Figure 15 shows the locomotive used in the test. Its basic frame construction has been described previously. Figure 16, a schematic of a lengthwise section of the locomotive, provides some information on the superstructure. The superstructure near the front end contains miscellaneous pieces of hardware, cabinets, and control panels. The significant superstructure items include the alternator and the engine, which are located behind the engineer's cab with some space allowed between as indicated in Figure 16. The impact relationship between the locomotive and the shipping system is seen in Figure 17 which is a photograph of the locomotive pushed up against the trailer.

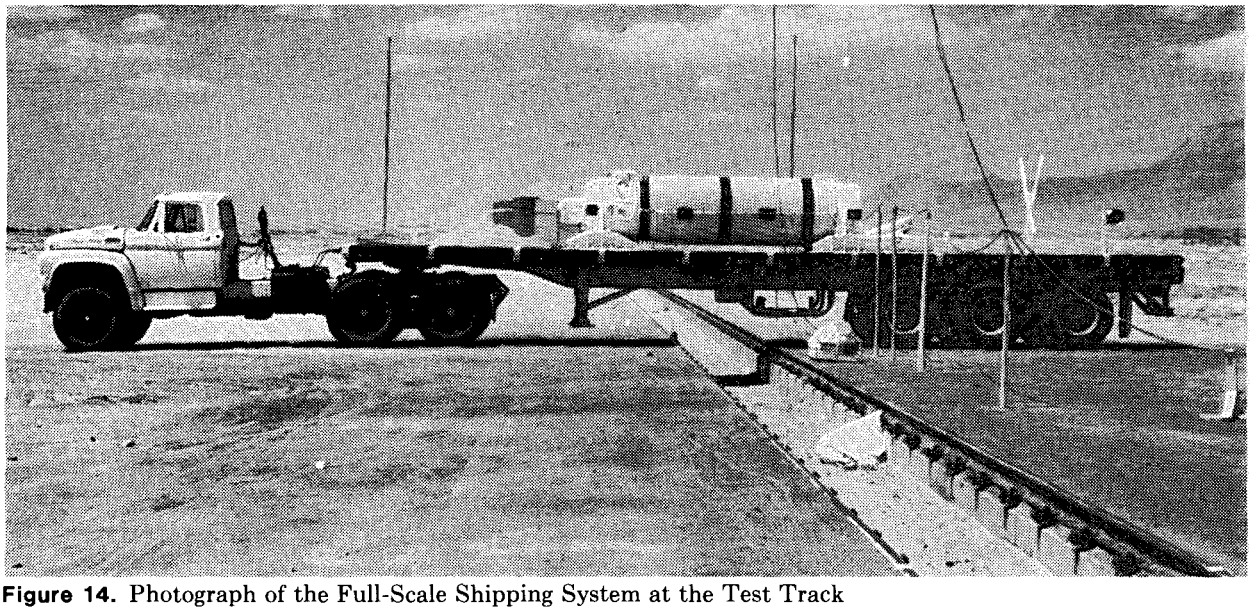

Figure 14. Photograph of the Full-Scale Shipping System at the Test Track

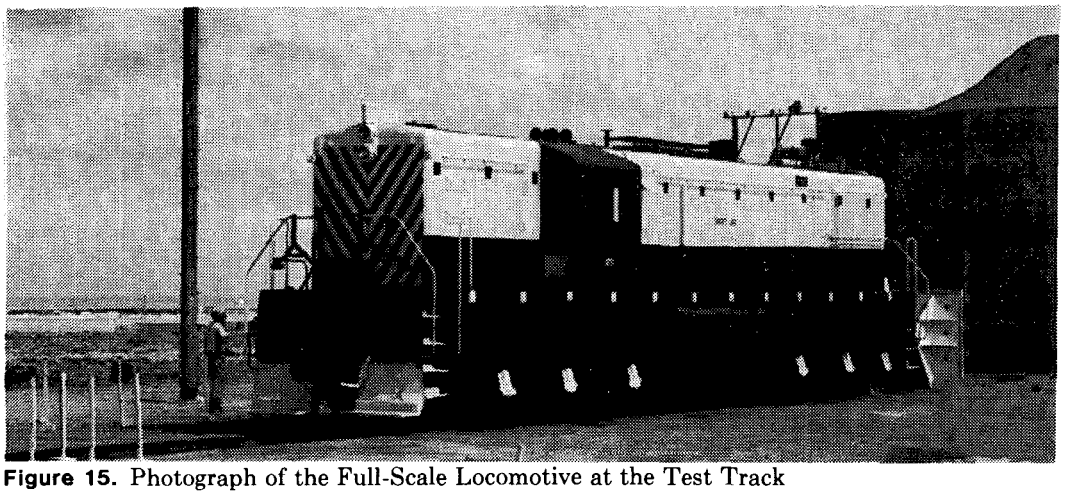

Figure 15. Photograph of the Full-Scale Locomotive at the Test Track

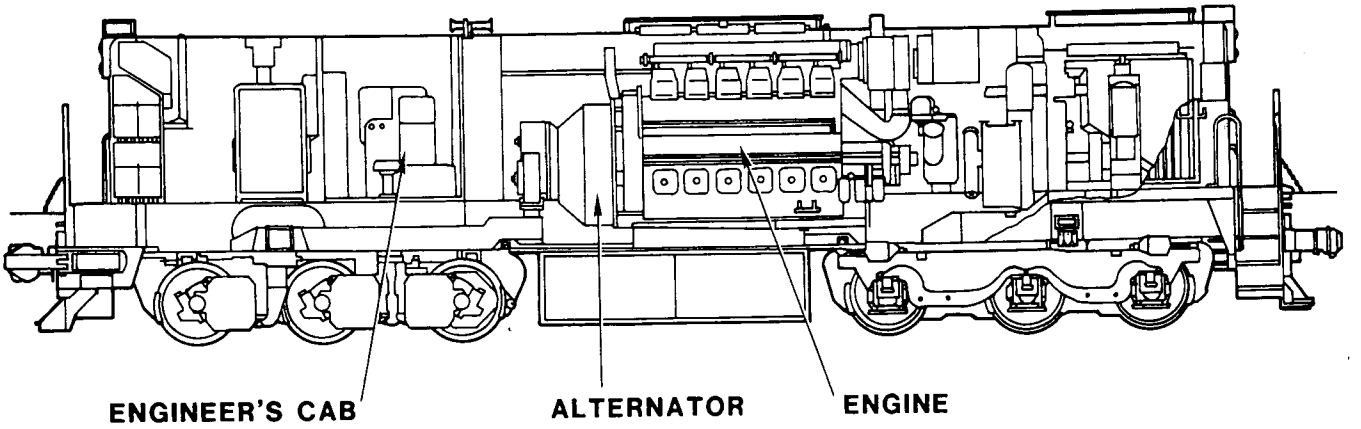

Figure 16. Schematic of Locomotive Cross Section

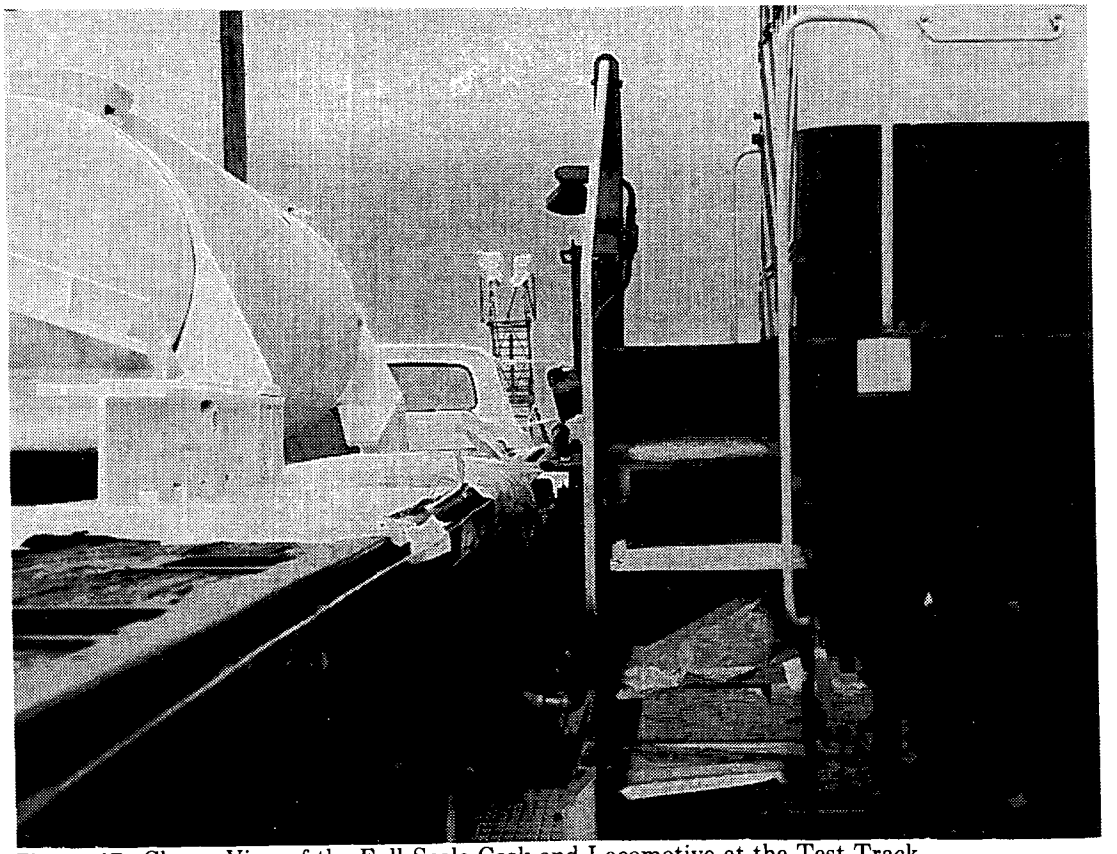

Figure 17. Closup View of the Full-Scale Cask and Locomotive at the Test Track

This full-scale hardware was monitored by 18 high-speed (framing rates of 400 to 2500 fps) cameras placed at different locations. In addition to the high-speed photography, the response of the cask was monitored by strain gages and accelerometers. A series of seven strain gages for reading axial strain were placed on the cask opposite the impact side. Four piezoresistive accelerometers were also located on the cask; these were placed on the back side of the cask with one centered directly opposite the impact and one centered on the top side of the cask. The other two were near the ends of the cask opposite the impact side. The accelerometers were uniaxial and were aligned horizontally in the direction of the locomotive motion. The locomotive was instrumented with an accelerometer on the frame 1.8 m (6 ft) from the front end; this accelerometer operated through its own telemetry pack. Aside from the telemetry systems, quantitative data were obtained from the high-speed films by means of a film analyzer that produced digitized data of the cask and locomotive motions. Data acquired from the full-scale test are included in Appendix D.

System Response

The system response is described with reference to a time frame where zero time is the instant when the front end of the locomotive contacts the side of the trailer. The right and left sides are as viewed from a position on the locomotive looking forward.

The general response was as follows:

1. The locomotive crushed and pushed the trailer structure under the cask; the cask remained stationary.
2. The underframe impacted the side of the cask at 30 ms, imparting a spin to it and two indentations to the outer shell. The locomotive underframe I-beams were buckled and the front plate severely bent backwards.
3. The cask impacted the superstructure 50 ms after the initial contact. The front cask-trailer tiedown broke at 60 ms; the rear one broke at 80 ms.
4. The cask plowed through about 3 m (10 ft) of the superstructure while spinning. It remained fairly perpendicular to the locomotive through the first 250 ms and then started rotating clockwise as viewed from the top.
5. The trailer completely wrapped itself around the locomotive by 250 ms.
6. The cask remained with the locomotive through the first 600 ms, then continued moving upward to a height several feet above the locomotive. It fell on the right side of the tracks in close to an end-on condition, hitting the ground at about 1.7 s. It first hit the ground about 46 m (150 ft) from the impact point. It then tumbled an additional 15 m (50 ft) before coming to rest in the middle of the tracks. (Figure D-18, in Appendix D, indicates the location of the hardware after the test.)

The impact can best be described by using series of photographs from the high-speed films. Views from both sides and from above are used. Figures 18 and 19 illustrate the view from the right from the instant of impact through 850 ms (at regular intervals through 180 ms and then skipping to a shot at 850 ms). The trailer-tractor connection was broken very early but the tractor remained almost undisturbed. At 180 ms the trailer almost completely wrapped itself around the locomotive, and the cask was hidden in the debris (Figure 19). Figures 20 and 21 show the view from the left. In this series, the cask remains visible longer and its motion into the superstructure can be better observed. The way in which the trailer wrapped itself around the locomotive can be clearly observed. Figure 22 shows two photographs taken from the overhead camera. This camera view revealed how the trailer structure was pushed out from under the cask while playing a relatively minor role in the impact of the cask with the underframe. Figure 23 shows two photographs also taken from above but slightly later: these indicate that at 250 ms the cask was well into the superstructure and had begun to rotate clockwise.

(a)

(b)

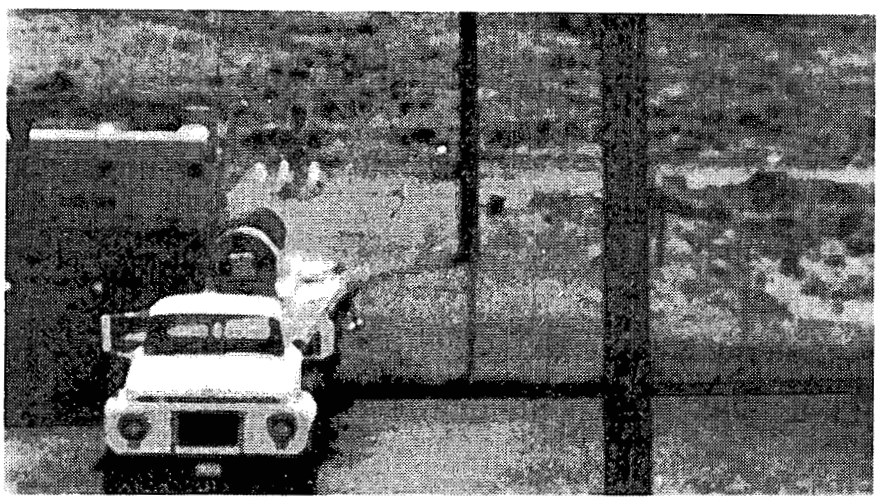

(c)

Figure 18. Right-Side View of the Full-Scale Test to 100 ms

(a)

(b)

(c)

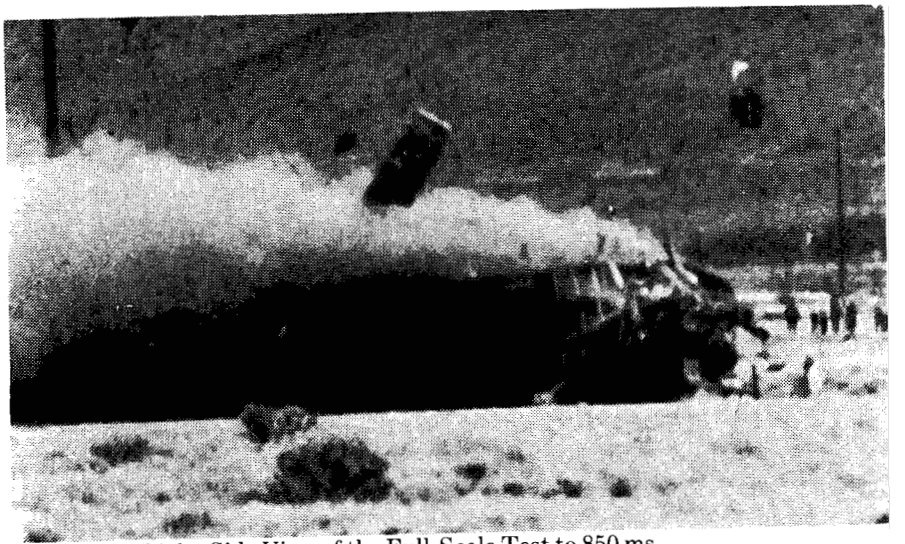

Figure 19. Right-Side View of the Full-Scale Test to 850 ms

(a)

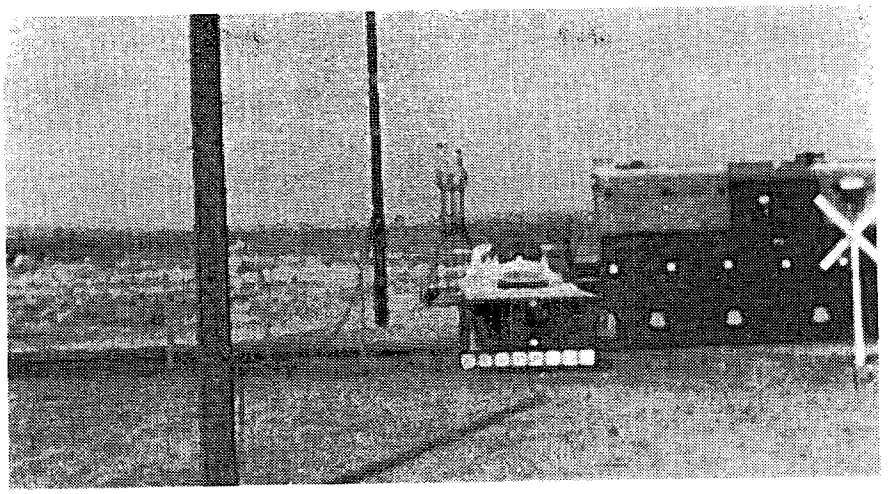

(b)

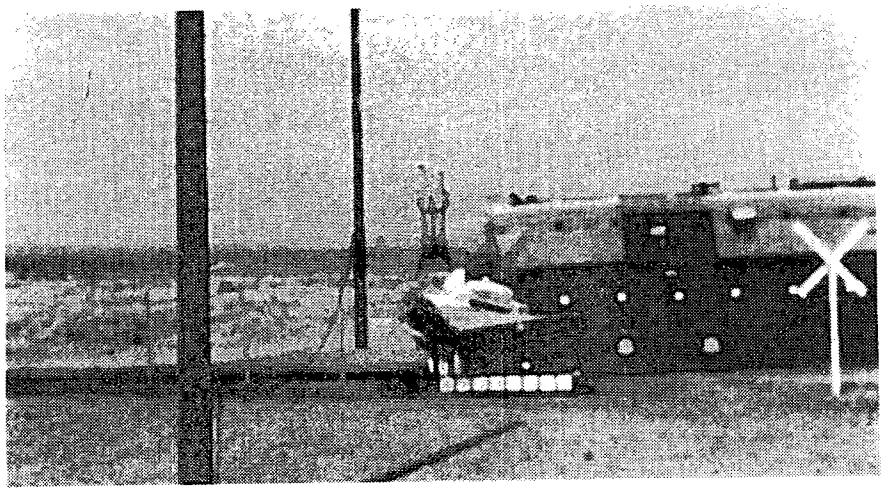

(c)

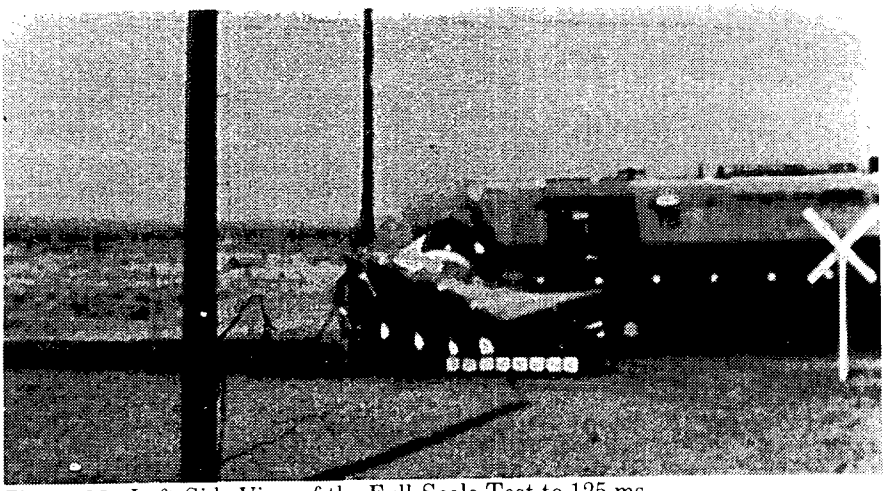

Figure 20. Left-Side View of the Full-Scale Test to 125 ms

(a)

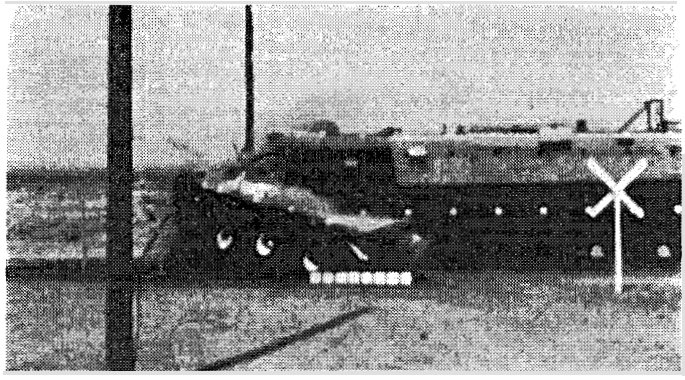

(b)

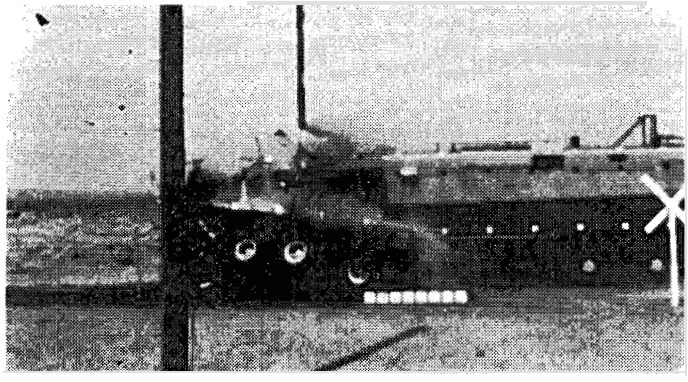

(c)

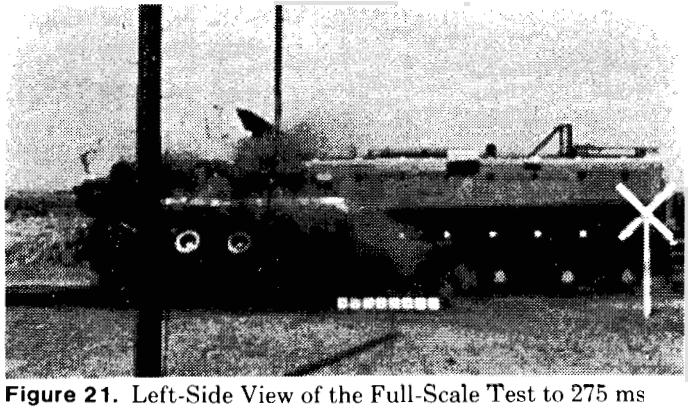

Figure 21. Left-Side View of the Full-Scale Test to 275 ms

(a)

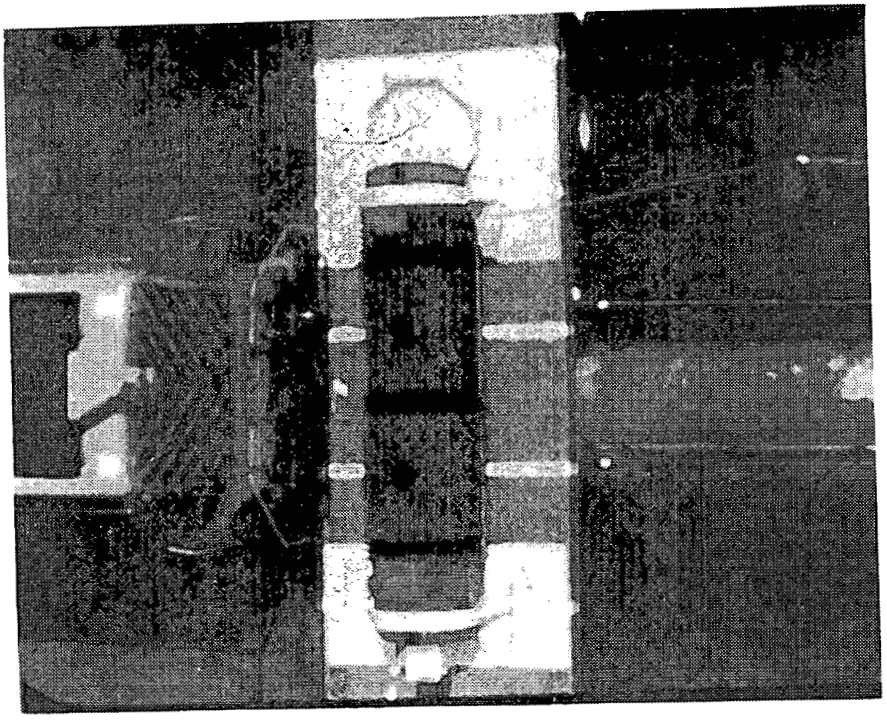

(b)

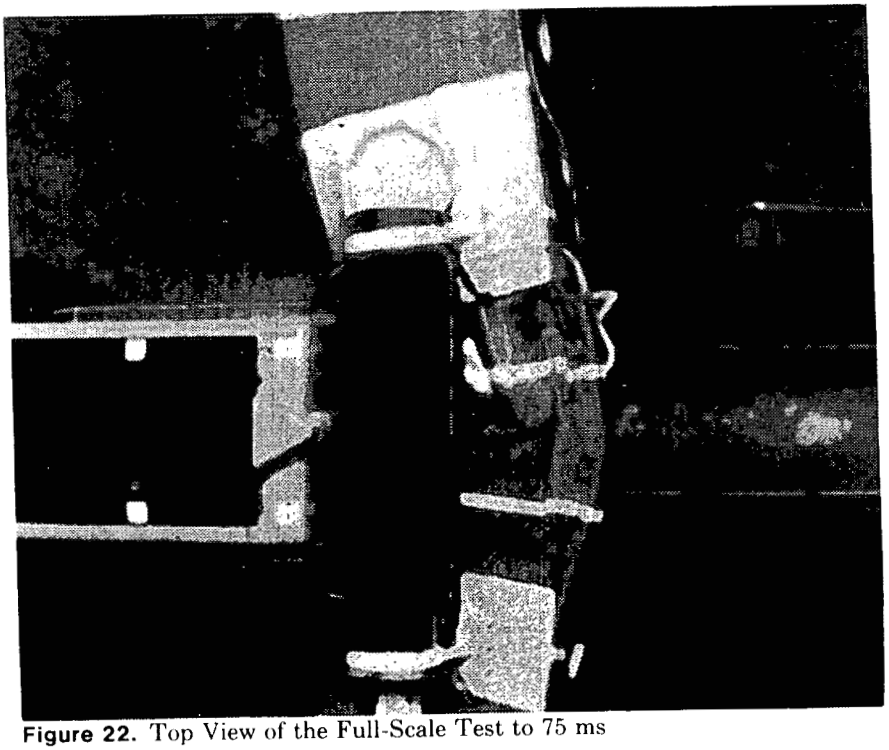

Figure 22. Top View of the Full-Scale Test to 75 ms

(a)

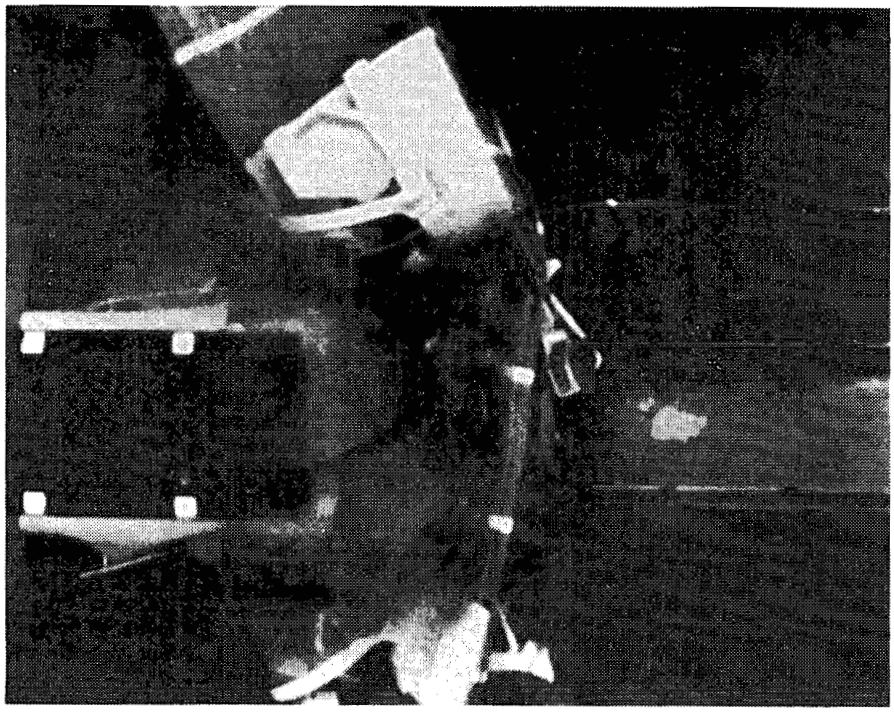

(b)

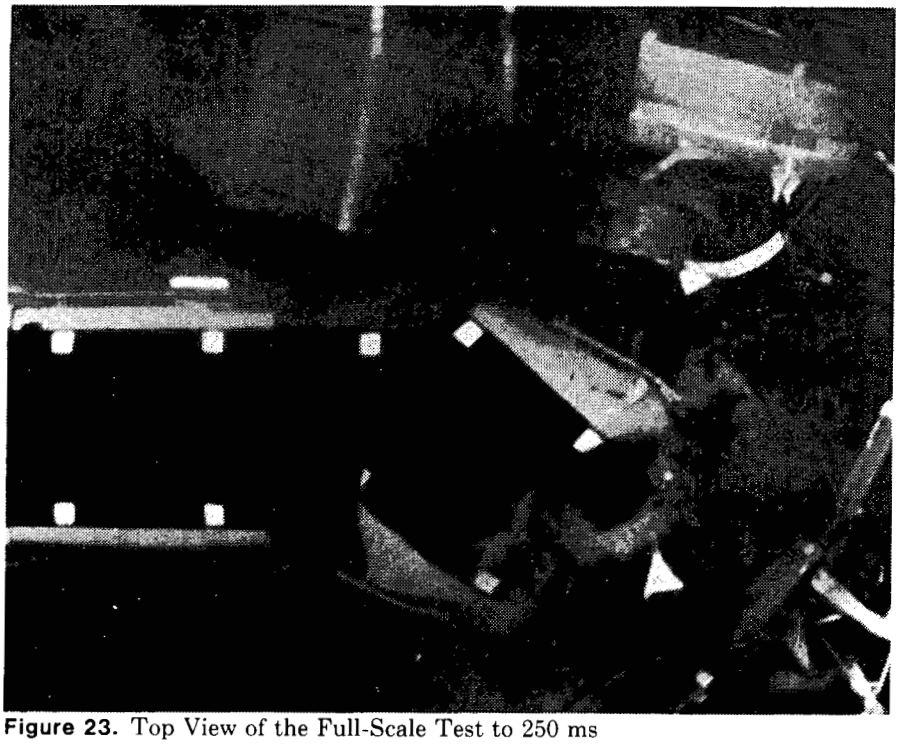

Figure 23. Top View of the Full-Scale Test to 250 ms

Film data for the cask and locomotive were obtained for the first 0.3 s of the impact. After this the structures became obscured by debris. The film data include displacement-time and velocity-time plots for the cask and locomotive, as well as a plot of cask rotation vs time. The cask-underframe impact gave a rotational velocity of about 150 rpm to the cask. (This value can be obtained by taking the slope of Figure D-7 at t = 0.0405). The impact caused the locomotive to pitch very little (3°) downward, although the front end pitched more. The downward force imparted to the locomotive by the cask caused the track rails to bow slightly at the point of impact, but the locomotive remained on the track. The cask attained a total velocity (vector sum of vertical and horizontal) of about 80 km/h (50 mph). Its velocity direction was nearly horizontal. (Although the cask moved vertically, the vertical component was small compared to the horizontal.)

Appendix D also includes some accelerometer and strain-gage data. Only two accelerometers produced credible traces. The center accelerometer directly opposite the impact point produced a peak reading of about 200 g's, and the accelerometer near the right end of the cask indicated a peak value of about 90 g's. These data were filtered to 800 Hz. Further filtering would bring down the peak values somewhat, but there would probably still be wide disagreement between the two readings. This is probably the result of local phenomena at the accelerometer installation points. Some doubt is also cast on the validity of these data because they were uniaxial accelerometers and the impact quickly imparted a high rate of spin to the cask, thus causing the instruments to be out of alignment. The strain-gage readings indicated that the cask tended to assume a bowed shape, with strains highest at the center and tapering off toward the ends. The peak strain reading produced was 100 x 10^{-6}, which is below the yield strain for the material.

Digitized film data for the cask motion were also used to obtain an estimate of what we will term the "rigid body" motion of the cask. This was done by following the central mark on the left end of the cask. This produced the g-time plot of Figure 24, which indicates a peak level of about 33 g's for the rigid body motion of the cask. Obtaining acceleration data from displacement film data is not an accurate procedure because successive differentiation is involved; however, the data of Figure 24 are presented as a rough approximation of the rigid-body acceleration of the cask. A check has been made by integrating this curve to see if the velocity change indicated by Figure D-4 is obtained for the time interval up to 0.10 s. The agreement was within 1%, and while this is not a positive check, it is a good indication that the data of Figure 24 are reasonable.

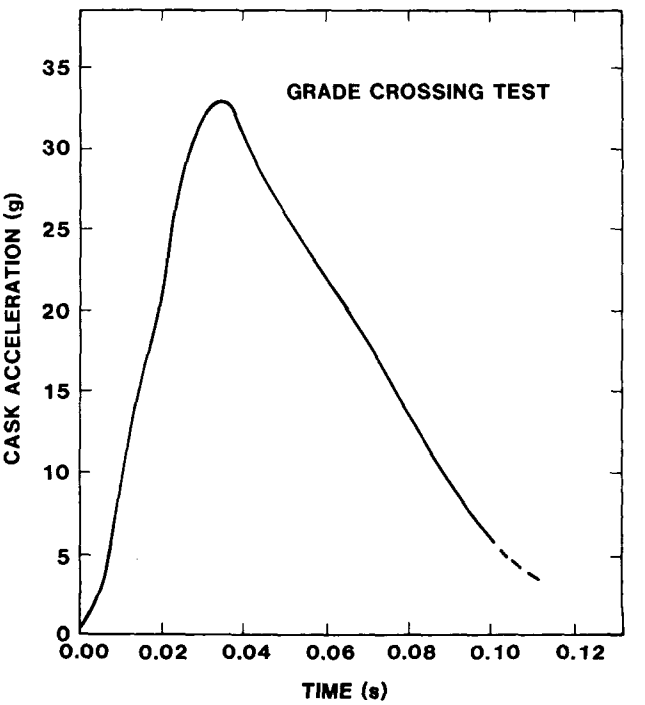

Figure 24. Acceleration-Time History for the Cask From Film Data

Figure 25 shows the condition of the cask after the impact; the impact produced two indentations at locations corresponding to the underframe I-beams. Here, the cooling fins were crushed and the outer cask shell was deflected inward. At their deepest points, the indentations averaged about 2.5 cm (1 in.) between the left and right side with the left side about 10% deeper. The I-beam flanges produced the deep portions of the dents. The inside diameter of the cask was measured at many locations from one end to the other. These measurements produced no indications of deformations to the inside cavity.

The fuel elements inside the cask were almost undamaged. Figure 26 is a photograph of the elements after removal from the cask. A visual inspection did not reveal any damage. Measurements on the fuel bundle indicated that the elements had bowed about 0.5 cm (0.2 in.) between the support points that existed at both ends and at the center. No fuel cladding was broken, and the support bracket was undamaged.

Figure 27, a side view of the locomotive after impact, shows severe damage to the front part of the superstructure. However, the deformation did not reach the hard components (alternator and engine). The cask crushed through the engineer's cab, leaving the rounded indentation in the superstructure seen in this figure. Figure 28 is an end view of the structure taken from an elevated height; this view clearly illustrates the wrapped-around condition of the trailer and extensive structural deformations. Figure 29 shows the condition of the impact end of the locomotive underframe. The buckled I-beam flange can clearly be seen just above the front plate. The manner in which the top of the front plate was severely bent back wards by the cask can also be clearly observed here. Measurements indicated that the top 7.5 in. of the front bumper plate were bent backwards through an angle of about 55°.

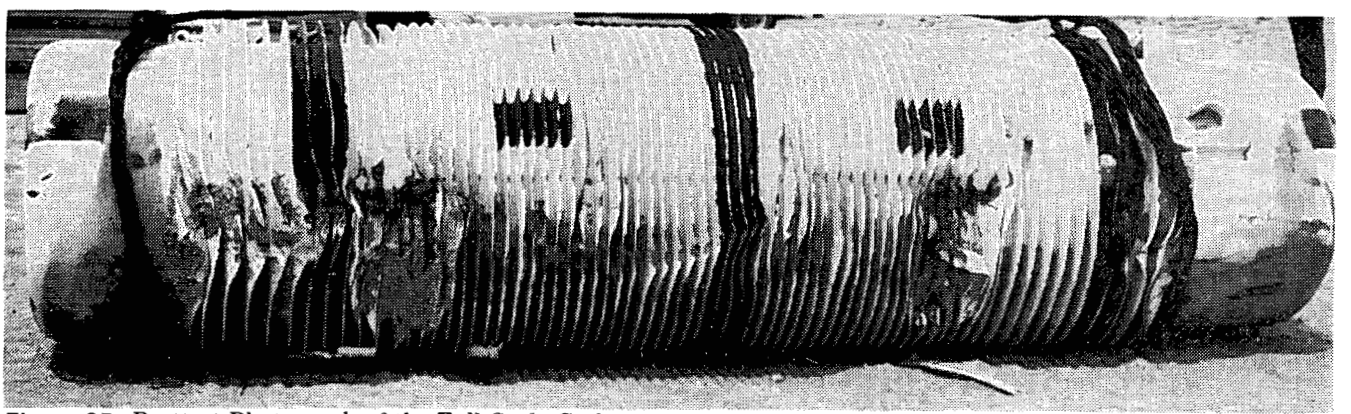

Figure 25. Posttest Photograph of the Full-Scale Cask

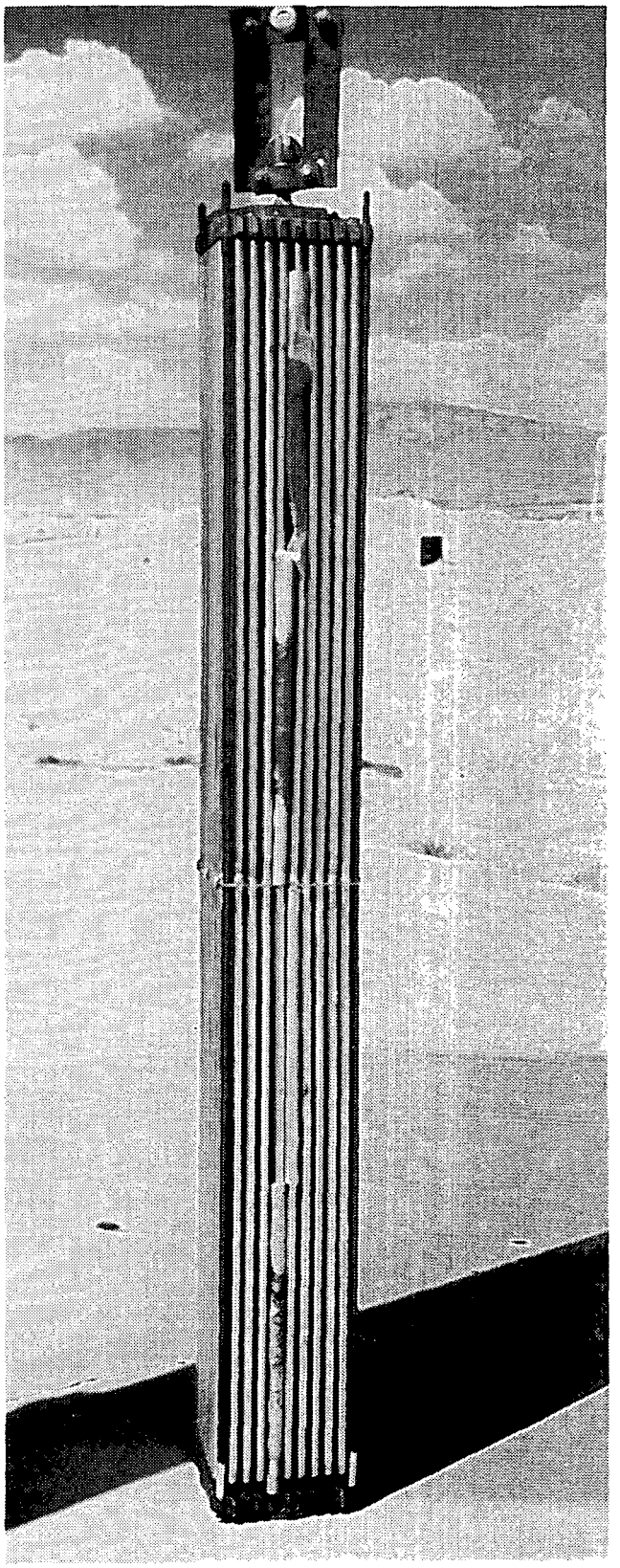

Figure 26. Posttest Photograph of the Fuel Bundle

Comparison of Analyses to the Results of the Full-Scale Test

The full scale test was analyzed by mathematical and physical scale modeling, both valuable analytical tools. This section discusses results obtained by both techniques in light of the observed results of the full-scale test. First, some comments about the mathematical analysis.

Mathematical Analysis

The mathematical analysis that used a very simplified 2D model produced conservative results when compared to results of the full-scale test. The deformations calculated with the finite-element model (Figure 6) are much more severe than those observed (Figure 25). The model did, however, indicate that the cask would not be breached by the impact. It also correctly predicted that the cask would buckle the corner of the underframe and the roll into the superstructure.

Scale Model

The scale model provided very detailed information on the response of the system. Before considering the results simply in terms of final damage to the cask, we will make a more detailed comparison by considering the cask's displacement and velocity after the impact. These comparisons are made first in terms of horizontal components and then in terms of vertical components. Final cask damage is then compared.

Figure 30 is a plot of horizontal cask displacement vs time both for the full-scale cask and the model. (To obtain a direct comparison for plotting against the prototype, we multiplied the model times and displacements by the scale factor of 8.) This plot indicates that the model predicted less cask displacement than was observed in the full-scale test, although again the agreement in early times (less than 0.06 s) is quite good. Figure 31 is a plot of the horizontal velocity of the cask as a function of time. This plot also shows good agreement in early time with the full-scale cask accelerating much quicker, but eventually leveling off in velocity.

In the vertical direction the full-scale cask exhibited much more displacement and velocity than in the model, although there was good agreement at early times. This comparison is seen in Figures 32 and 33.

At 300 ms, which is as far as the full-scale cask could be followed, the model predicted a vertical displacement that was about 60% low. The predicted vertical velocity was off by an even greater amount (Figure 33) at this same time in the impact.

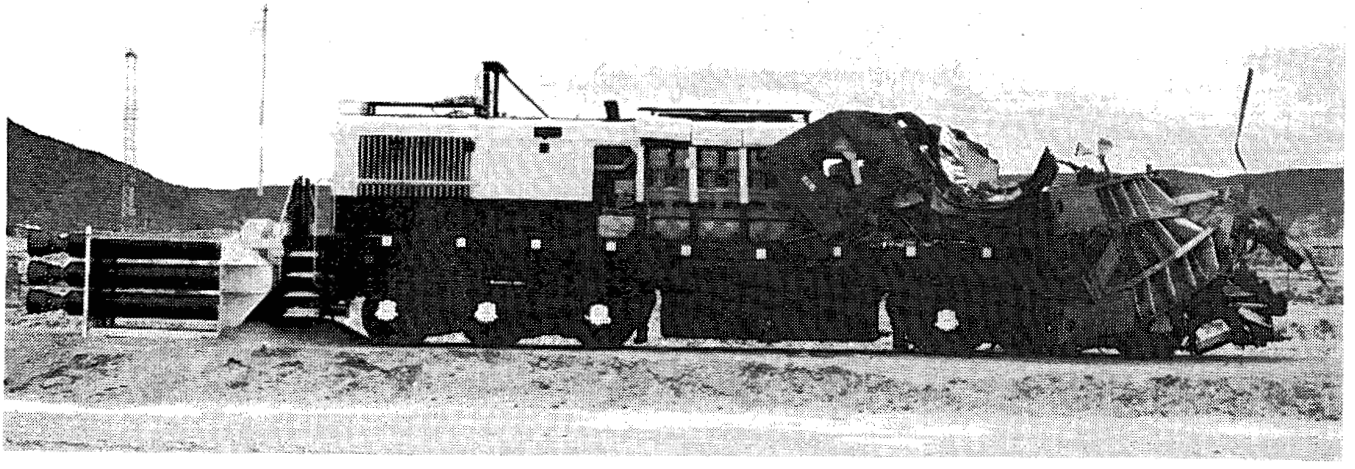

Figure 27. Posttest Side View of the Locomotive

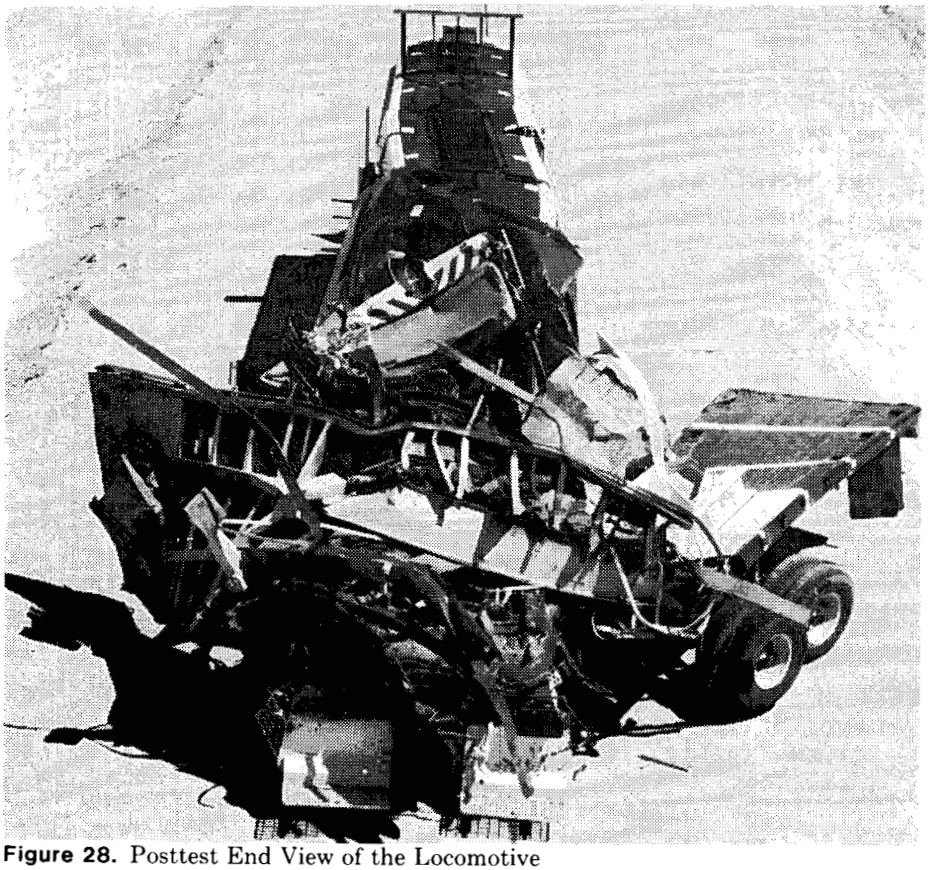

Figure 28. Posttest End View of the Locomotive

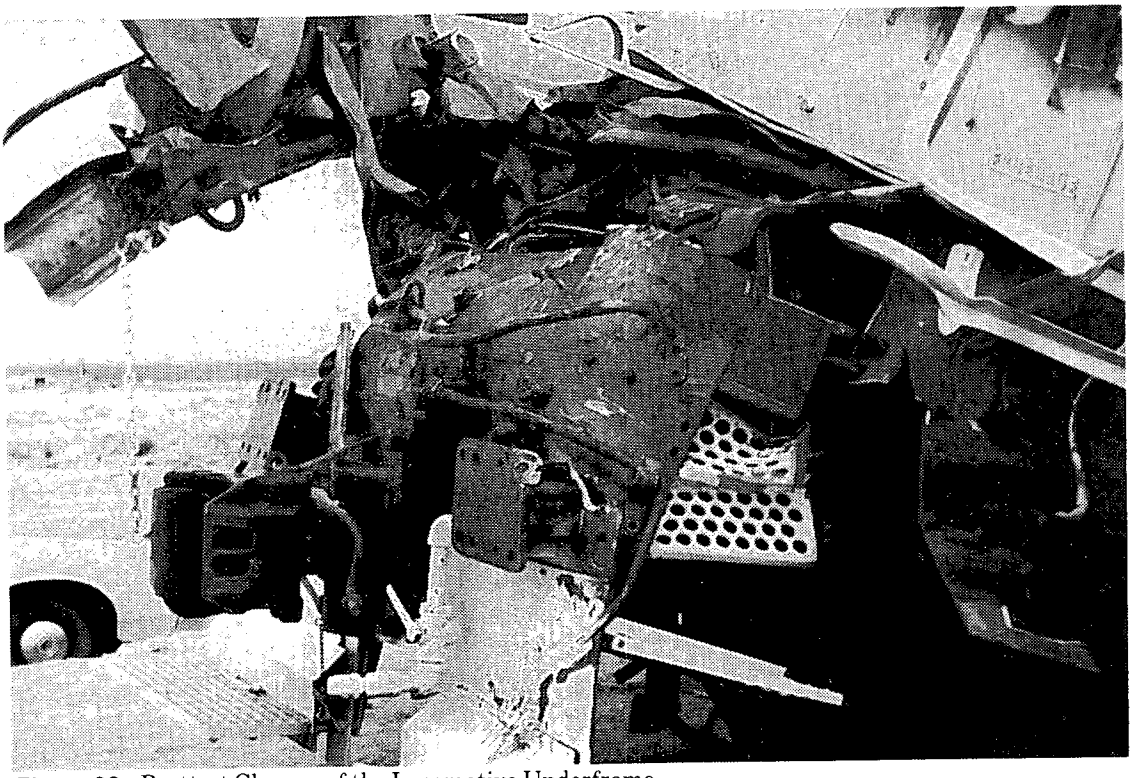

Figure 29. Posttest Closeup of the Locomotive Underframe

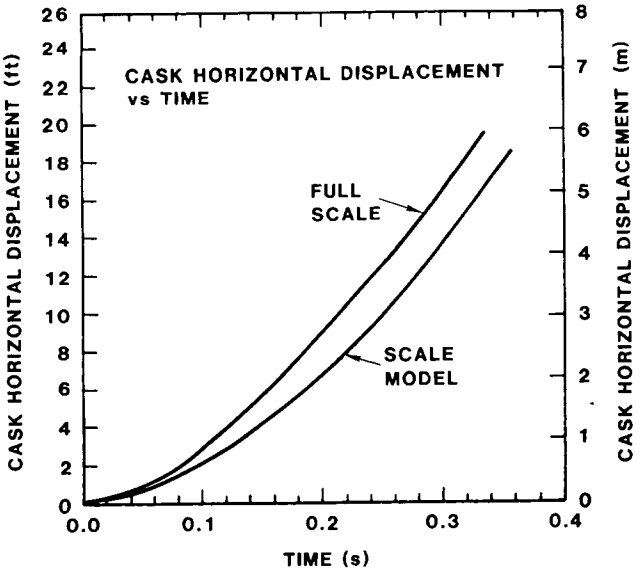

Figure 30. Cask-Horizontal Displacement vs Time for Model and Full-Scale System

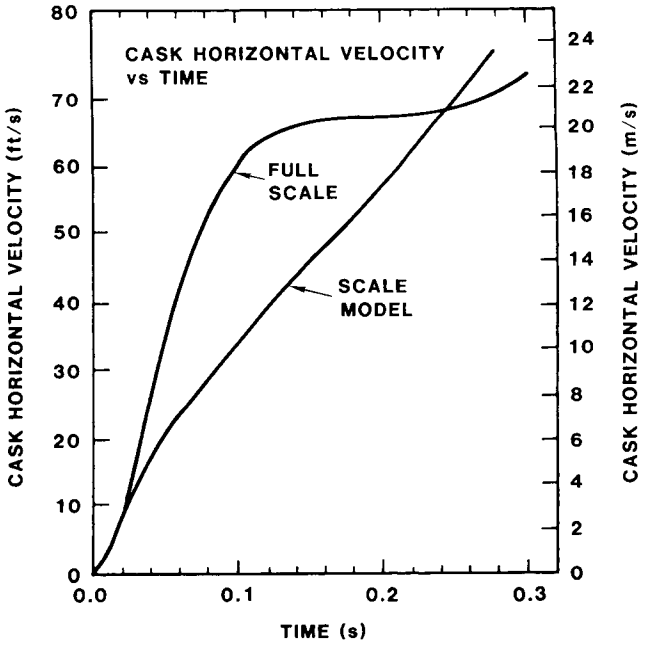

Figure 31. Cask-Horizontal Velocity vs Time for Model and Full-Scale System

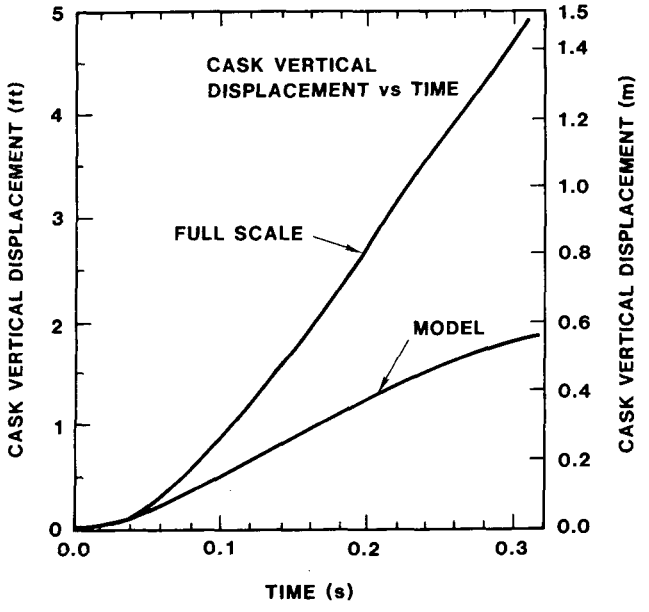

Figure 32. Cask Vertical Displacement vs Time for the Model and the Full-Scale System

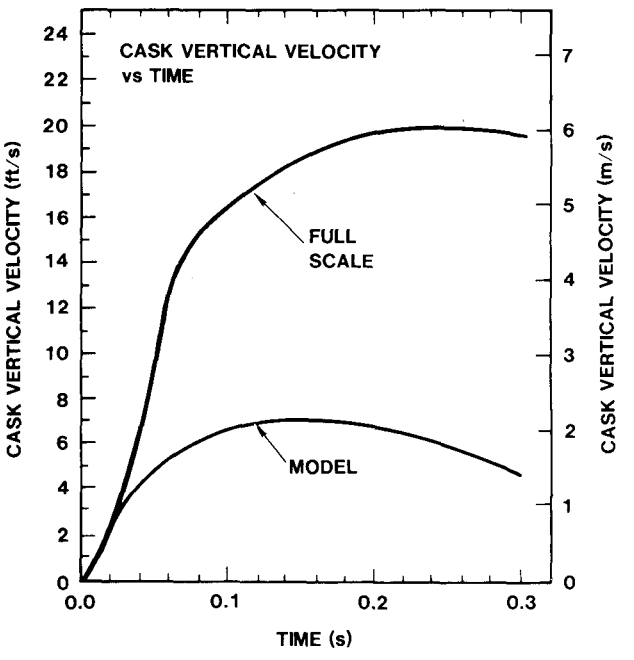

Figure 33. Cask Vertical Velocity vs Time for the Model and Full-Scale System

Figure 34 shows the posttest condition of both the full-scale and model casks. Here the great similarity in damage sustained by the casks is clearly observed. Both casks sustained indentations in the area where the underframe I-beams made contact with the cask. The horizontal impressions made by the I-beam flanges can clearly be seen in both the model and the prototype. These flange indentations produced the deepest parts of the damaged area. In the model cask the left and right indentations averaged about 0.254 cm (0.1 in.) in depth at their deepest point. The left side was about 10% deeper. The full-scale cask had a corresponding deformation of 2.54 cm (1 in.), with the left side also about 10% deeper. Internal measurements of both casks did not reveal any internal cavity deformation.

Besides comparing the cask damage, we now compare the post test condition of the model underframe to the full-scale by examining Figures 12 and 29. Here it is seen that the deformation pattern of the front bumper plate and the underframe I-beams is very similar. Measurements on the hardware indicated that the upper portion of the full-scale bumper plate was bent back through an angle of about 55°; the same measurement on the model indicated an angle of 50°. The maximum spin imparted to the cask scaled very well. The model was given a spin 8.66 times higher (1300 rpm vs 150 rpm) than the full-scale cask and close to the theoretical scale factor value of 8.0.

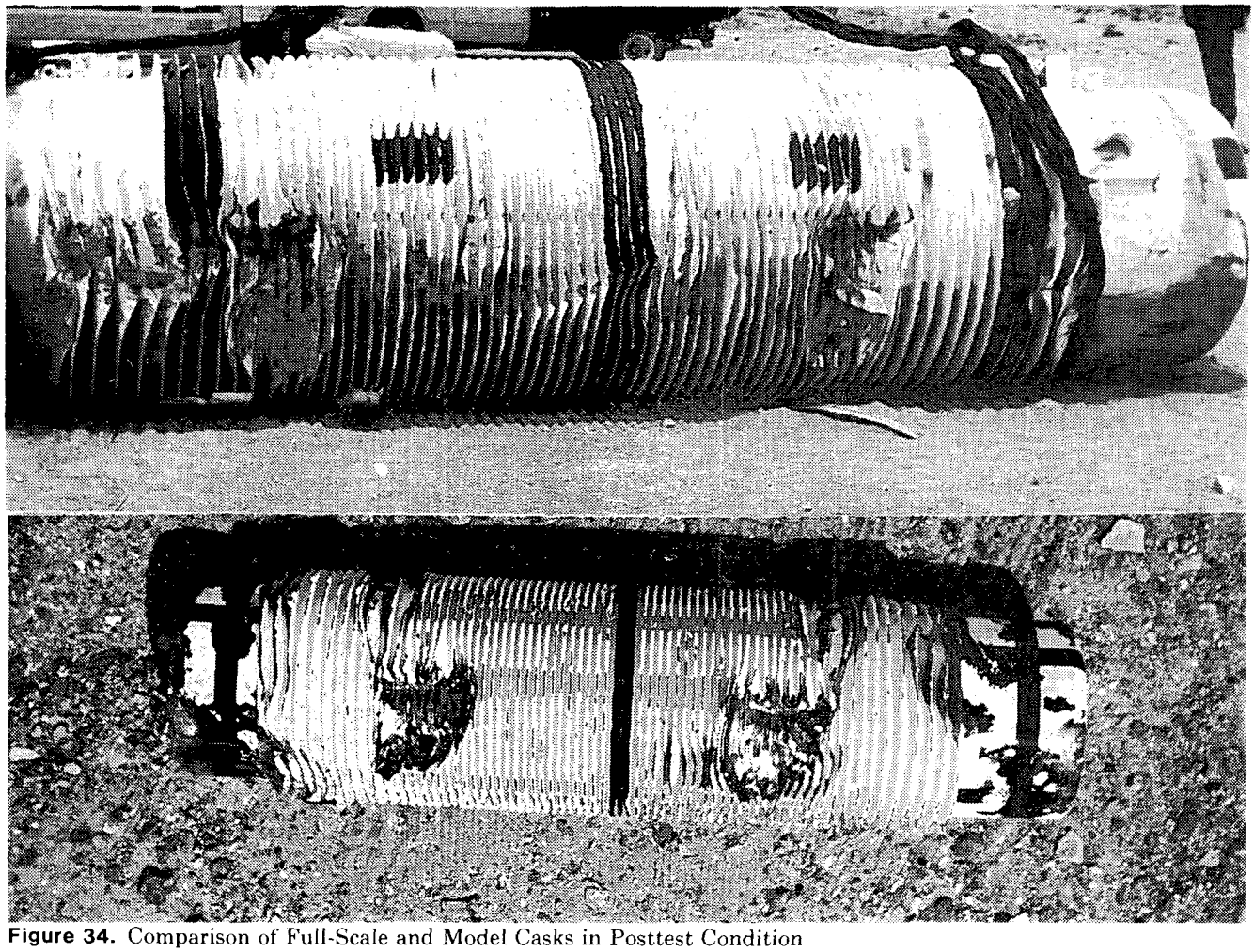

Figure 34. Comparison of Full-Scale and Model Casks in Posttest Condition

Discussion of Results

The mathematical analysis served the purpose of bounding the problem very well. Results indicated that the locomotive underframe would yield and that the cask would sustain some deformation, but not large enough to jeopardize the containment capability of the cask. The model, because of various factors, was conservative, as verified by the full-scale test. The finite-element calculations, however, did provide very good estimates of the results of the accident scenario. The model, designed to be conservative, yielded fairly conservative results.

The results comparing the scale-model cask displacement and velocities showed great differences between the model and the prototype. The differences, however, occurred after the underframe impact and at the point where the cask encountered the superstructure. The full-scale superstructure proved stiffer, as evidenced by the greater displacement and velocity given the cask. These differences can be explained by the fact that the scale-model design ignored all hardware in front of the engine and alternator (Figure 8) and provided only a sheet-metal cover in this area. The hardware located in this area in the full-scale locomotive (Figure 16) proved significant enough to cause differences between the cask's displacement-time and velocity-time curves because the cask never reached the engine-alternator. This hardware caused differences not only in the horizontal direction because of increased stiffness but also in the vertical direction because of a ramping effect. This is readily seen by examining the crushed superstructure. The model superstructure (Figure 12) was completely stripped clean of the underframe without providing much of a ramp effect. On the other hand, the full-scale superstructure (Figure 27) provided much more of a ramp because this structure was not stripped off the underframe like the model; it remained attached to the underframe while being crushed below the cask and provided an upward force. The result was that the full-scale cask was given more vertical displacement,

even though scaling laws dictate that because of gravity effects[2] the model cask should have exhibited the greater vertical displacement. Differences in the superstructure also caused a difference in the rates at which the model and full-scale locomotives slowed down.

The differences in superstructures between model and prototype, however, did not affect cask damage. The reason for this is that the only significant deformations sustained by the cask were inflicted by the locomotive underframe. This part of the structure as well as the cask were very accurately modeled, with excellent agreement in cask damage between model and prototype (Figure 34). The model cask sustained a maximum indentation depth of 0.254 cm (0.1 in.). This then indicates that the full-scale maximum depth should have been 2 cm (0.8 in.) instead of 2.54 cm (1 in.) as measured. On the surface this represents a 20% error; however, because the model impact velocity was 3.7% low, representing about an 8% difference in locomotive kinetic energy, the error becomes less.

The agreement is then considered to be excellent especially, because the correlation is for a parameter that is very difficult to predict with any accuracy. Even though very complex mechanics were involved in the test, the damage pattern observed in the model gave an excellent indication of what to expect in the full-scale test.

Conclusions

The problem of analyzing a locomotive-cask impact is very difficult to handle analytically. A finite-element program capable of handling large plastic deformations is needed. In the present study a 3D impact problem was simplified into a 2D problem by making several assumptions. This requires considerable engineering judgment; but if the assumptions are conservative it is fairly certain that the response, in terms of cask damage in this case, is bounded. If the solution indicates only moderate cask deformations, then it is fairly certain that the cask will not be breached because the solution is an upper bound on damage. Finite-element calculations of the 2D type are well within the state of the art and are not difficult to do once the model characteristics are determined. The amount of computer time is also not too high; for example, the calculational results presented here took about 8000 seconds of computer time on a CDC 7600 machine.

In this case, finite-element results gave good indications of the cask response and somewhat overpredicted the cask deformation, as expected. The utility of such calculations is that such an analysis does not require any hardware and can be done fairly inexpensively. In many situations, especially when trying to estimate a response, this approach makes the most sense.

The next step in an analytical analysis is to use a 3D finite-element model, which is roughly an order of magnitude more difficult than using a 2D model. At the time that the full-scale test was conducted, such an analysis was beyond the state of the art; however, recent advances in software and computers indicate great promise.[10] Reported computer run times of this type of problem are now as much as two orders of magnitude faster than those encountered only a few years ago.[5] These times are for what is generally known as Class VI machines with optimized software. Even with this capability, some simplifying assumptions must be made. The modeling of buckling and crushing phenomena of complicated shapes is still beyond the state of the art. The problem of modeling a locomotive to impact a cask is still not straightforward, but it is recommended that more 3D analyses be attempted. The state of the art may be at such a point that 3D large-deformation finite-element modeling is beginning to be feasible. Some effort in this area should be expended to evaluate its utility and feasibility.

Physical scale modeling has long been a reliable analytical tool in many areas. The present study as well as the work reported in References 2 and 3 indicates that this technique gives excellent results for the impact analysis of lead-shielded shipping casks in situations of severe impact (large deformation). It has been demonstrated that simplified models of vehicle structures such as tractor-trailer rigs,[2] railroad cars,[3] and locomotive underframes can give excellent results. The scale used in these studies has been one-eighth, but larger scales can be constructed to include more detail and provide greater resolution. The cost of the models has been reasonable, and larger scales can probably be constructed with a relatively small increase in cost.

In view of previous results and the results of the current study, scale modeling is recommended as the means of analyzing complex accident situations where a high reliability in results is desirable, or when it is desirable to confirm an analytical solution. A simple analytical solution should always be attempted to obtain some feeling for the problem.

The analyses and testing of the present study have demonstrated that a typical lead-shielded, steel, spent-fuel cask is very rugged and able to withstand great impact forces. In this case the major impact was applied by a locomotive underframe, with the driving force provided by the mass of the locomotive. The force delivered to the cask, however, was limited by the buckling or crush force of the locomotive underframe. Adding more driving mass by the addition of railroad cars, for example, would not have affected the results.

The question of how much force was applied to the cask may be of some interest. The force-time curve must contain a sharp spike because of the buckling phenomenon encountered; it is characteristic that during crush a structure such as this produces a spike with the force then coming down to a much lower level. An average crush level can be estimated by simple means as in Appendix E. The results indicate that an approximate average force of about 6.66×10^6 N (1.5×10^6 lb) was applied while the cask was in contact with the underframe.

The results of this study have further verified that current engineering analytical techniques can predict the structural response of shipping casks subjected to very complicated and severe accident environments. The degree of accuracy achieved with these analyses has been very high. These same techniques can be applied to the design of new equipment or to answer questions about hypothetical accident environments.

References

[1]H. R. Yoshimura, and M. Huerta, *Full Scale Tests of Spent-Nuclear-Fuel Shipping Systems*, SAND76-5707, (Albuquerque, NM: Sandia Laboratories, July 1976).

[2]M. Huerta, *Analysis, Scale Modeling, and Full Scale Tests of a Truck Spent-Nuclear-Fuel Shipping System In High Velocity Impacts Against a Rigid Barrier*, SAND77-0270, (Albuquerque, NM: Sandia Laboratories, April 1978).

[3]M. Huerta, *Analysis, Scale Modeling, and Full Scale Test of a Railcar and Spent-Nuclear-Fuel Shipping Cask in a High Velocity Impact Against a Rigid Barrier*, SAND78-0458, (Albuquerque, NM: Sandia National Laboratories, August 1980).

[4]A. W. Dennis, *Analytical Investigation of a Grade-Crossing Accident Between a Railroad Train and a Spent Reactor Fuel Cask*, SAND74-0317, (Albuquerque, NM: Sandia Laboratories, January 1975).

[5]C. M. Stone, Sandia National Laboratories, private communication, June 1981.

[6]J. H. Biffle, and M. H. Gubbels, *WULFF--A Set of Computer Programs for the Large Displacement Dynamic Response of Three-Dimensional Solids*, SAND76-0096, (Albuquerque, NM: Sandia Laboratories, August 1976).

[7]S. W. Key, Z. E. Beisinger, and R. D. Krieg, *HONDOII A Finite Element Computer Program for the Large Deformation Dynamic Response of Axisymmetric Solids*, SAND78-0422, (Albuquerque, NM: Sandia Laboratories, October 1978).

[8]A. W. Dennis, Sandia National Laboratories, private communication, December 1979.

[9]R. E. Jones, *QMESH: A Self-Organizing Mesh Generation Program*, SLA-73-1088, (Albuquerque, NM: Sandia Laboratories, July 1974).

[10]J. O. Hallquist, "Preliminary User's Manuals for DYNA3D and DYNAP," (Livermore, CA: Lawrence Livermore Laboratory, October 1979).

APPENDIX A

Details of the Finite-Element Model

This appendix describes in some detail the finite-element model used to analyze the impact of the locomotive with the cask. The HONDO finite-element program was used for the analysis, as mentioned in the text. The geometric configuration of the model is illustrated in Figure 4 of the text. The analysis was plane strain, and it was done on the basis of a per-unit thickness.

Because the cask is wider than the underframe, some adjustments had to be made to the material property data. One was to increase the density of the lead material in the cask so that the full mass of the cask would be acting on the underframe. The analysis was done on the basis of the 188 cm (74 in.) underframe.

The artificial lead density was calculated as follows. The cross-sectional area of the outer stainless-steel shell was calculated as 696.8 cm^2 (108.0 $in.^2$), and the inner one 239.35 cm^2 (37.1 $in.^2$). The total weight for a 188 cm (74 in.) length was then calculated as 1464.1 kg (3221 lb). Because the total weight of the cask was 25454.5 kg (56,000 lb), the necessary weight of the lead in this section was then calculated as 23990 kg (52,778 lb). The lead volume in a 188-cm (74-in.) section was calculated as 824597.1 cm^3 (50,320 in^3). This dictated that, to include the full weight of the cask in the 74-in. section, the lead should be given a weight density of 288.1 x 102 kg/m^3 (1.04 $lb/in.^3$). This is the value that was used in the model.

Because the model was 2D, the I-beam webs had to be assumed as solid through the width of the underframe. Therefore the stiffness of the webs was distributed through the underframe width. This was done by multiplying the yield strength and modulus of the steel web material by the fraction of the frontal underframe area actually covered by the webs. By taking the web height of 50.8 cm (20 in.) and the web width of 1.27 cm (0.5 in.), it was calculated that the web cross sections were only 1.35% of the total frontal area. The modulus and yield stress of the steel underframe material were multiplied by this factor to simulate the web behavior in the underframe. Also, the material was given a very low value of Poisson's ratio to better simulate the buckling behavior that was anticipated. The locomotive portion of the model was given a density that would equal 113.6 metric tons (250,000 lb) to correspond to the locomotive mass. Because the analysis was done on a unit thickness basis (when the width of the locomotive is considered), the area corresponding to the locomotive (see Figure 7) had to represent 1533.6 kg (3374 lb m). A very high elastic modulus was also given to this material so that this portion of the finite-element model represented a very dense and rigid mass driving the underframe into the cask.

The I-beam flanges were modeled as solid steel extending through the width of the underframe. The front plate (see Figure 7) was modeled in a similar manner.

The elastic-plastic material model available in the HONDO program was used to model the behavior of each of the materials. The input parameters for the materials include the weight density of the material, ρ; Young's modulus, E; Poisson's ratio, μ; yield stress, t_o; and the plastic modulus, E_t. The following values were used for the various materials.

Material	ρ, kg/m^3 ($lb\ m/in.^3$)	E, mPa ($lb/in.^2$)	μ	t_o, mPa ($lb/in.^2$)	E_t, mPa ($lb/in.^2$)
Locomotive mass	$1296. \times 10^2$ (4.5)	3102.3×10^3 (450×10^6)	0.3	3447 (500×10^3)	3447 (500×10^3)
Locomotive underframe	83.1×10^2 (0.3)	206.8×10^3 (30×10^6)	0.3	241.3 (35×10^3)	1103 (160×10^3)
I-beam web material	1.11×10^2 (0.004)	3.10×10^3 (0.45×10^6)	0.01	3.27 (0.475×10^3)	31 (4.5×10^3)
Stainless Steel (cask shells)	31.1×10^2 (0.3)	199.9×10^3 (29×10^6)	0.3	241.3 (35×10^3)	2068.2 (300×10^3)
Lead Shielding (Material)	288.1×10^2 (1.04)	13.8×10^3 (2×10^6)	0.42	17.23 (2.5×10^3)	17.02 (2.47×10^3)

APPENDIX B

Construction Details for the Scale Models

DESIGN AGENCY PART NO.	REVISIONS				
	ISSUE	SHEET ZONE	DESCRIPTION	PREPARED BY	DATE
T45453-000	A			R.YOSHIMURA,5432 J.PUHARA,9652	1/6/17

NOTES:

1. ALL EXTERIOR WELDS TO BLEND AND BE GROUND SMOOTH.
2. MINIMUM WELD THICKNESS TO BE EQUAL TO THINNEST ITEM BEING JOINED.
3. ALL WELDS ARE SEAL WELDS.
4. PAINT PER ENG'G INSTRUCTIONS.

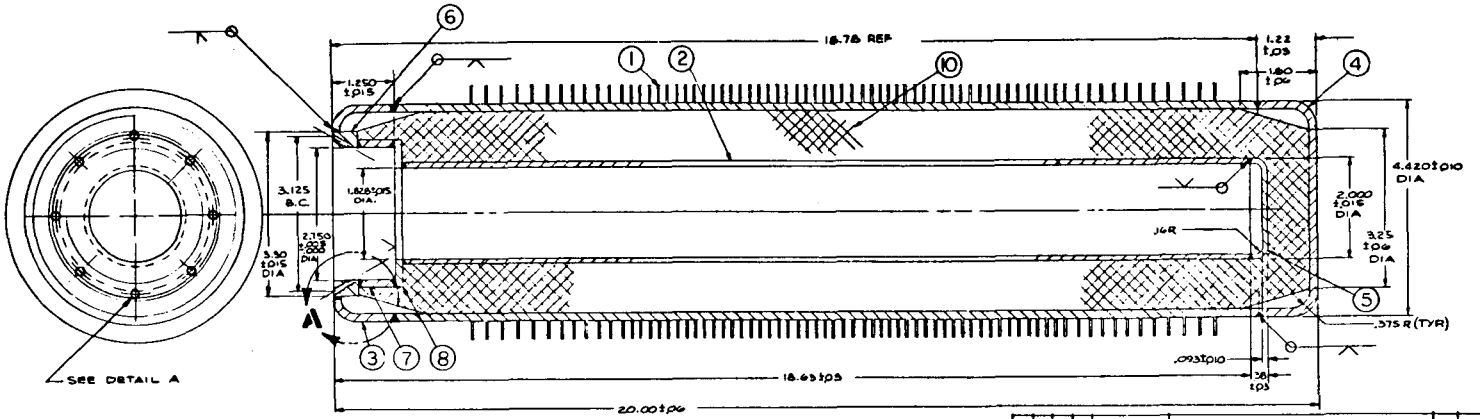

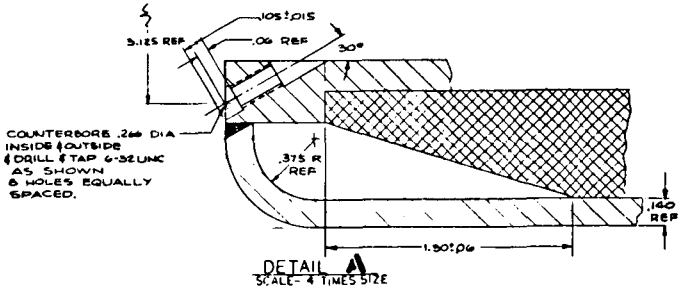

DETAIL A
SCALE- 4 TIMES SIZE

ITEM	QTY	PART NUMBER	DESCRIPTION	MATERIAL
10	AR		LEAD	
9	1		PLATE, RING-STAINLESS STL -TYPE 304 - .141 THK	
8	1		TUBE, STAINLESS STL -TYPE 304 3.000 O.D. X .120 WALL	
7	1		PLATE, RING-STAINLESS STL -TYPE 304 - .500 THK	
6	1		HEAD FLG. -STAINLESS STL -TYPE 304	
5	1		HEAD FLG. -STAINLESS STL -TYPE 304	
4	1		HEAD FLG. -STAINLESS STL -TYPE 304	
3	1		TUBE, STAINLESS STL, TYPE 304, 2.000 O.D. X .083 WALL	
2	1	T45454-00	OUTER SHELL	
1				

LIST OF MATERIAL

AGENCY APPROVALS		SHEET	1
ORG	DATE	APPROVALS	ISSUE A

HELP INDEX

PART CLASSIFICATION: UNCLASSIFIED

DWG CLASSIFICATION LEVEL: UNCLASSIFIED

TITLE: CASK ASSEMBLY
MODEL-GENERAL ELECTRIC
15X140 SPENT FUEL SHIPPING CASK

SIZE	CAGE MATL NO	DWG NUMBER
D	14213	T45453

SCALE FULL SHEET 1 OF 1

NOTES:

1. MATERIAL: STAINLESS STEEL, TYPE 304.
2. PASSIVATION TREATMENT FOR CORROSION-RESISTING STEEL PER QQ-P-35.

DESIGN AGENCY PART IDENTIFICATION NO.	REVISIONS					
	ZONE	LTR	DESCRIPTION	PREPARED BY	DATE	
T45454-000		A		R.YOSHIMURA 5432/PUHARA, 9652	11/17	

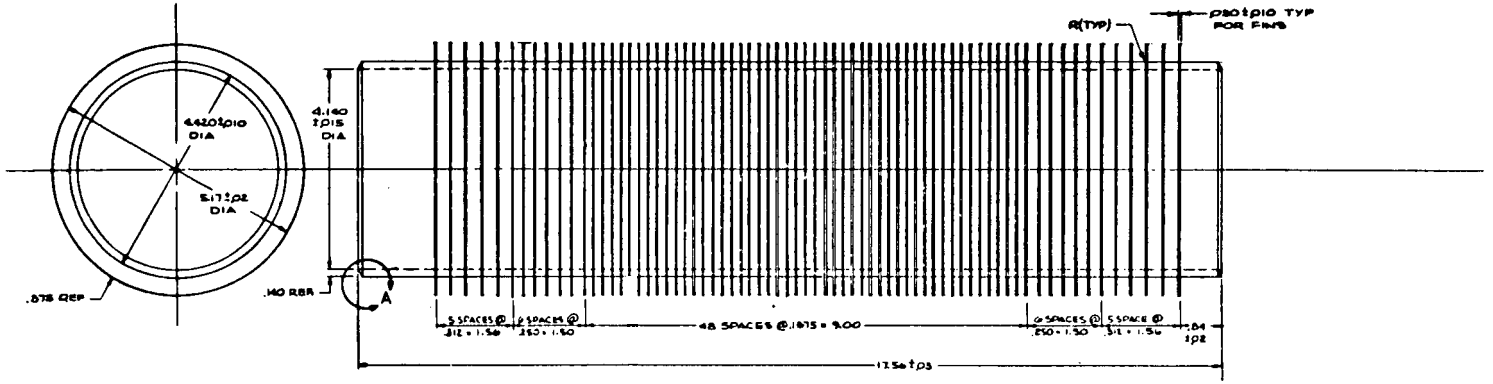

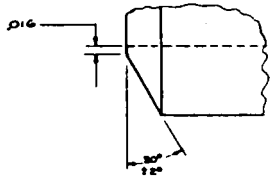

DETAIL A
TYP BOTH ENDS

AGENCY APPROVALS			SHEET	1							TITLE
ORG	DATE	APPROVALS	ISSUE	A							OUTER SHELL
			SHEET INDEX								
			PART CLASSIFICATION	UNCLASSIFIED							
			DWG CLASSIFICATION LEVEL	UNCLASSIFIED							SIZE D / CAGE IDENT. NO. 14213 / DWG NUMBER T45454
			SCALE FULL								SHEET 1 OF 1

DESIGN AGENCY PART NO.	REVISIONS: ISSUE	DESCRIPTION	PREPARED BY	DATE	CHKD	APPD
T45426-000	A		R.YOSHIMURA,5432/ PUHARA,9652	1/14/11		

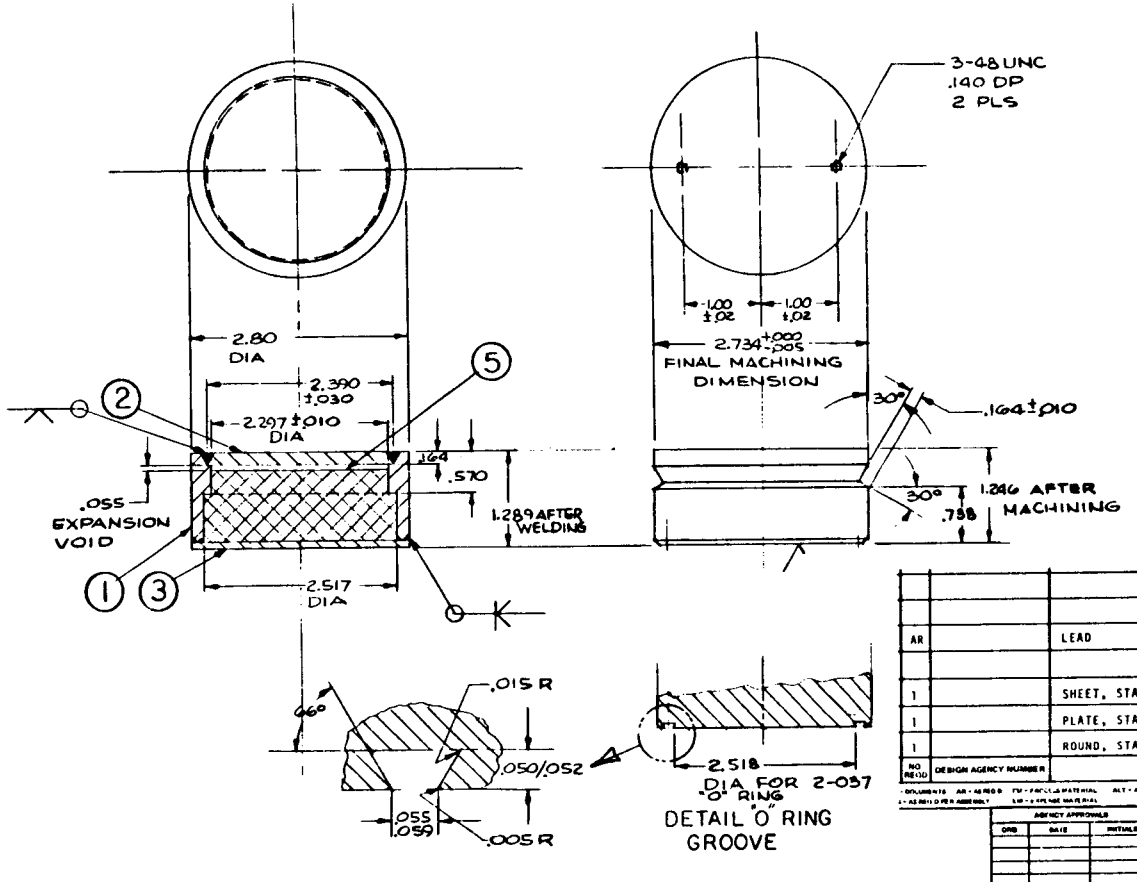

NO REQD	DESIGN AGENCY NUMBER	DESCRIPTION	NOTE	SHEET ZONE	ITEM
AR		LEAD			5
					4
1		SHEET, STAINLESS STL-TYPE 304-.135 THK.			3
1		PLATE, STAINLESS STL-TYPE 304-.188 THK.			2
1		ROUND, STAINLESS STL-TYPE 304-3 DIA.			1

LIST OF MATERIAL

AGENCY APPROVALS	ORG	DATE	INITIALS

SHEET 1 ISSUE A

SHEET INDEX

PART CLASSIFICATION: UNCLASSIFIED

DWG CLASSIFICATION LEVEL: UNCLASSIFIED

TITLE: CLOSURE HEAD

SIZE C | CODE IDENT. NO. 14213 | DWG. NUMBER T45426

SCALE FULL | SHEET 1 OF 1

NOTES:

1. STRESS RELIEVE AND STRAIGHTEN AFTER WELDING.
2. PRIME COAT AND PAINTING TO BE DONE AT THE DIRECTION OF ENGINEERING.

DESIGN AGENCY PART [redacted] NO.	ISSUE	SHEET	DESCRIPTION / PREPARED BY	DATE	CHKR	ENGR
T4 5764-000	A		R YOSHIMURA 5432/PUHARA 5652	1/6/77		

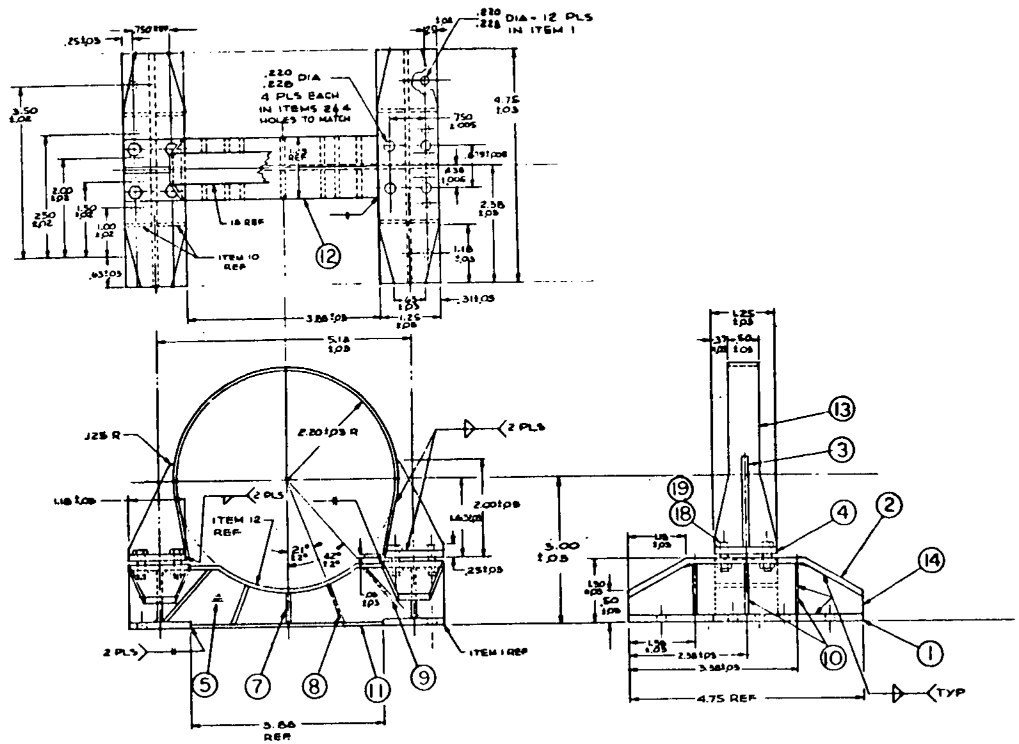

QTY REQD	DESCRIPTION	ITEM
		20
8	NUT, HEX, HD STEEL 8-32 UNC	19
8	SCREW, HEX HD, 8-32UNC x .75 LG (HIGH STRENGTH)	18
		17
		16
		15
2	SHEET, 10 GA (.1345) STEEL LOW CARBON	14
1	SHEET, 16 GA (.064) STEEL LOW CARBON	13
1	SHEET, 16 GA (.064) STEEL LOW CARBON	12
1	SHEET, 16 GA (.064) STEEL LOW CARBON	11
10	SHEET, 16 GA (.064) STEEL LOW CARBON	10
4	SHEET, 16 GA (.064) STEEL LOW CARBON	9
4	SHEET, 16 GA (.064) STEEL LOW CARBON	8
2	SHEET, 16 GA (.064) STEEL LOW CARBON	7
		6
1	SHEET, 10 GA (.1345), STEEL, LOW CARBON	5
2	SHEET, 10 GA (.1345), STEEL, LOW CARBON	4
2	SHEET, 10 GA (.1345), STEEL, LOW CARBON	3
2	SHEET, 10 GA (.1345), STEEL, LOW CARBON	2
2	SHEET, 10 GA (.1345), STEEL, LOW CARBON	1

LIST OF MATERIAL

SHEET 1 — ISSUE A

PART CLASSIFICATION: UNCLASSIFIED

DWG CLASSIFICATION LEVEL: UNCLASSIFIED

TITLE: TIE DOWN SHIPPING SUPPORT AND TIE DOWN STRAP ASSYS

SIZE: D — CODE IDENT. NO. 14213 — DWG NUMBER T45764

SCALE FULL — SHEET 1 OF 1

Part or identifying no.	Rev		Description
T40385-000	A		YOSHIMURA 5432 PUHARA 9652
T40385-001	B		ADDED 16 BOLTS (ITEM 16) TO BASE/PRESS. PLATE; R'MD 1 T40396-000 BASE (ITEM 9) FROM P/L; R'MD 1 T39563-000 UNDERFRAME (ITEM 12) ALSO R'MD 4 BOLTS (ITEM 16) HOLDING THE UNDERFRAME TO THE BASE; ITEM 10 DWG NO. T40397-001 WAS T40397-000; ITEM 4 DWG NO. T40393-001 WAS T40393-000; DIM. 87.20 REF WAS 85.156 REF; ADDED ITEM 11 ASSEMBLY, UNDERFRAME/BASE DWG NO. T59826-000; ADDED 12 NUTS (ITEM 22), 12 LOCK WASHERS (ITEM 25), 4 NUTS (ITEM 23) 4 LOCK WASHERS (ITEM 26), 2 NUTS (ITEM 24), 2 LOCK WASHERS (ITEM 27). I. BOHL 9651 (MRL)/ D STENBERG 4552 (MRL)

NOTES

1. FINAL PAINTING TO BE UNDER THE SUPERVISION OF ENGINEERING.
2. BALLAST TO TOTAL MODEL WEIGHT OF 480±5#

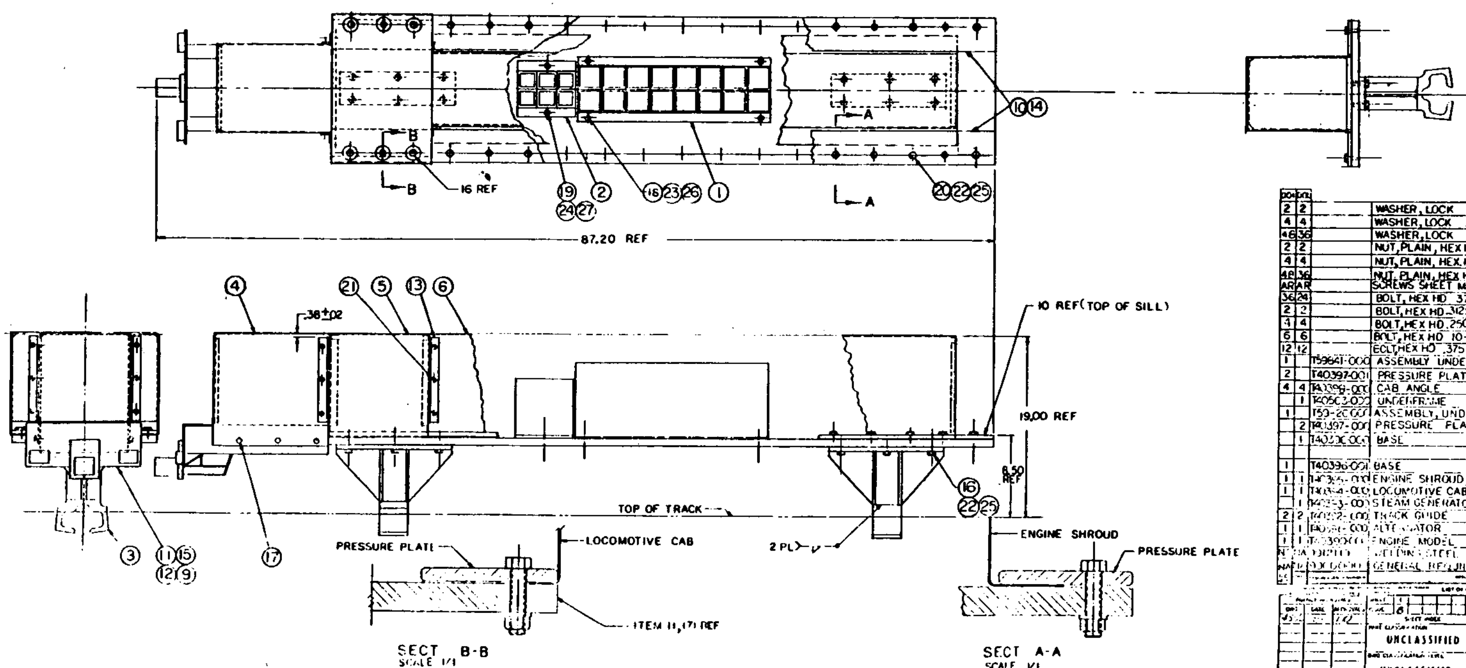

-000	-001	Part no.	Description	Item
2	2		WASHER, LOCK .3125	27
4	4		WASHER, LOCK .250	26
48	36		WASHER, LOCK .375	25
2	2		NUT, PLAIN, HEX HD .3125-18 UNC	24
4	4		NUT, PLAIN, HEX HD .250-20UNC	23
48	36		NUT, PLAIN, HEX HD .375-16 UNC	22
AR	AR		SCREWS SHEET METAL NO 8	21
36	24		BOLT, HEX HD .375-16UNC X 1.75	20
2	2		BOLT, HEX HD .3125-18 UNC X 1.500	19
4	4		BOLT, HEX HD .250-20UNC X 1.250	18
6	6		BOLT, HEX HD 10-24 UNC X .375	17
12	12		BOLT, HEX HD .375-16UNC X 2.00	16
1		T59641-000	ASSEMBLY UNDERFRAME	15
2		T40397-001	PRESSURE PLATE	14
4	4	T40398-000	CAB ANGLE	13
	1	T40503-000	UNDERFRAME	12
1		T59-2C000	ASSEMBLY, UNDERFRAME/BASE	11
	2	T40397-000	PRESSURE PLATE	10
	1	T40396-000	BASE	9
				8
1		T40396-001	BASE	7
1	1	T40395-000	ENGINE SHROUD	6
1	1	T40394-000	LOCOMOTIVE CAB	5
	1	T40393-000	STEAM GENERATOR COVER	4
2	2	T40392-000	TRACK GUIDE	3
1	1	T40391-000	ALTERNATOR	2
1	1	T40390-000	ENGINE MODEL	1
[illegible]	[illegible]	[illegible]	WELDING STEEL ALLOYS	
[illegible]	[illegible]	[illegible]	GENERAL REQUIREMENTS	

LIST OF MATERIAL

UNCLASSIFIED

⅛ SCALE SIMULATED ALCO-1600 DIESEL LOCOMOTIVE

UNCLASSIFIED

E T40385

NOTES:

1. MATERIAL: LOW CARBON STEEL - 750 THK STK
2. CALC. WT. 224#
3. ZINC CHROMATE PRIMER PER 5031201/5031202.
4. GENERAL REQUIREMENTS ARE DEFINED IN 9900000.

SENDER AGENCY PART OR CONTROL NO.	REVISIONS				
	ZONE	LTR	DESCRIPTION	DATE	APPROVED
40396-001		C	REPLACED ALL TAPPED HOLES WITH CLEARANCE HOLES THRU, DELETED 4 EA 375-16 UNC HOLES ON END OF BASE, REVISED DIM TO T.P, REDRAWN FOR CLARITY COWLEY 9651 (MRL) / STENBERG 4552 (MRL)		

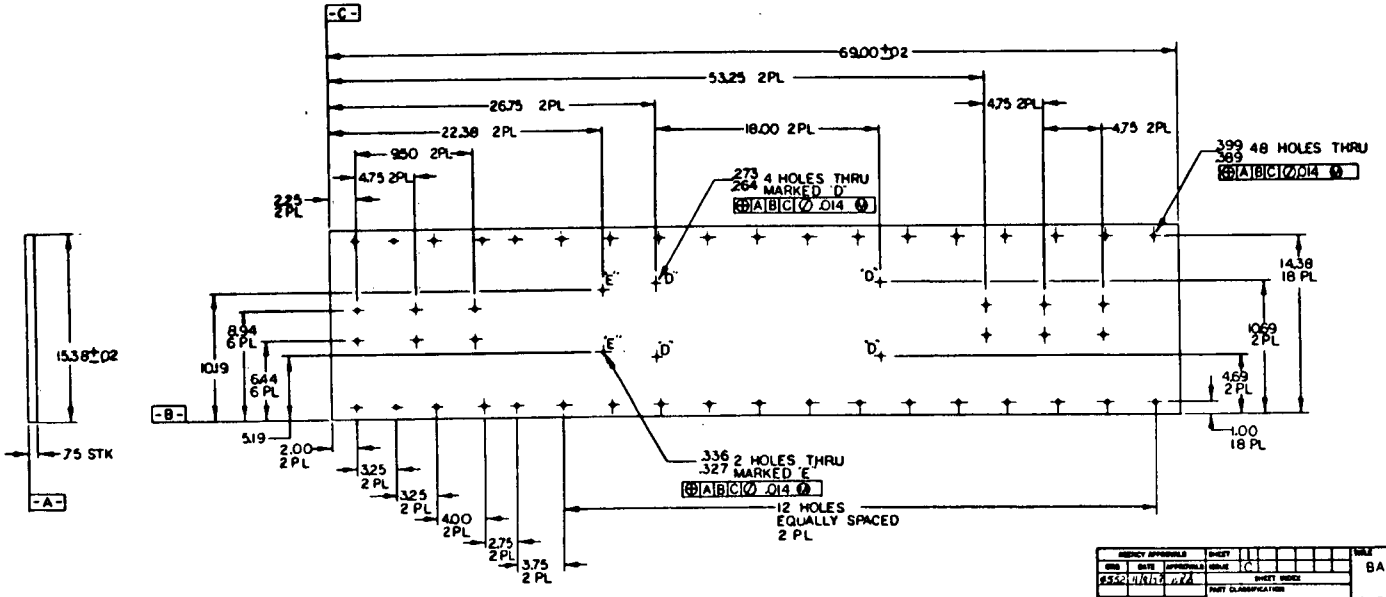

AGENCY APPROVALS			SHEET	
ORG	DATE	APPROVALS	ISSUE	C
8352	11/11/74		SHEET INDEX	
			PART CLASSIFICATION	UNCLASSIFIED
			SHG CLASSIFICATION LEVEL	UNCLASSIFIED
DC51				

TITLE	
	BASE
	ALCO 1600
SIZE	D
CODE IDENT. NO.	14213
SHG NUMBER	T40396
SCALE	1/4
SHEET	1 OF

T59826000	A	1. BOHL 9651/(MPL) D. STENBERG 4552(MPL)	4/4

NOTES:

1. NOTE ORIENTATION OF HOLES IN ITEM 2 (BASE) IN RELATION TO ITEM 1 (NOSE).
2. WELD AND INSPECT PER 9912119 CLASS II.

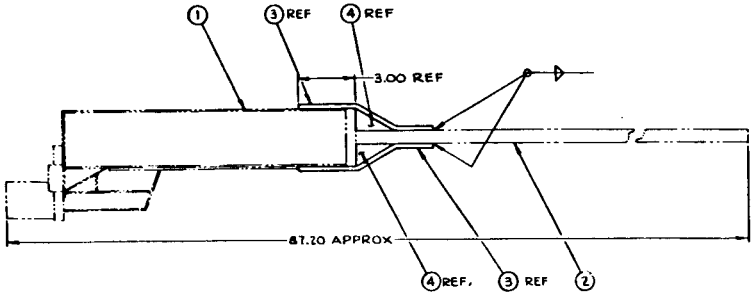

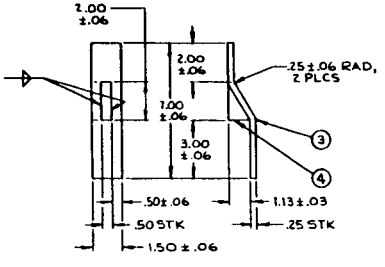

DETAIL A

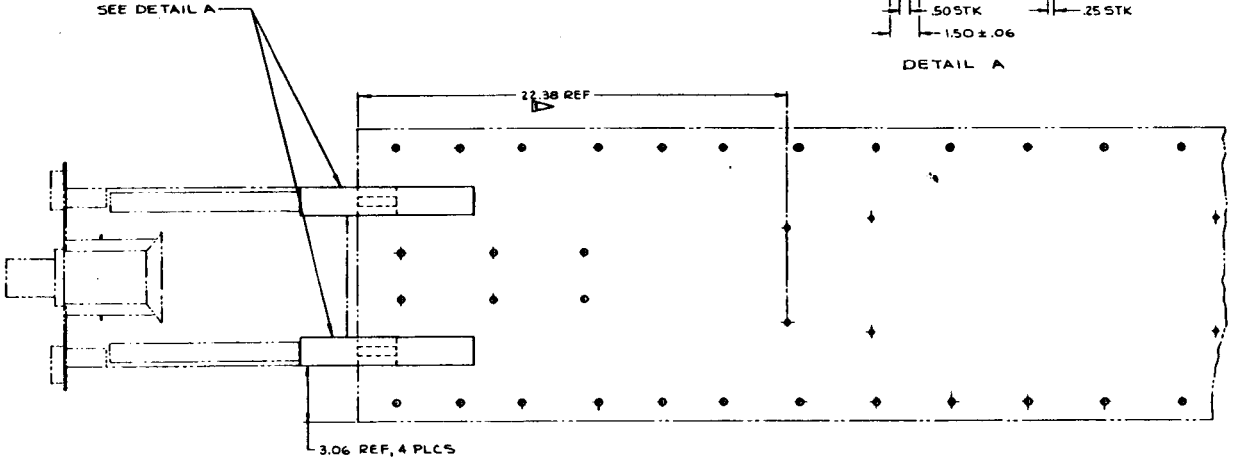

4		STEEL, C.R. .50 STK	4
4		STEEL, C.R. .25 STK	3
1	T40396001	BASE	2
1		ASSEMBLY, UNDERFRAME	1
NA	9912119-00	WELDING, STEEL ALLOYS	
NA	9900000	GENERAL REQUIREMENTS	

DES.	JRD	4/4	
		UNCLASSIFIED	
		UNCLASSIFIED	

ASSEMBLY, UNDERFRAME/ BASE

ALCO 16610

E 14213 T59826

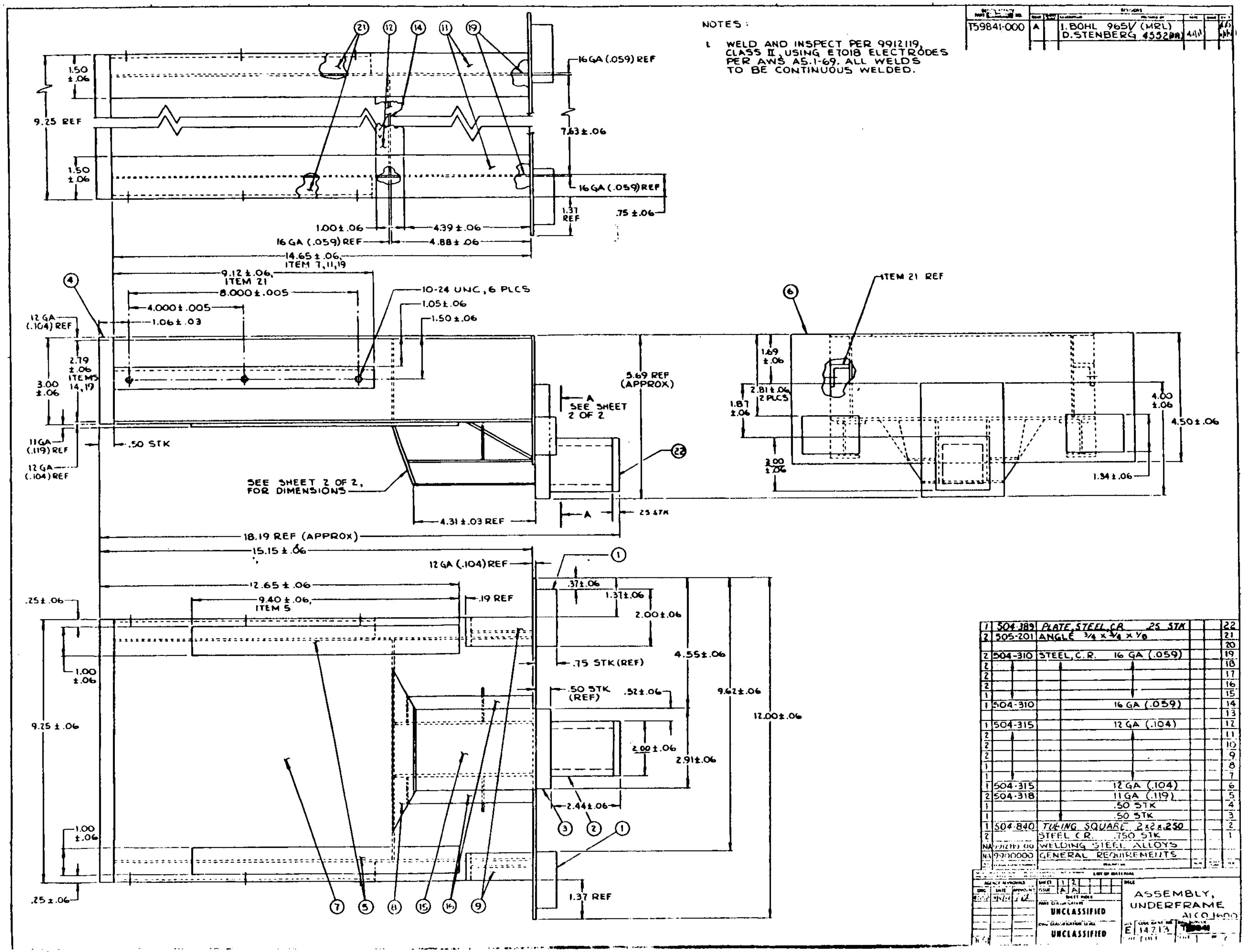
NOTES:
1. WELD AND INSPECT PER 9912119, CLASS II, USING E7018 ELECTRODES PER AWS A5.1-69. ALL WELDS TO BE CONTINUOUS WELDED.
T59841-000 A I. BOHL 965V (MRL) D. STENBERG 4552(PA)
16 GA (.059) REF
9.25 REF
7.63 ±.06
1.50 ±.06
1.37 REF
.75 ±.06
1.00 ±.06
4.39 ±.06
4.88 ±.06
14.65 ±.06, ITEM 7, 11, 19
9.12 ±.06, ITEM 21
8.000 ±.005
4.000 ±.005
1.06 ±.03
10-24 UNC, 6 PLCS
1.05 ±.06
1.50 ±.06
12 GA (.104) REF
11 GA (.119) REF
2.79 ±.06 ITEMS 14, 17
3.00 ±.06
.50 STK
5.69 REF (APPROX)
SEE SHEET 2 OF 2
SEE SHEET 2 OF 2, FOR DIMENSIONS
4.31 ±.03 REF
.25 STK
18.19 REF (APPROX)
15.15 ±.06
12.65 ±.06
9.40 ±.06, ITEM 5
.19 REF
.37 ±.06
1.37 ±.06
2.00 ±.06
4.55 ±.06
9.62 ±.06
12.00 ±.06
.75 STK (REF)
.50 STK (REF)
.52 ±.06
2.91 ±.06
2.44 ±.06
.25 ±.06
9.25 ±.06
ITEM 21 REF
1.69 ±.06
2.81 ±.06 2 PLCS
1.87 ±.06
4.00 ±.06
4.50 ±.06
1.34 ±.06
1 | 504-389 | PLATE, STEEL, C.R. .25 STK | 22
2 | 505-201 | ANGLE 3/4 x 3/4 x 1/8 | 21
20
2 | 504-310 | STEEL, C.R. 16 GA (.059) | 19
1 | 504-310 | 16 GA (.059) | 14
1 | 504-315 | 12 GA (.104) | 12
1 | 504-315 | 12 GA (.104) | 6
2 | 504-318 | 11 GA (.119) | 5
1 | .50 STK | 4
1 | .50 STK | 3
1 | 504-840 | TUBING SQUARE 2 x 2 x .250 | 2
2 | STEEL C.R. .750 STK | 1
NA | 9912119 00 | WELDING STEEL ALLOYS
NA | 9900000 | GENERAL REQUIREMENTS
UNCLASSIFIED
UNCLASSIFIED
ASSEMBLY, UNDERFRAME ALCO 1600
E 14213 [redacted]

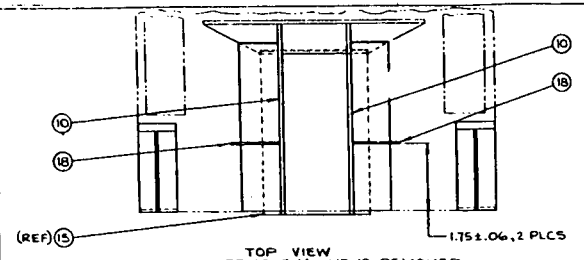

TOP VIEW
WITH ITEMS 7, 14, AND 19 REMOVED
FOR CLARITY

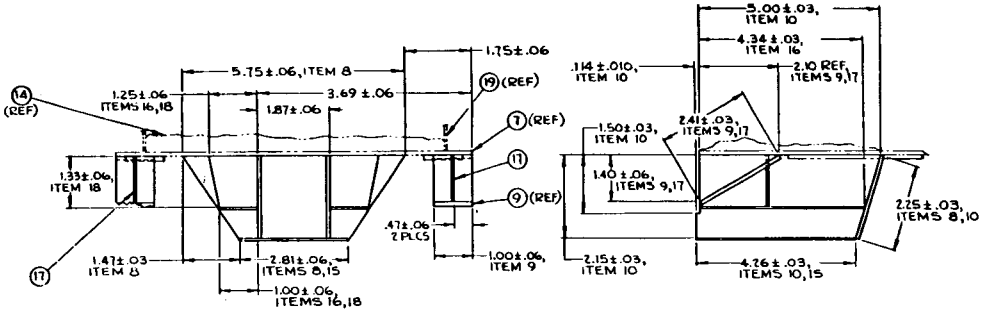

VIEW A-A
WITH ITEMS 1, 2, 3, AND 6
REMOVED FOR CLARITY

UNCLASSIFIED

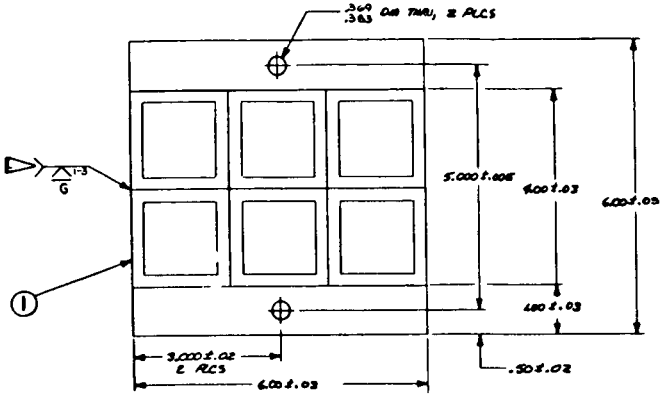

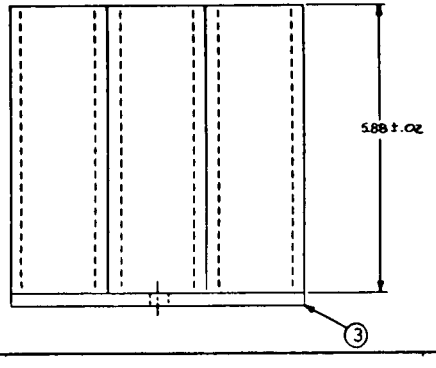

NOTES:

1. ASSEMBLE TUBES IN PAIRS, ALTERNATING WELD TO ALLOW CLOSE FIT. ASSEMBLE PAIRS AS SHOWN AND WELD TOGETHER 10 WELDS IN ALL.
2. APPROX. WT. = 18.4

DESIGN AGENCY PART NO.	REVISIONS					
	ZONE	REV LTR	DESCRIPTION	PREPARED BY	DATE	
T40391-000		A		VAN THEEMSCHE 5652/ YOSHIMURA 5432	2376	

				5
				4
1	504-425	SHEET, LOW CARBON STEEL, .250 THK		3
				2
6	504-840	TUBE, STEEL, 2 X 2 X .250 WALL		1
	9900000	GENERAL REQUIREMENTS		

LIST OF MATERIAL

AGENCY APPROVALS			SHEET	
ORG	DATE	APPROVALS	ISSUE	A
5132			SHEET INDEX	
			PART CLASSIFICATION	UNCLASSIFIED
			DWG CLASSIFICATION LEVEL	UNCLASSIFIED
DCF 2				

TITLE: ALTERNATOR 2 ALCO 1600

SIZE	CODE IDENT. NO.	DWG NUMBER
D	14213	T40391
SCALE FULL		SHEET OF

NOTES:

1. ASSEMBLE TUBES IN PAIRS, ALTERNATING WELD TO ALLOW CLOSE FIT. ASSEMBLE THE EIGHT PAIRS AS SHOWN AND WELD TOGETHER. 30 WELDS IN ALL.
2. APPROX. WT. = 62.5#

DESIGN AGENCY PART NUMBER NO.	REVISIONS					
	ISSUE	ENGR. ORDER	DESCRIPTION	DATE	CHKD	APPD
T40390-000	A		VAN THEEMSCHE 96527 YOSHIMURA 5432	3-3-76		

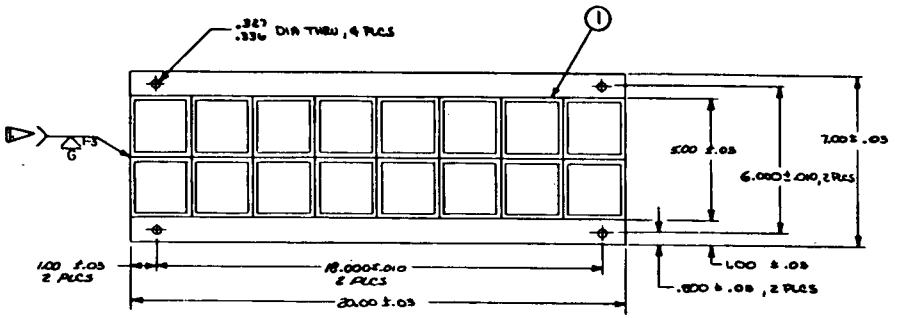

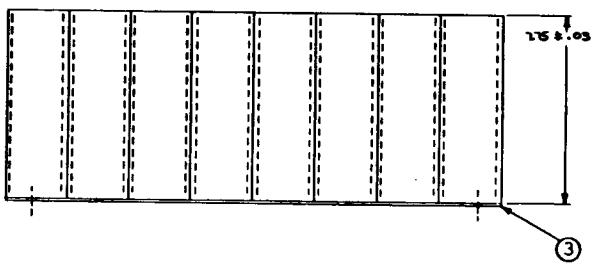

ITEM	PART NUMBER	DESCRIPTION	
1	504-318	SHEET, LOW CARBON STEEL, 11 (.1191 GAGE	
16	504-842	TUBE, STEEL, 2.5 X 2.5 X .188 WALL	
	9900000	GENERAL REQUIREMENTS	

LIST OF MATERIAL

AGENCY APPROVALS: ORG | DATE | APPROVALS — 6432 — 5652

SHEET ISSUE

SHEET INDEX

PART CLASSIFICATION: UNCLASSIFIED

DOD CLASSIFICATION LEVEL: UNCLASSIFIED

TITLE: ENGINE MODEL 2 ALCO 1600

SIZE: D | CLARK DRAWING NO. 14213 | DWG NUMBER T40390

SCALE 1/2 | SHEET 1 OF 1

NOTES:

1. MATERIAL: SHEETMETAL (STEEL), LOW CARBON, HR OR CR 20(.0359) GA.
2. ZINC CHROMATE PRIMER PER 5031201 / 5031202.
3. ALL BEND RADII = .125 R MIN.
4. INSTALL RIVETS PER 9914001.
5. CALC. WEIGHT = 7.25#

DESIGN AGENCY PART NO.	REVISIONS				
	SCALE	SHEET SIZE	DESCRIPTION	PREPARED BY	DATE
T40394-000		A	R.YOSHIMURA, 5432 J.PUHARA, 9652		2-3-76
		B	ADDED 2EA. 1.25 DIA. HOLES, REVISED NOTE 4, REPLACED NO.8 SCREWS WITH .125 DIA. RIVETS. COWLEY 9C51 (MRL) / STENBERG 4552 (MRL)		4-1-11

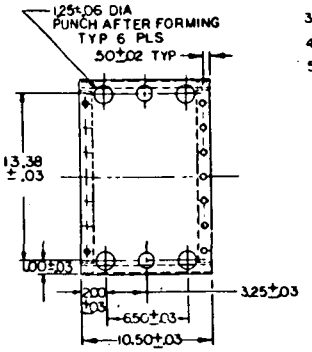

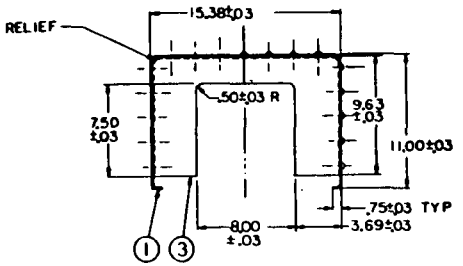

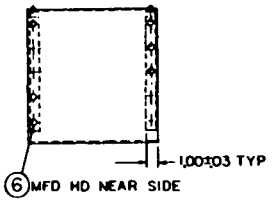

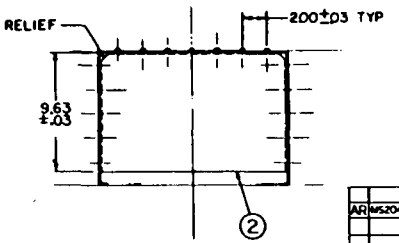

QTY	PART NO.	DESCRIPTION			ITEM
AR	MS20470AD4-6	RIVET .125 DIA.			6
1		FORWARD BULKHEAD			3
1		AFT BULKHEAD			2
1		MAIN COVER			1
NA	9914001	RIVET INSTALLATION			
NA	9900000	GENERAL REQUIREMENTS			

LIST OF MATERIAL

AGENCY APPROVALS			SAFETY ISSUE	TITLE
ORG	DATE	APPROVALS		LOCOMOTIVE CAB "B"
453			SHEET INDEX	ALCO 1600
			PART CLASSIFICATION	
			UNCLASSIFIED	
			ORG CLASSIFICATION LEVEL	SIZE / CODE IDENT NO. / DWG NUMBER
9651			UNCLASSIFIED	D 14213 T40394
				SCALE 1/4 SHEET 1 OF 1

NOTES:

1. MATERIAL: SHEET STEEL, LOW CARBON, H.R. OR C.R. #20 (.0359) GA.
2. ZINC CHROMATE PRIMER PER 5031201 OR 5031202.
3. CALC. WEIGHT = 19.6#

DESIGN AGENCY PART NO.	REV	DESCRIPTION
T40395-000	A	R. YOSHIMURA, 5432 J. PUHARA, 9652
	B	REPLACED NO 8 SCREWS (ITEM 4) WITH .125 DIA RIVETS COWLEY 9651 (MRL)/ STENBERG 4552 (MRL)

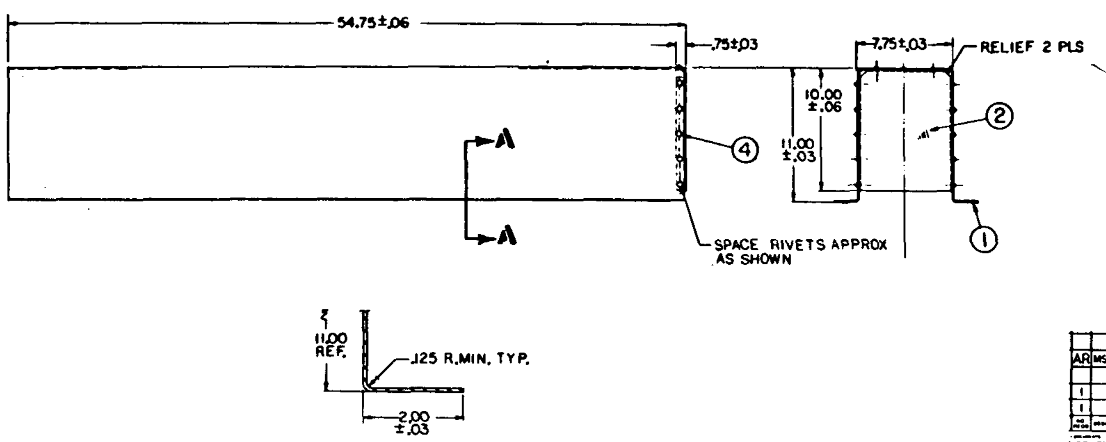

SECT A-A
SCALE - FULL

QTY REQD	DESIGN AGENCY NUMBER	DESCRIPTION	NOTE		ITEM
					5
AR	MS20470AD4-4	RIVET .125 DIA.			4
					3
1		END COVER	1		2
1		MAIN COVER	1		1

LIST OF MATERIAL

AGENCY APPROVALS			
DRG	DATE	APPROVALS	SHEET 1 / ISSUE B
4552			
9651			

PART CLASSIFICATION: UNCLASSIFIED

DWG CLASSIFICATION LEVEL: UNCLASSIFIED

TITLE: ENGINE SHROUD "B"

ALCO 1600

SIZE D | CODE IDENT. NO. 14213 | DWG NUMBER T40395

SCALE 1/4 & NOTED | SHEET 1 OF 1

NOTES:

1. MATERIAL: STEEL SHEET, LOW CARBON H.R. OR C.R., 20(.0359) GA.
2. ZINC CHROMATE PRIMER PER 5031201 / 5031202.
3. ALL BEND RADII - .125 R MIN
4. LOCATE .125 DIA. RIVETS APPROX. AS SHOWN.
5. ESTIMATED WEIGHT = 3.7#

DESIGN AGENCY PART [redacted] NO.	ISSUE	DESCRIPTION	PREPARED BY	DATE	CHKD	ENGR
T40393-000	A		R.YOSHIMURA, 5432; PUHARA, 9652	2.2.76		
	B	REPLACED NO. 8 SCREWS (ITEM 3) WITH .125 DIA RIVETS COWLEY 9651 (MRL)/ STENBERG 4552 (MRL)		11/4/78		11/15/78

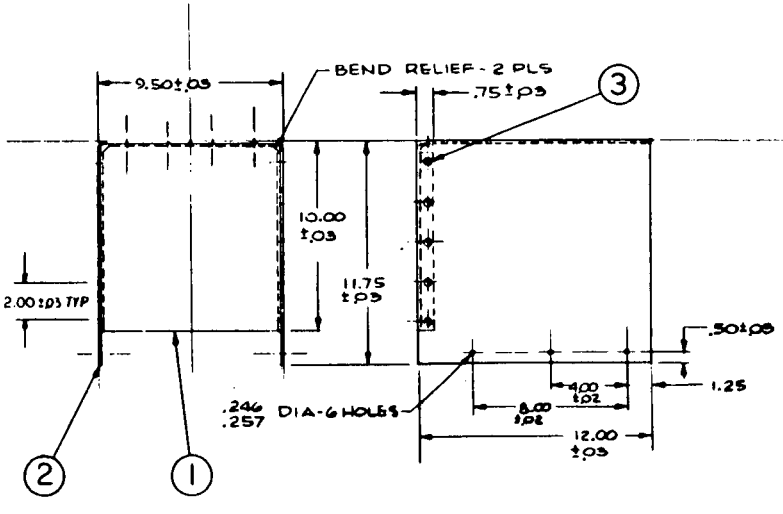

NO REQD	DESIGN AGENCY NUMBER	DESCRIPTION	NOTE	SHEET ZONE	ITEM
					5
					4
AR	MS20470AD4-4	RIVET .125 DIA.	4		3
1		COVER	1,3		2
1		FRONT BULKHEAD	1,3		1

LIST OF MATERIAL

AGENCY APPROVALS		
CAGE	DATE	INITIALS
4552	11/9/78	[redacted]
9651		

SHEET INDEX: SHEET 1, ISSUE B

PART CLASSIFICATION: UNCLASSIFIED

CHG. CLASSIFICATION LEVEL: UNCLASSIFIED

TITLE: STEAM GENERATOR & BATTERY COVER ALCO 1600

SIZE C | CODE IDENT. NO. 14213 | DWG. NUMBER T40393

SCALE 1/4 | SHEET 1 OF 1

NOTES

1. ZINC CHROMATE PRIMER PER 5051201/5051202.
2. CALC. WT =23.5#
3. MATERIAL: LOW CARBON STEEL.
4. GENERAL REQUIREMENTS ARE DEFINED IN 3900000

T40397-000	A		R. YOSHIMURA, 5432 J. PUHARA, 9652	2-3-76		
T40397-001	B		ADDED 8 EA. .386/.399 DIA HOLES, REVISED DIM TO T.P., ADDED NOTE 4 COWLEY 9651 (MRL) STENBERG 4562 (MRL)			

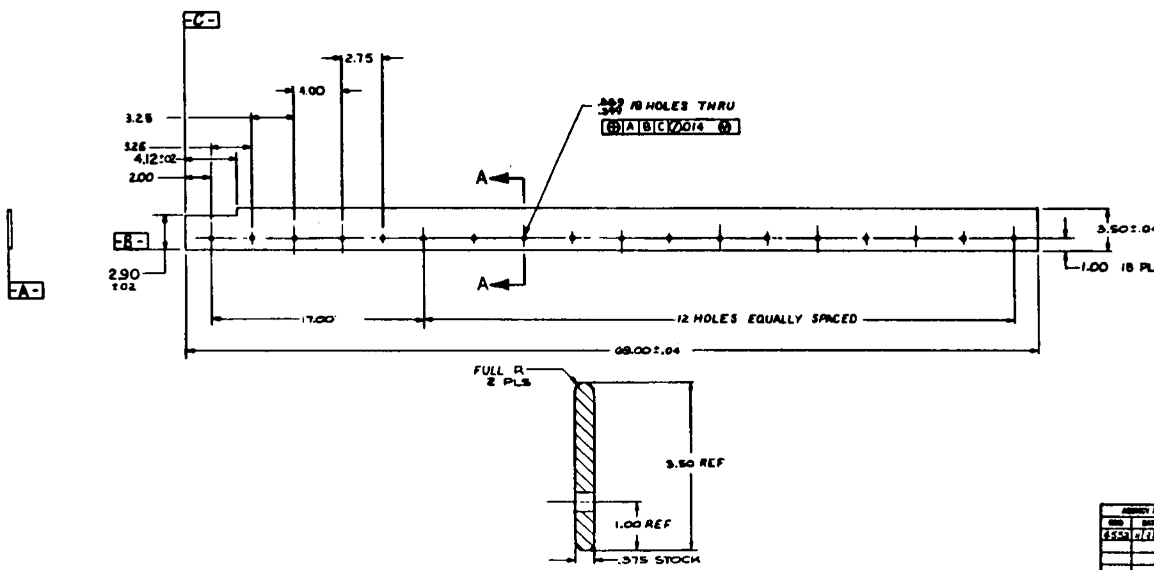

SECT A-A
SCALE - FULL

4552			B	
			UNCLASSIFIED	PRESSURE PLATE
				ALCO 1600
			UNCLASSIFIED	D 14213 T40397
3C5				SCALE 1/4 SHEET 1 OF 1

DESIGN AGENCY PART [redacted] NO.	REVISIONS				
	ISSUE	DESCRIPTION	PREPARED BY	DATE	CHKR	ENGR.
T40398-000	A	R.YOSHIMURA, 5432 J.PUHARA 9652		2-3-76	-	

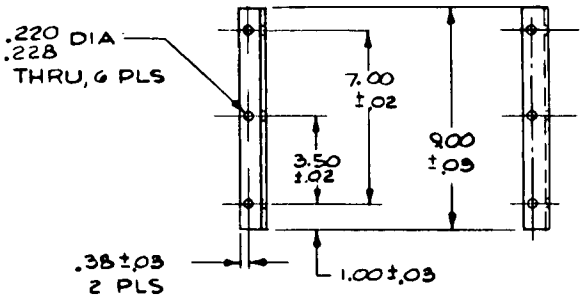

NOTES:

1. MATERIAL: STEEL, 1" x 1" x 1/8" ANGLE
2. CALC. WT = .6 #

AGENCY APPROVALS			SHEET	1					
ORG	DATE	INITIALS	ISSUE	A					
			SHEET INDEX						
			PART CLASSIFICATION	UNCLASSIFIED					
			DWG CLASSIFICATION LEVEL	UNCLASSIFIED					

TITLE: ANGLE, CAB
ALC0 1600

SIZE	CODE IDENT NO.	DWG NUMBER
B	14213	T40398

SCALE 1/4 SHEET 1 OF 1

NOTES:

1. TO BE FURNISHED BY 4552 ENG'G DIV..
2. MATERIAL: MEDIUM CARBON STEEL.
3. CALC. WT ~21.5#
4. ZINC CHROMATE PRIMER PER 5031201/5031202.

DESIGN AGENCY PART NO.	REVISIONS					
	ISSUE	DESCRIPTION	PREPARED BY	DATE	CHKD	APPD
T40392-000	A	R.YOSHIMURA, 5432, PUHARA, 9652		2-3-76		

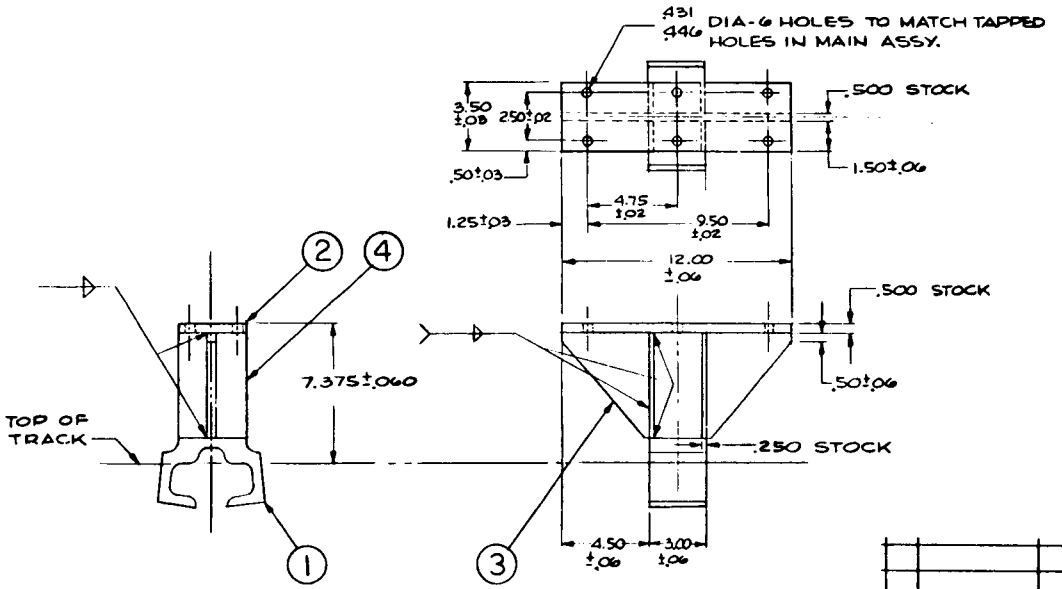

NO REQD	DESIGN AGENCY NUMBER	DESCRIPTION	NOTE	SHEET ZONE	ITEM
					5
4		GUSSET	2		4
1		COLUMN	2		3
1		CAP	2		2
1		SHOE, TRACK			1

LIST OF MATERIAL

AGENCY APPROVALS			SHEET	1
ORG	DATE	INITIALS	SIZE A	

SHEET INDEX

PART CLASSIFICATION: UNCLASSIFIED

DWG. CLASSIFICATION LEVEL: UNCLASSIFIED

TITLE: TRACK GUIDE ALCO 1600

SIZE	CODE IDENT. NO.	DWG. NUMBER
C	14213	T40392

SCALE 1/4 SHEET 1 OF 1

APPENDIX C

Data From the Scale-Model Test

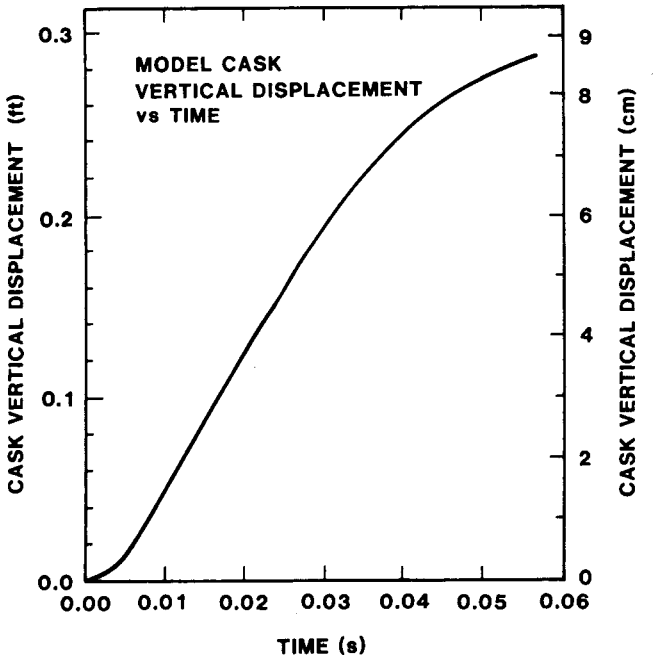

Figure C-1. Model Cask Vertical Displacement vs Time

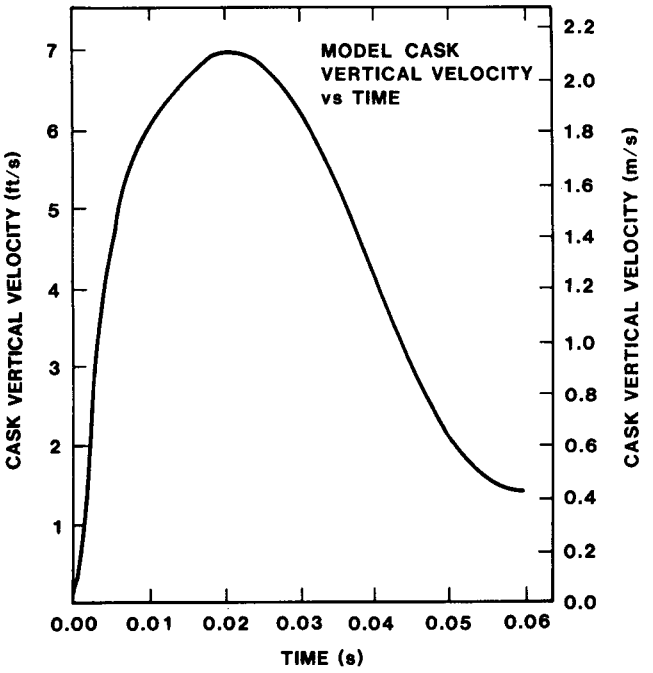

Figure C-2. Model Cask Vertical Velocity vs Time

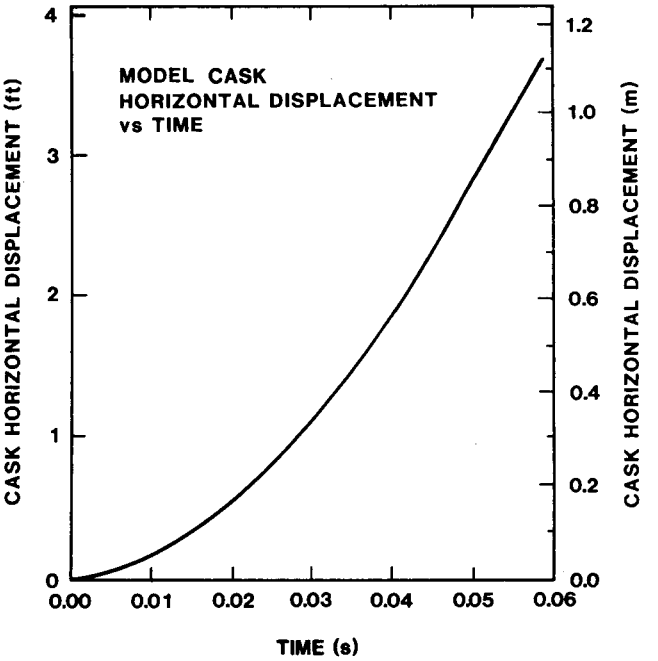

Figure C-3. Model Cask Horizontal Displacement vs Time

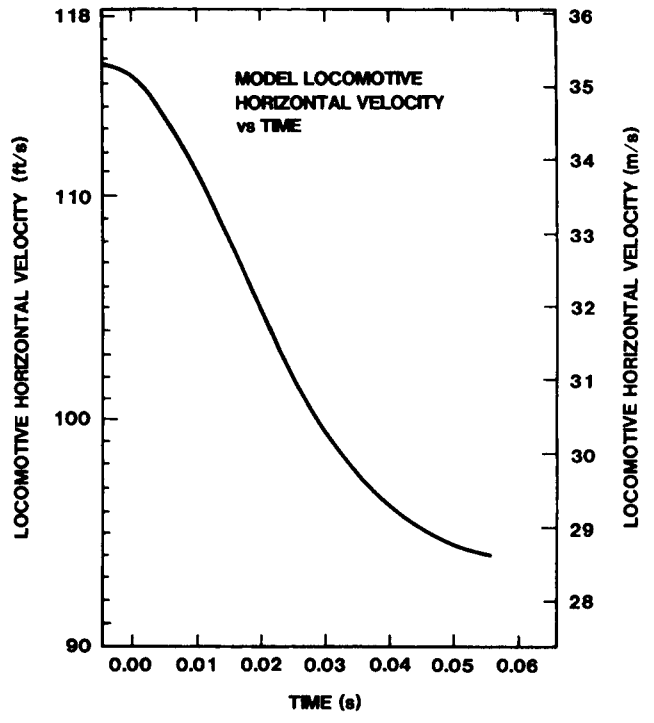

Figure C-4. Model Locomotive Horizontal Velocity vs Time

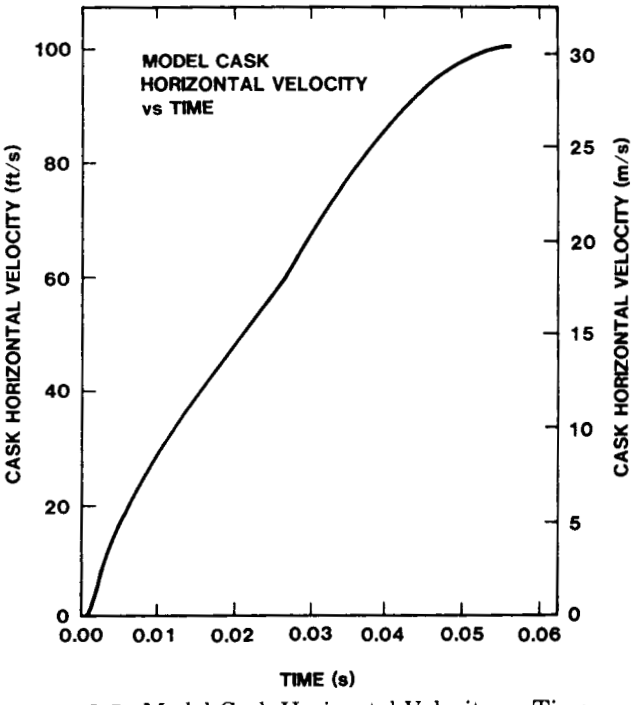

Figure C-5. Model Cask Horizontal Velocity vs Time

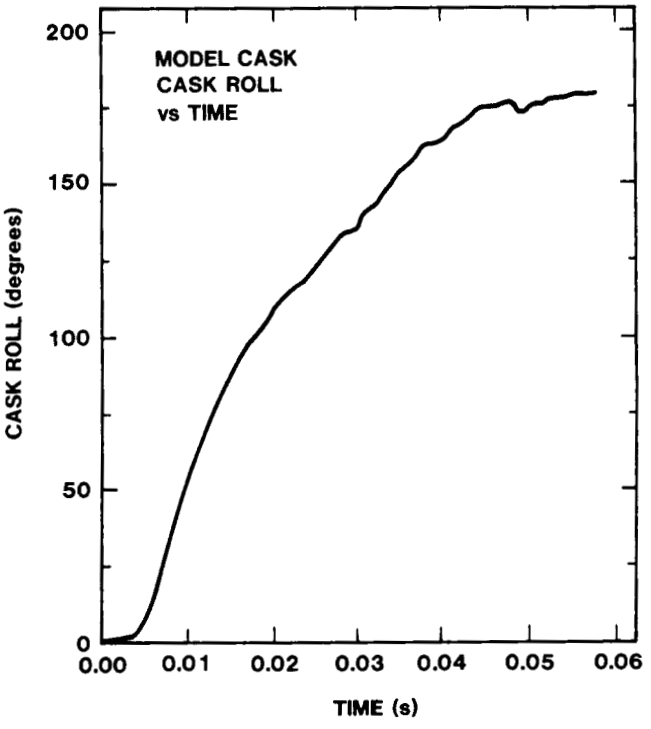

Figure C-6. Model Cask Roll vs Time

APPENDIX D

Data From the Full-Scale Test

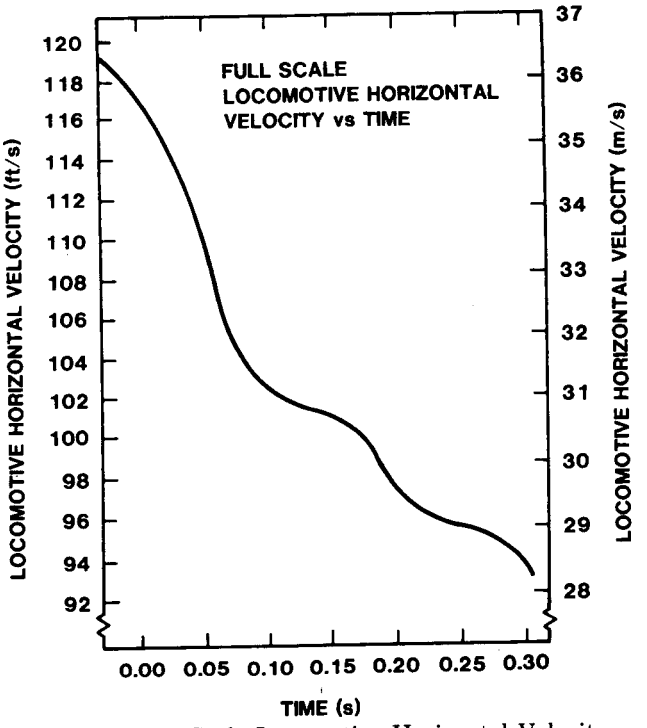

Figure D-1. Full-Scale Locomotive Horizontal Velocity vs Time

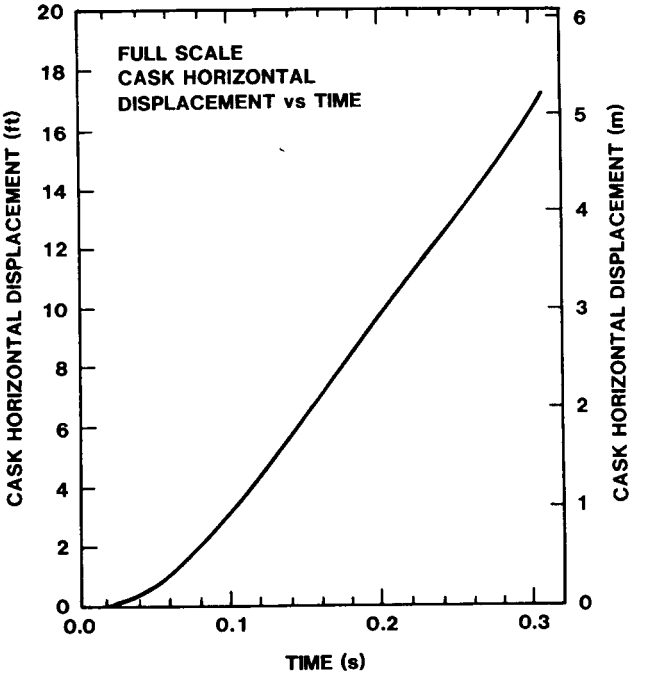

Figure D-3. Full-Scale Cask Horizontal Displacement vs Time

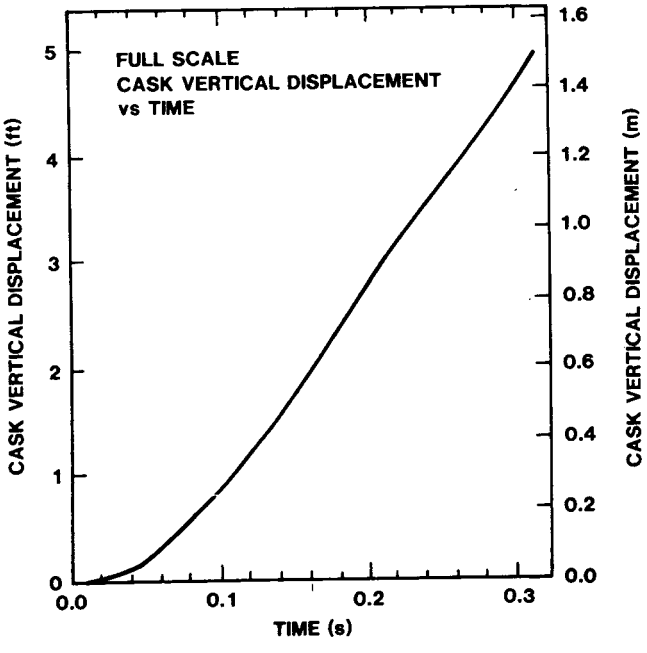

Figure D-2. Full-Scale Cask Vertical Displacement vs Time

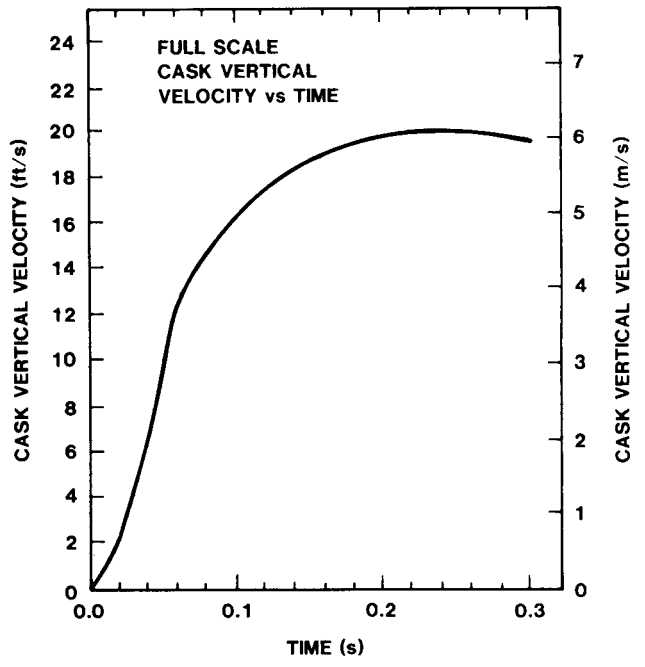

Figure D-4. Full-Scale Cask Vertical Velocity vs Time

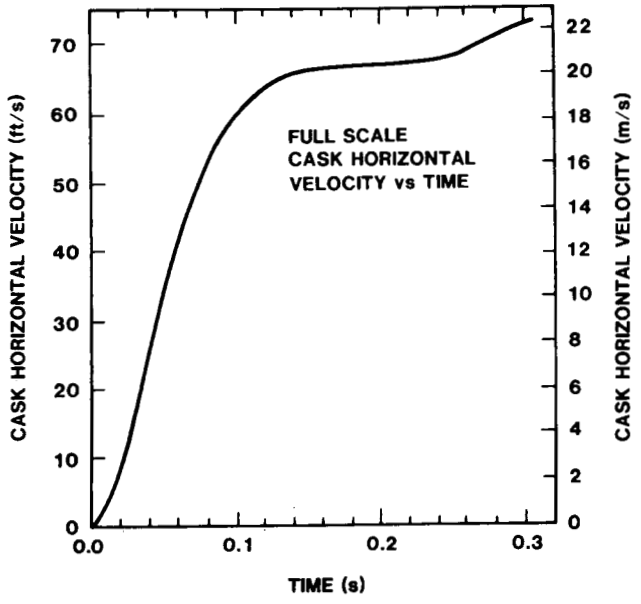

Figure D-5. Full-Scale Cask Horizontal Velocity vs Time

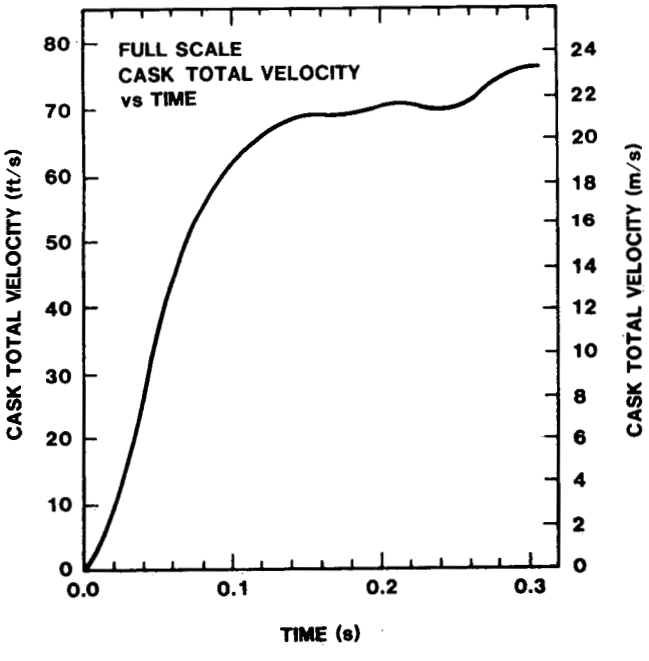

Figure D-6. Full-Scale Cask Total Velocity vs Time

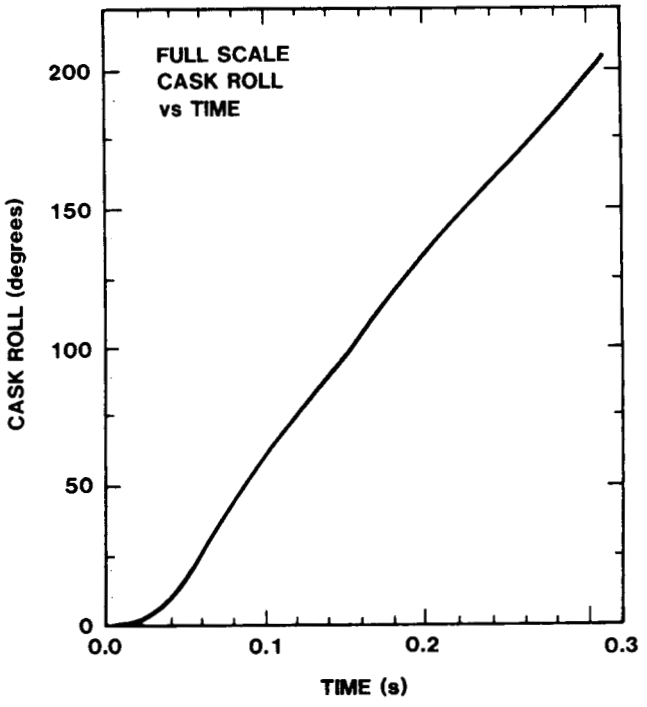

Figure D-7. Full-Scale Cask Roll vs Time

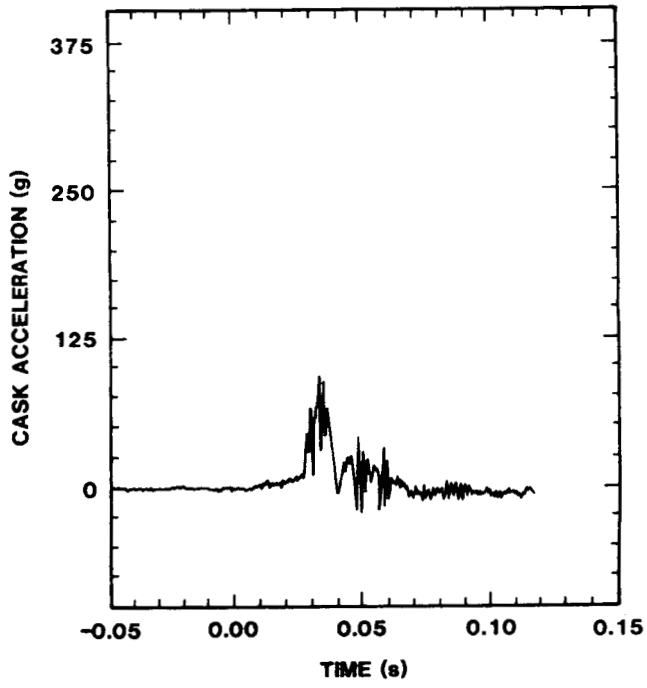

Figure D-8. Full-Scale Cask Acceleration vs Time From Accelerometer Near Right End

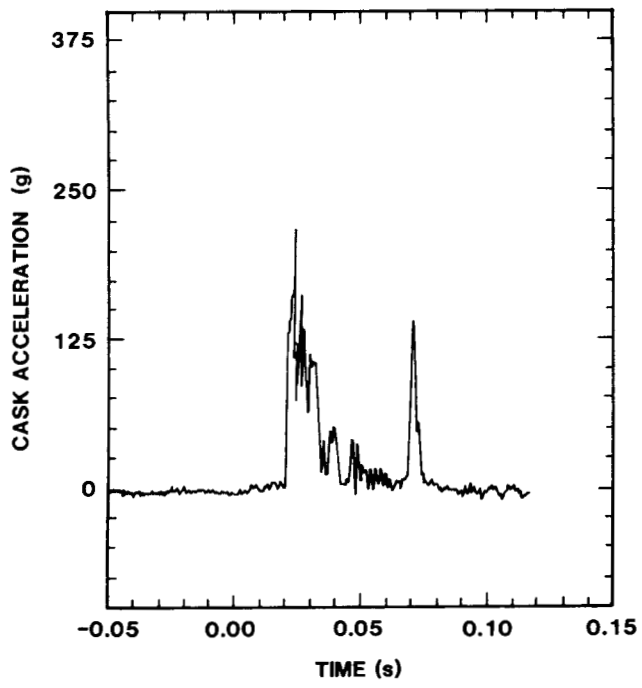

Figure D-9. Full-Scale Cask Acceleration vs Time From Center Accelerometer

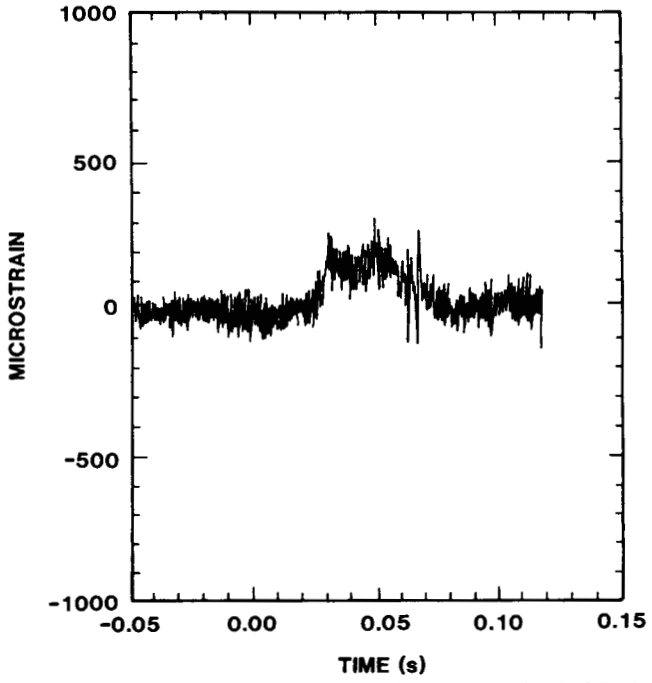

Figure D-11. Cask Strain at a Location 23.6 cm (60 in.) Left of Center

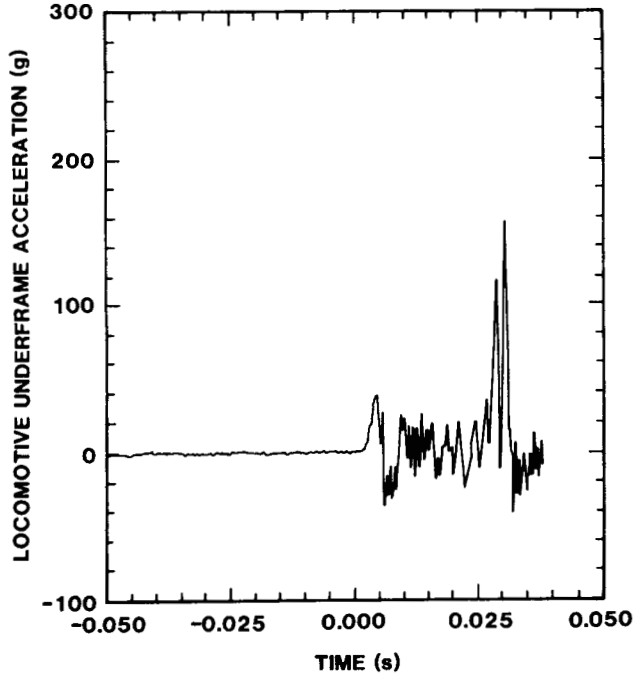

Figure D-10. Acceleration Trace From the Locomotive Underframe at a Location 2 m (6.6 ft) From the Front End

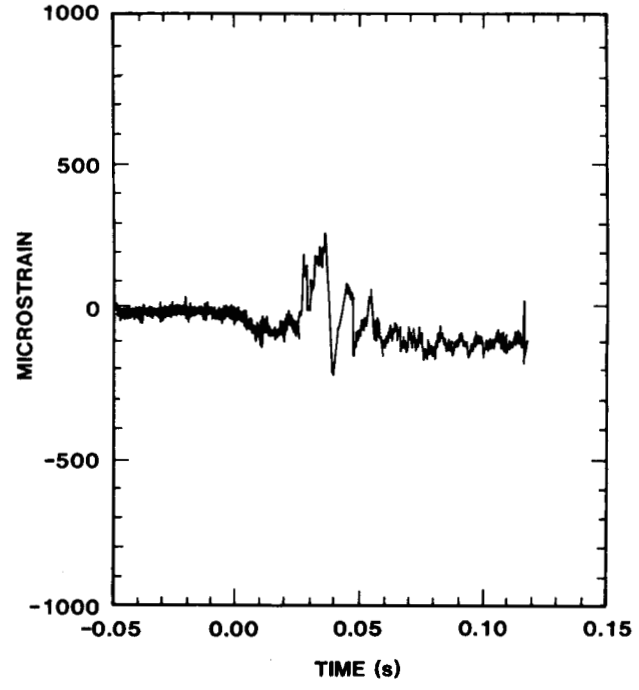

Figure D-12. Cask Strain at a Location 15.7 cm (40 in.) Left of Center

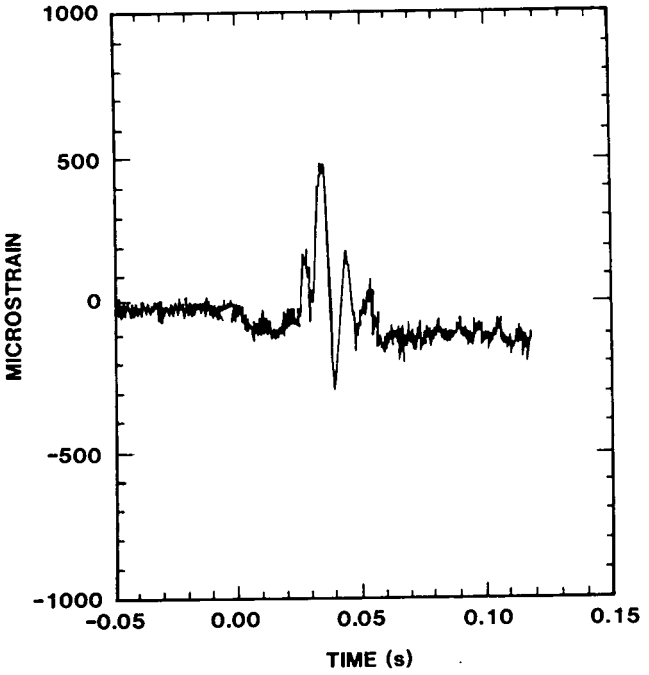

Figure D-13. Cask Strain at a Location 7.9 cm (20 in.) Left of Center

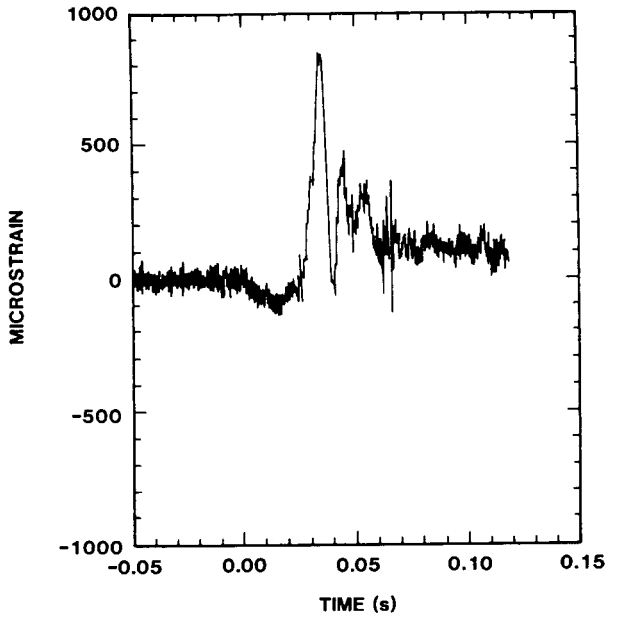

Figure D-15. Cask Strain at a Location 7.9 cm (20 in.) Right of Center

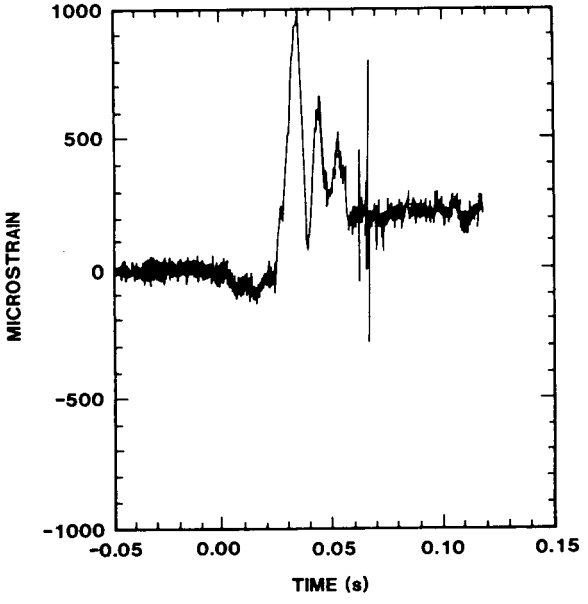

Figure D-14. Cask Strain at Center Location Opposite Impact Side

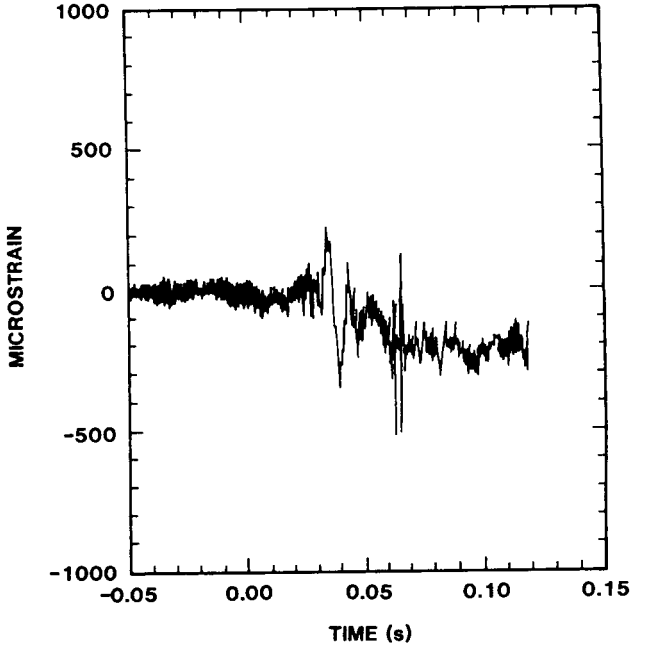

Figure D-16. Cask Strain at a Location 15.7 cm (40 in.) Right of Center

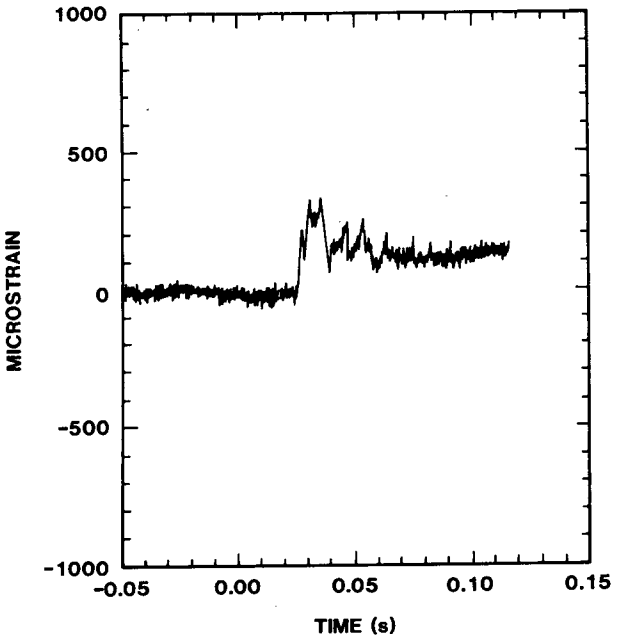

Figure D-17. Cask Strain at a Location 23.6 cm (60 in.) Right of Center

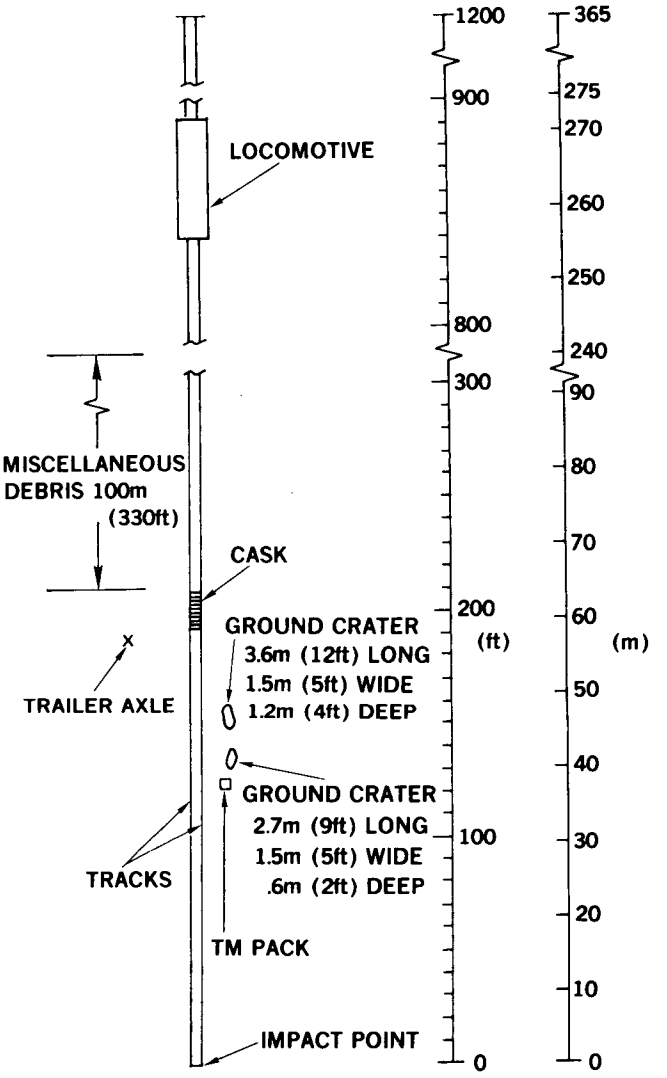

Figure D-18. Map of Hardware Location After Testing

APPENDIX E

Calculation of Horizontal Force Delivered to the Cask

In this appendix the average horizontal force delivered to the cask by the locomotive underframe is calculated. The purpose of the calculation is not to obtain a precise force-time history, but to estimate the average force applied to the cask during the short time that the underframe was in contact causing the two indentations reported. The calculation will be done three different ways for comparison. First, the velocity change given the cask during the almost 30-ms contact with the corner of the underframe will be used. Second, the angular velocity imparted to the cask will be used, again with a contact time of 30 ms. Third, the observed damage to the underframe will be used to roughly estimate the force. The 30-ms contact time was obtained from the finite-element analysis presented in the report.

The velocity change, Δv, imparted to the cask during the time interval from 0.030 to 0.060 s as observed in Figure D-5 is 7.6 m/s (25 ft/s). Assuming the force to be constant, we calculate the force level by using the following formula:

$$\int_{t_1}^{t_2} F\,dt = m \cdot \Delta v \qquad \text{(E-1)}$$

where

F = force
m = mass of the cask
Δv = velocity change
$t^1 = 0.030$ s
$t^2 = 0.060$ s

The force is then given by

$$F = \frac{m\,\Delta v}{t_2 - t_1} \qquad \text{(E-2)}$$

This equation gives a value of 6.44×10^6 N (1.449×10^6 lb) when a cask mass of 25,400 kg (1741 slugs) is used.

The force can also be estimated from the spin imparted to the cask. As mentioned previously, this value was about 150 revolutions/minute or 15.7 rad/s. For this calculation the following formula over the same time frame can be used:

$$\int_{t_1}^{t_2} M\,dt = I\omega \qquad \text{(E-3)}$$

where

M = moment or torque applied to the cask
I = mass movement of inertia of the cask
ω = angular velocity of the cask

In this calculation a moment arm, R, has to be assumed to estimate the force. Because the corner of the underframe impacted the cask 20.32 cm (8 in.) below center, this value will be used for R. The moment, M, will then be replaced by F R in Equation (E-3), and the expression for the force becomes

$$F = \frac{I\omega}{R(t_2 - t_1)} \qquad \text{(E-4)}$$

The moment of inertia of the cask about its longitudinal axis now needs to be calculated. This is done by treating the cask as a thick-wall cylinder of uniform density. The expression for I is

$$I = \frac{1}{2} m\,(R_o^2 + R_i^2) \qquad \text{(E-5)}$$

where

R_o = outside radius of cask
R_i = inside radius of cask
m = mass of cask

If we take R_o as 44.9 cm (17.68 in.), R_i as 19.05 cm (7.5 in.), and the mass of the cask used previously, the moment of inertia of the cask, I, is 6067 kg-m^2 (2227 slug-ft^2). Using these values and Equation (E-4) we calculate,the force as 7.82×10^6 N (1.75×10^6 lb). This value is slightly higher but still very much in the same range. It is very dependent on the value of R chosen; however, the off-center distance between the top of the underframe and the center of the cask seems a reasonable number to use.

The force level delivered to the cask can also be roughly estimated by considering the damage sustained by the underframe (Figure 29). The upper 21.6 cm (8.5 in.) of the I-beams was deformed plastically and the front bumper plate was permanently bent back. It is assumed that the force level causing this damage is close to the total force delivered to the cask. The damaged area in the I-beams includes the upper flange and the top 19.05 cm (7.5 in.) of the webs. If both sides are considered, these two T-shaped areas add up to 227.4 cm^2 (35.25 in.^{2}). Multiplying these areas by the yield stress of 241.3 mPa (35,000 lb/in.^{2}) gives a force level of 5.48×10^6 N (1.233×10^6 lb). Simple hand calculations, not included here, indicate that the plastic deformation of the front bumper added about 4.44×10^5 N (1×10^5 lb) to the force level delivered to the cask. This brings the force level estimated by this technique to 5.91×10^6 N (1.33×10^6 lb). This is probably a low estimate because there are other structural components that contributed secondary forces.

The force delivered to the cask in the vertical direction is not calculated here, but has been estimated to be less than one-third of the horizontal component. When this is vectorially added to the horizontal component, the resulting vector sum is only very slightly higher than the horizontal component.

In view of the above calculations, we estimate that the average force delivered to the cask by the underframe during the 30 ms of contact was about 6.67×10^6 N (1.5×10^6 lb).

DISTRIBUTION:

DOE/TIC–4500–R70 UC 71 (277)

US Department of Energy (3)
Routing DP123
Washington, DC 20545
Attn: G. Oertel
J. Jicha
F. P. Falci

US Department of Energy (2)
Albuquerque Operations Office
Albuquerque, NM 87115
Attn: K. A. Carlson
E. C. Hardin

1520 T. B. Lane
1521 R. D. Krieg
1522 T. G. Priddy
1523 R. C. Reuter
1523 R. A. May
1530 L. W. Davison
9000 G. A. Fowler
9700 E. H. Beckner
9780 R. M. Jefferson
Attn: TTC Master File
9781 TTC Library (10)
9781 R. E. Luna
9782 R. B. Pope
9783 G. C. Allen
9783 H. R. Yoshimura (50)
9783 M. Huerta (10)
9783 D. R. Stenberg (4)
8214 M. A. Pound
3141 L. J. Erickson (5)
3151 W. L. Garner (3)
For DOE/TIC (Unlimited Release)